DESIGN AND MODELING OF INTAKE AND EXHAUST SYSTEMS OF A RECIPROCATING INTERNAL COMBUSTION ENGINE

A Final Year Project Report

Presented to

SCHOOL OF MECHANICAL & MANUFACTURING ENGINEERING

Department of Mechanical Engineering

NUST

ISLAMABAD, PAKISTAN

In Partial Fulfillment
of the Requirements for the Degree of
Bachelor of Mechanical Engineering

by

Muhammad Arsal Rehman
Muhammad Izaam bin Riaz
Munam Ahmed

June 2021

EXAMINATION COMMITTEE

We hereby recommend that the final year project report prepared under our supervision by:

MUHAMMAD ARSAL REHMAN	218391
MUHAMMAD IZAAM BIN RIAZ	209458
MUNAM AHMED	217750

Titled: *"DESIGN AND MODELLING OF INTAKE AND EXHAUST SYSTEMS OF A RECIPROCATING INTERNAL COMBUSTION ENGINE"* be accepted in partial fulfillment of the requirements for the award of BACHELOR'S IN MECHANICAL ENGINEERING degree with grade ___

Supervisor: Dr. Samiur Rahman Shah, Assistant Prof.	______ Dated:
Co - Supervisor: Dr. Emad-Ud-Din, Associate Prof.	______ Dated:
Committee Member: Dr Jawad Aslam, Assistant Prof.	______ Dated:
Committee Member: Dr Khalid Akhtar, Assistant Prof	Dated: ______

______________________ ___________

(Head of Department) (Date)

COUNTERSIGNED

Dated: ________________ __________________________

(Dean / Principal)

ABSTRACT

Engine is a machine that is designed to convert heat energy produced by combustion of fuel to useful mechanical energy. They have diverse applications everywhere around us; from driving cars, trucks, bikes, to generating electricity or propelling a ship or a small aircraft. These applications are just a few to mention. Whichever be the application area, the sole purpose of engine is to generate power. In any industry of application, whenever engine is developed, it goes through some iterative tuning techniques to obtain best possible performance.

In this project, the flow of fluid (air) during the intake and exhaust are studied using thermodynamic equations. The state of fluid at the points of interest such as orifice formed due to opening and closure of intake and exhaust valves is observed. Study of intake and exhaust flows is of great importance for engine development and advancement of technology. The scope of our project covers; analytical model of the flows under discussion, use of the model to achieve a tuned runner length and suggest the required mechanical component change in mechanism operating opening and closing of valves.

Most engine manufacturers in the world tend to maximize engine volumetric efficiency for a specific range of operating RPMs. There are several methods to achieve an increased volumetric efficiency. Whatsoever be the method, the importance of knowing the operational intake and exhaust flows can never be neglected.

ACKNOWLEDGMENTS

We are extremely grateful to Allah Almighty for satisfactory progress in our Final Year Project. We have, till now, learnt significantly about project management, analytical and critical problem solving, market awareness, manufacturing processes, and other aspects important while progressing in an FYP. We are also thankful to our supervisor Dr. Sami-Ur Rehman Shah who provided us an opportunity to learn and gain practical knowledge. We are also very thankful to Dr. Emad_ud_Din and other faculty members for guiding and helping us. We hope this fruitful project will enable us to apply our skills and knowledge to polish ourselves as good mechanical engineers.

ORIGINALITY REPORT

FYP Report

ORIGINALITY REPORT

1%	1%	0%	0%
SIMILARITY INDEX	INTERNET SOURCES	PUBLICATIONS	STUDENT PAPERS

PRIMARY SOURCES

1	www.ijstr.org Internet Source	1%

Exclude quotes	Off	Exclude matches	< 1%
Exclude bibliography	Off		

TABLE OF CONTENTS

LIST OF TABLES

LIST OF FIGURES

ABBREVIATIONS

RPM	*Revolutions Per Minute*
TDC	*Top Dead Center*
BDC	*Bottom Dead Center*
PV Diagram	*Pressure – Volume Diagram*
TS Diagram	*Temperature – Entropy Diagram*
V.E	*Volumetric Efficiency*
AFR	*Air Fuel Ratio*
FAR	*Fuel Air Ratio*
EVO	*Exhaust Valve Opening*
IVO	*Inlet Valve Opening*
EVC	*Exhaust Valve Closing*
IVC	*Inlet Valve Closing*
DOHC	*Dual Overhead Cam Engines*
SOHC	*Single Overhead Cam Engines*
MEP	*Mean Effective Pressure*
ASTM	*American Society for Testing and Materials*
AISI	*American Iron and Steel Institute*
OEM	*Original Equipment Manufacturers*
HCCI	*Homogeneous Charge Compression Ignition*
RCCI	*Reactivity Controlled Compression Ignition*

SUBSCRIPTS

atm	*Atmosphere states*
o	*Stagnation states*
gen	*Generated*
1	*Inlet*
2	*outlet*
v	*Volume processes*
p	*Pressure processes*

NOMENCLATURE

γ	*Adiabatic Index*
v	*Volume Flow Rate (m^3/s)*
ω	*Angular Velocity (rad/s)*
P	*Pressure (Pa)*
T	*Temperature (K)*
δU	*Change in Internal Energy*
δQ	*Change in Heat Energy*
δW	*Change in Work done*
C_v	*Specific Heat at Constant Volume*
C_p	*Specific Heat at Constant Pressure*
Ma	*Mach Number*
c	*Speed of Sound*
S_{gen}	*Total Generated Entropy*
h_0	*Stagnant Enthalpy*
T_0	*Stagnant Temperature*
C_d	*Coefficient of Discharge*
V_{p_avg}	*Average Piston Speed*
NOx	*Nitrous Oxides*
COx	*Carbon Oxides*

CHAPTER 1: INTRODUCTION

In the past century, the world has evolved immensely through technical revolutions. From once famous man-pulled carts and wagons to the vast variety of automobiles available today, the world has been through a lot. In all so, the engine of a vehicle lies at the core of this advancement. Although, electric vehicles and other newer technologies are uprising in the market, it is safe to say that engines will be the crux of the working world for the coming years. Therefore, it is crucial that they keep on getting better with time. Even now, constantly working on the technicalities of combustion, mixture flow and operating conditions to improve the engine efficiency is popular.

An engine has many parts that control the entirety of the energy production process. To better understand the project, consider the three main parts:

- Intake: the manifold that holds the air and transfers it to the combustion chamber through special channels called “runner”.
- Engine cylinder: this is the combustion chamber where the fuel is burnt to generate energy.
- Exhaust: this manifold extracts the burnt air and fuel and discharges them to the open environment.

Engines may be diesel operated or they may work on petrol. The diesel engine, named after Rudolf Diesel, is an internal combustion engine in which ignition of the fuel is caused by the elevated temperature of the air in the cylinder due to the mechanical compression; thus, the diesel engine is a so-called compression-ignition engine (CI engine). Generally, diesel engines have a greater efficiency as compared to the other engines because there is no need of a spark plug in them. A diesel engine may be 2-stroke or 4-stroke. In most applications, a 4-stroke engine is used for better performance and emission control.

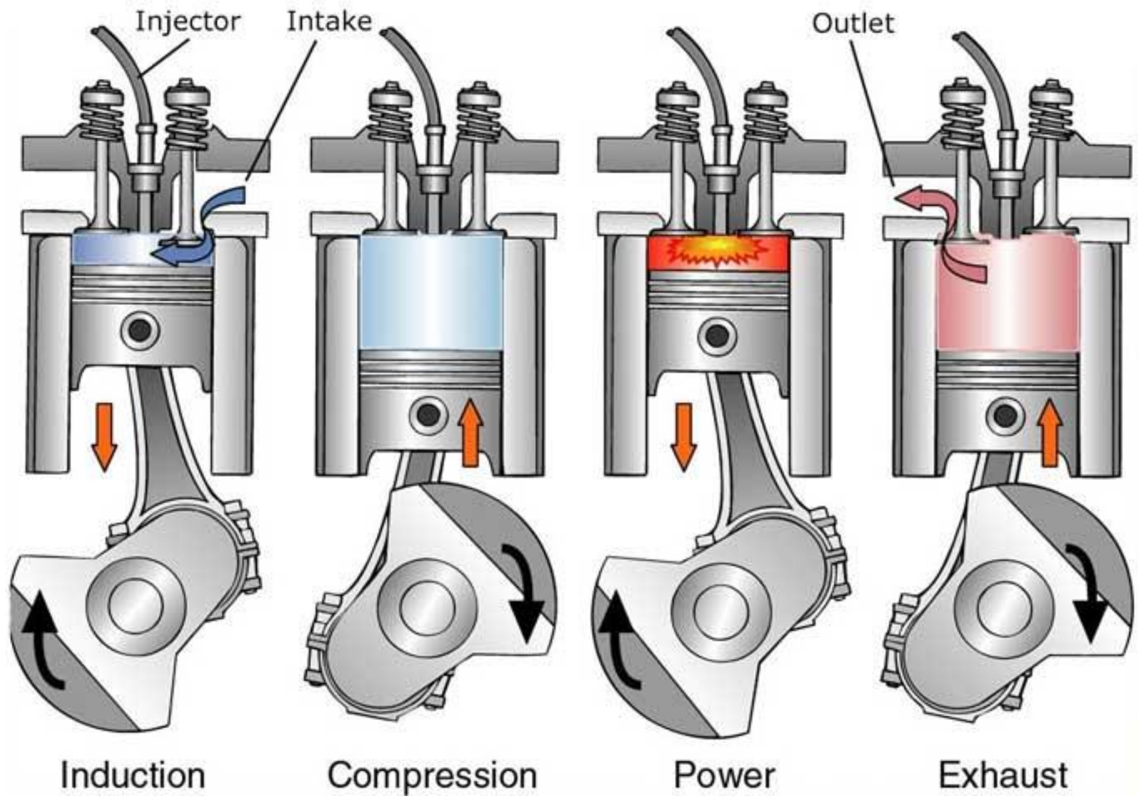

Figure 1: General Cycle Indication of a 4-stroke diesel engine [1]

1.1 Problem Statement

To study these concepts better and to indulge ourselves into the study of thermal and fluid fields, the suitable problem statement of our project narrows to:

"Design and Modelling of Intake and Exhaust Systems of a Reciprocating Internal Combustion Engine"

In this project, we will work on **MATLAB** to study the flows at the intake and exhaust manifolds. The plots obtained for different cylinder states and flow properties will further highlight our studies. All this will come in the later part of the report.

1.2 Objectives

The core goal of our project is to study the 2000 cc 4-stroke diesel engine, design its parameters and analyze the results for improvements. Our objective is to model the engine on a software, study the flows and tune the components for a better volumetric efficiency. The key aims of our project are as follows:

(i) To design the model an engine with the experimentally known initial data. We will work on the intake and exhaust systems.

(ii) To model the flows of intake and exhaust. Use their developed states and iterate with different variables such as length, diameter and area to change the mass-flow and hence the volumetric efficiency.

(iii) To tune the runner for the intake manifold and observe the effect on volumetric efficiency as compared to forced induction systems

(iv) For the mass-flow and high pressure, suggest critical design to keep the operation of intake and exhaust smooth.

1.3 Motivation

The major motivation of our project is to develop a learning and working experience with engines. By studying the fluid flows we will be better able to equip ourselves with the practical knowledge and skills. By touching both the thermal and fluid sides, we will be solidifying our foundation as mechanical engineers.

As electric vehicles only shift the pollution from fuel operated vehicles to the production facilities, it is essential to keep working on the engines to make them more sustainable. So, our project has the following scopes:

(i) The results from our studies can be used to better understand the efficiencies of engines and their working cycles.

(ii) Our MATLAB code can be further utilized to develop some tuning software that tunes the runner lengths of intake manifolds which can in turn increase the volumetric efficiency.

(iii) By studying the basics of a working engine, the project can be extended in any direction such as fluid analysis on ANSYS or combustion analysis.

The study of intake and exhaust flows is quite diverse and important. It does not restrict us to the scope of this project rather this study can be used as an established method and a first step towards more modern concepts of research in the IC Engine realm.

CHAPTER 2: LITERATURE REVIEW

Volumetric efficiency is defined as the ability with which engine can take the charge of air into and expel out of itself. The ratio of air fuel charge getting into the cylinder to the total swept volume is called the volumetric efficiency. There are certain pressure losses and other constraints that will not allow an engine to breathe at the maximum capacity and in turn is unable to achieve volumetric efficiency of 100%.

There are several methods by which the volumetric efficiency of the engine can be increased. Forced induction is one way i.e., by using superchargers or turbochargers. Naturally aspirated engines are also designed to get better volumetric efficiency. This can be done by using several methods, such as, cam phasing for variable valve timing, reducing the temperature of intake charge (this is difficult to implement and has many complexities), or using carefully tuned and arranged intake and exhaust systems.

Pressure wave is generated inside the intake and exhaust system and when specifically tuned the resonance hence created will result in a compressed air chunk to enter into the cylinder. And a negative pressure gradient pulls the exhaust out of the engine more effectively.

Study of flows of intake and exhaust and knowing the respective mass-flows, pressure and temperature are important in order to apply in of the method to obtain a good volumetric efficiency. The development of the engine flow model will help in engine development. Over the period of time many advancements have been made in this field but the significance of intake and exhaust flows have not yet diminished.

2.1 Choice of engine to model

Internal combustions engine can be segregated into various kinds depending on the fuel they use, method of combustion, state of intake air, number and orientation of cylinders, fuel injection technique etc. For our analytical model development, it is important that we choose a practically existing engine so that we have an actual product to base our study upon. The simpler yet realistic model should be chosen. We look forward to weigh different options and then go for the one best suited to our requirement.

2.1.1 List of requirements

The most widely used in daily drivers' car or even commonly used portable or fixed generators is an inline orientation of cylinders. Most engine use 4 cylinders as this is neither too miserly for power nor a fuel chugging beast.

1. **Diesel engine**

   Reason: Diesel is widely used fuel. Produces good power. Intake air is free of fuel so easier for analysis and less assumptions required.

2. **Inline 4 cylinder**

   Reasons: Any fancier orientation or more cylinder engine can be selected and physics would probably obey same laws. But for basing the study on a more basic application these characteristics are preferred

3. **Availability of resource**

   Reason: Our project requires experimentally obtained data from the engine and availability of either this data or the engine itself is necessary to move on with the project.

2.1.2 Peugeot DW10 [2]

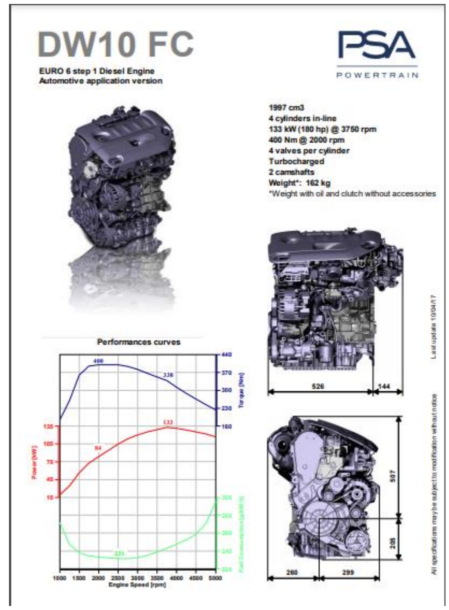

Figure 2: PSA DW10 Peugeot Engine book cover

Peugeot DW10 diesel 2000 cc inline 4 cylinder meet our requirements. This engine manufacturer is quite renowned and engine has been tested time and time again to perform well. DW10 has a bore of 85 mm and stroke of 88 mm. This engine is used widely by the PSA in cars like Citroen C4 and Peugeot 206. It was the first engine to feature common rail direct injection. In this system fuel from tank is first supplied to the accumulator and a high-pressure relief valve is used to inject fuel into the cylinder.

2.2 Research and Development on the DW10

DW 10 is a well-developed engine by PSA Peugeot Citroën. In 1999, it was first time used as a replacement of its predecessor XUD9. The most obvious difference between the two was the injection system used in both engines. DW10 made a good name in the category and was not only used by Citroën and Peugeot in their cars ranging from hot-hatches, to MPV, crossover SUVs and even sedans. In European market this engine with its reputation was also used by other car manufacturers such as Suzuki, Ford, Volvo and Fiat. DW 10 has seen three major upgrades ever since production.

(i) **Improvement in emission standards**: when the production of this engine started, the emission standards were up to the mark according to the standards of that time. DW10 operated on EURO 3 technology. After the improvement in technology, the manufacturer worked their way around to get the engine suited to EURO 5 standards. This EURO 5 version is still allowed to be used in most countries. However, a modified version of DW10 is also compliant to EURO 6 emission standards. This variant uses selective catalytic reduction emissions control technology.

(ii) **Life Cycle of DW10**: Developed from the basic design of UDX9, an engine developed by PSA. Some parts such as crankshaft etc. were used as it is with the change in material. DW10 was quite lighter than its predecessor. From 1999 to the present date DW10 is currently used in automobiles. The good reputation of engine led the companies like Jaguar and Land Rover to use a modified version of this engine by the name of Ingenium engine family in their high performance and SUVs.

(iii) **Research papers based on this engine** [3]: Many research papers have been published with this engine model as a basis. Water cooled technology research, NOx emissions control, in-cylinder emission control etc.

In this project the wide diversity of work that has been done will help us to achieve our required experimental data. Moreover, a better comparison and insight of our interpreted results can be gathered.

2.3 CFD of in engine cylinder Flows

Finite volume is the most popular numerical approach used in Computational Fluid Dynamics (CFD). In this study, Tumble motion, which is popular in automotive engines, and the RNG k-e turbulence model were used as significant, common fluid flow patterns in CFD simulations. Using a CFD code based on finite volume and codes written in the visual C++ setting, the air flow in a two-valve engine cylinder during 720 degrees of crank angle was investigated. This model made use of Dynamic Mesh and Moving Boundary capabilities.

This approach was used to base our physics and a comparison to the peak indicated pressure practical vs calculated comparison was used. The graph based on CFD analysis of the above-mentioned study is less accurate and hence a better fit plot of cylinder pressure as compared to this result will ensure the superiority of study. [4]

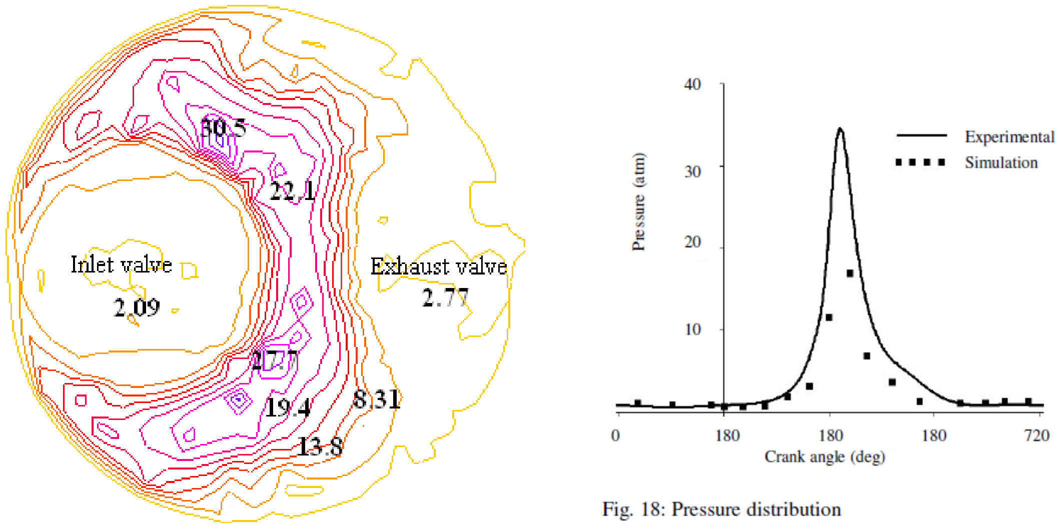

Figure 3: Velocity Contours and Pressure Distribution results as shown in mentioned literature

2.4 Fundamentals of Internal Combustion Engine

Combustion engines are complex machines. They have moving parts, exchange of heat, high pressure working fluid and application of all major concepts of mechanical engineering. Even with the development of electronic control systems, ICEs have a diverse application of electronics. The scope of our project does not require us to deal with the

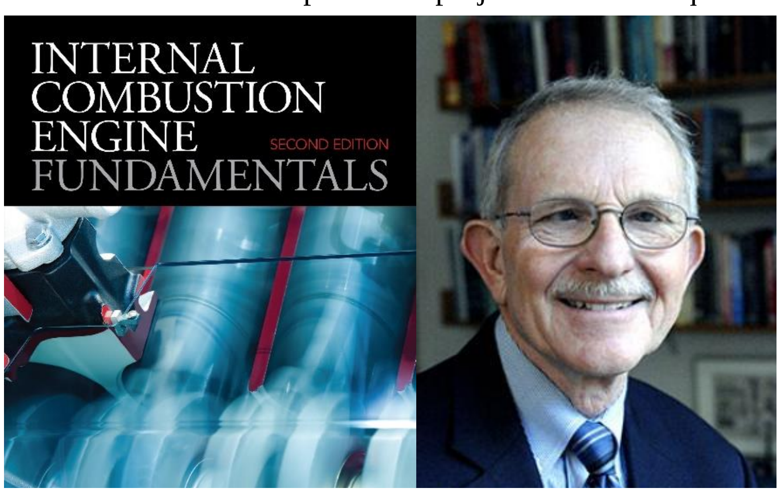

Figure 4: ICE Fundamentals Book cover and Author John B Heywood

electronic or major mechanics portion such. To seek help on any concept and comparison to established practices of literature, a consultation to the book "Internal Combustion Engines Fundamentals by John B. Heywood" will be made. This book discusses the engine types and design parameters, thermochemistry of fuels, working properties of fluids, fuel metering and manifold phenomena, engine cycles, motion and combustion of fuel, emission and environmental effects, heat transfer, lubrication and many more concepts deeply. [5]

This book by John B. Heywood is a paradise for the engineers and can help them with concepts of Internal Combustion Engines at whatever stage of their professional career they are.

2.5 Design of a 4-cylinder Internal Combustion engine

Radoslav Plamelov Georgiev, a researcher of Universidad Publica de Navarra, in 2011 has published his paper on design of Internal Combustion engine. All basic development calculations for mechanical component design. Kinematic calculations and use of established design calculation for different parts such as piston, cylinder head, valves, connecting rods etc. The aim of this thesis is to introduce you to the fascinating world of internal combustion engines and to explain what an I.C.E. is. What are the key components and design of it? This is how the engine really works. Also, to build a real engine, taking into account all required kinematics, dynamics, and strength estimates. [6]

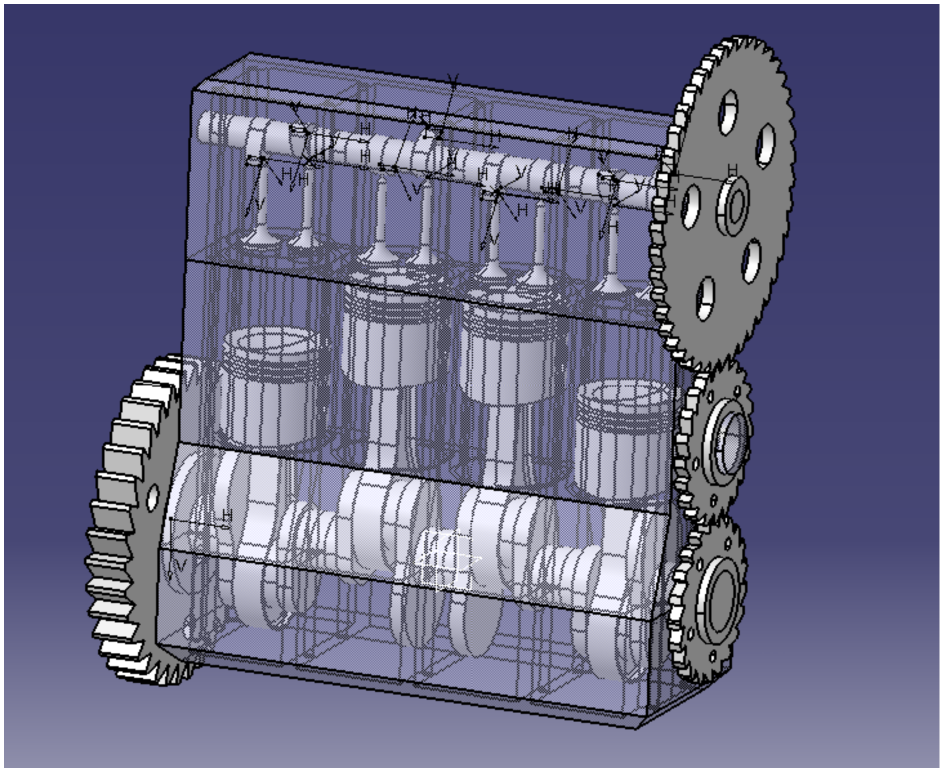

Figure 5: Assembly designed on CATIA by the author of mentioned literature

This piece of literature could be of help when any general calculation is required anywhere. As the scope of our project is not related to the kinematics of moving parts such as piston or connecting rod etc. but this paper will help us build a relation to the stream if we might require at any point during our project.

2.6 Compressibility effect and Tuned Runner Concept [7]

The gas dynamics of the intake system are crucial in determining an engine's output. Fuel injected and carbureted engines have various dynamics, which vary depending on the type of engine, the number of cylinders, the temperature at the inlet, valve timing, valve angle, and other variables. The engineer (designer) can control the characteristics by carefully designing the manifolds. This paper details on how intake runner lengths can affect the performance of engine and uses a software technique to address the issue. It was found that change in runner length had a considerable effect on the rpm at which peak value of torque was obtained (occurred). Accordingly, a system to adjust the manifold length (tuned adjustable intake pipe) was designed and developed. According to the simulation graphs, in order to increase the torque performance, plenum length must be extended for low engine speeds and shortened as the engine speed increases. A wave is divided into two parts: a compression wave and a rare faction wave. Both of these waves can be used to improve the volumetric performance of the engine, thus increasing its breathability.

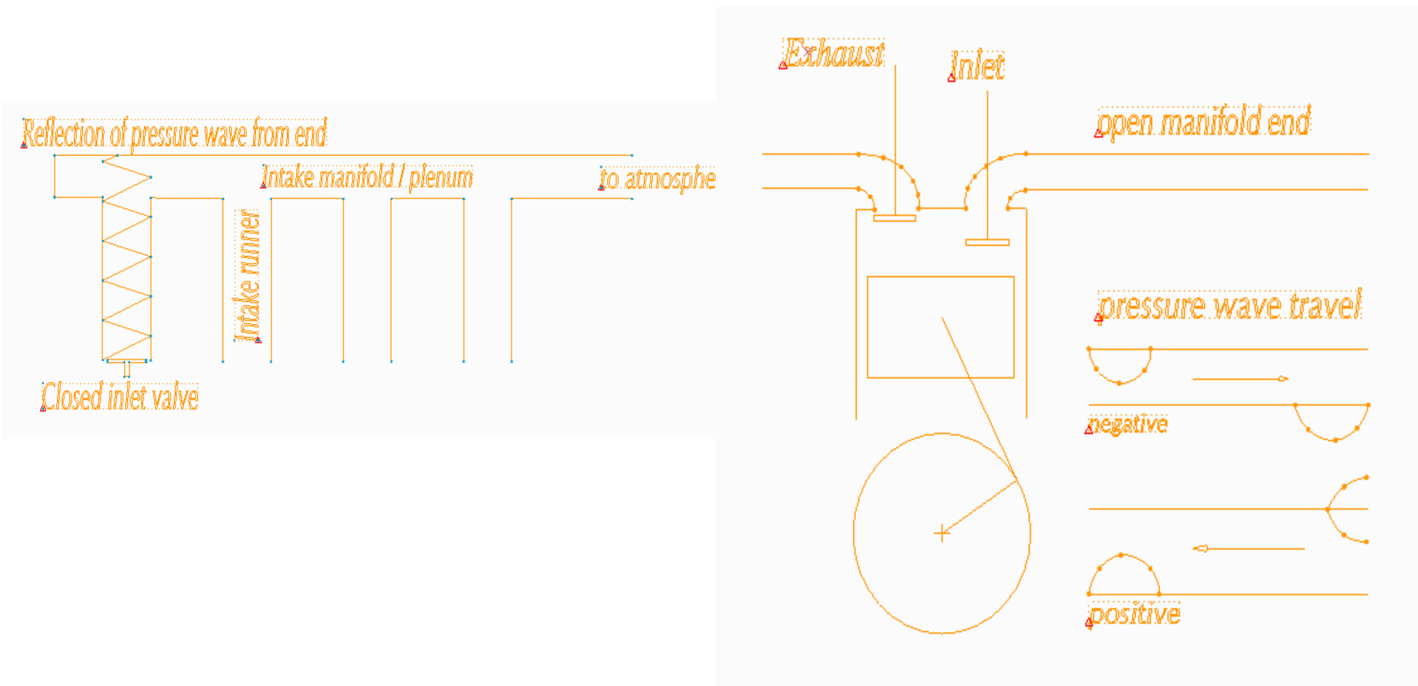

Figure 6: Explanatory image of Pressure wave propagation from the mentioned literature

Two major concepts of our target are discussed in literature.

(i) Chryslers RAM Theory

The pressure wave formed moves back and forth inside the intake manifold. According to this theory the length is adjusted in such a way that the compression part of the wave resides over the opening of valve. Due to inertial effect the compressed part enters into the cylinder.

(ii) Acoustic Tuning Theory

The negative pressure gradient can be created to suck in more air into the cylinder. This can be achieved by proper acoustic tuning and using the rarefaction part of the wave.

Another important concept is of Helmholtz Resonance which is actually useful in calculating and assuming length and frequency of the pressure wave formed.

CHAPTER 3: METHODOLOGY

The project, as we can conclude from the earlier sections pertains to the study of parameters effecting the volumetric efficiency of a ***naturally aspirated*** engine, the evolution of these parameters throughout the cycle and an attempt to incorporate Ram effect, i.e. the increase in volumetric efficiency by accurately timing the high-pressure wave to hit the inlet valve. This effect alludes at the "ramming" of air inside the cylinder, similar to forced induction, however the major difference lies in the "pulsation" of air inside manifold which, in multicylinder, forced induction engines is not the case. It is to be, however, noted that the increase in volumetric efficiency is limited to a specific RPM range, in the case of Ram effect. For the rest of the RPM range, the air does not resonate, and the "ramming" effect is not achieved. Hence, when the intake manifold opens, the compressed air, formed due to stagnation of air on the closed valve wall, does not reside over the inlet valve, as it opens for the next cycle and the effect is lost.

This is also to be noted that such a compression wave is generated after a rarefaction wave, created by sudden suction of air from the intake manifold, gets reflected, but this does not fall within the purview of this project.

An important aspect of the project is to study the physical phenomena taking place inside an engine and developing appreciable understanding of factors chiefly effecting the volumetric efficiency, and the second step is to optimize these parameters to achieve maximum volumetric efficiency, with justified cost. To practically achieve this, engineers generally rely on dynamometers and instrumentation to study the curves of power and torque, varying these parameters and tune the engine accordingly. However, the cost to carry out such operations is exorbitant especially sans experience. It is to be noted, these parameters usually are:

i. **Valve Timing:**

   This is the time of the cycle, **at** which the valves (intake and exhaust) open. This effects the efficiency, since pressures on both ends of each valve varies throughout the cycle, e.g., the pressure difference across exhaust valve will be higher if exhaust valve timing is advanced i.e., exhaust valves open earlier. This has been discussed later in the results section.

ii. Valve Lift:

Valve lift is the distance the valves cover as they are pushed by the cam/pushrod from their **seat** i.e., closed position, to the point of maximum opening. This effects the volumetric efficiency, as the area through which the flow occurs increases, thereby increasing the mass flow rate by the formula:

$$\dot{m} = \rho * A * V$$

Where $\dot{m}$	=	mass flow rate	[kg/s]
ρ	=	density	[kg/m^3]
A	=	Cross-sectional Area	[m^2]
V	=	Velocity	[m/s]

Thus, the volumetric efficiency increases.

iii. Valve Duration:

This is the time duration for which the valves remain open. This greatly effects the volumetric efficiency as this in combination with Valve timing, dictate the scavenging effect, i.e., the fresh charge pushing the burnt gases out of the clearance volume during the overlap (the degrees of rotation for which both the intake and exhaust valves remain open). There is an optimum valve duration for a particular RPM range. If it is less than optimum, the pressure gradient is not completely utilized and if beyond optimum, due to compressibility of air, it will start flowing in the reverse direction. The Valve duration of

Peugeot DW10 is:

Table 1: Valve Duration Represented in Crank Degree Rotation

Inlet valve	Opens 19^0 *bTDC*	Closes 49^0 *aBDC*	Total Degrees = 248^0
Exhaust Valves	Opens 62^0 *bBDC*	Closes 28^0 *aTDC*	Total Degrees = 270^0
Overlap	Exhaust closes 28^0 *aTDC*	Inlet Opens 19^0 *bTDC*	Total Overlap = 47^0

It is to be however noted, a clear picture of the understanding developed has been provided in the results and discussion section of the report however, any variation in the three afore mentioned parameters and its effect has not been quantified, as this is a project of its own.

iv. Intake Runner Diameter:

This is a factor is similar to lift, as this does dictate the amount of air that can flow into the cylinder without restriction. This dictates the cross-sectional area available to the air to flow from atmospheric conditions to the cylinder. The effect of this parameter has been explicitly studied and quantifiable results are provided in the results and discussions section.

v. Intake Runner Length:

This Parameter dictates the resonance of air inside the manifold. The effect of length falls within the scope of this project and is studied in a quantifiable manner. For a detailed discussion on the theory of this topic refer to section 2.6.

vi. Forced Induction Mechanisms:

These techniques refer to an entirely different domain of turbomachinery and are well beyond the scope of this project. Forced induction mechanisms generally include Turbo-exhaust-charging (i.e., turbine run through high-pressure exhaust) or Turbo-super-charging (i.e., turbine run mechanically).

3.1 Thermodynamics of a Diesel Cycle:

Diesel Cycle as it is known is a compression ignition (CI) cycle and relies on the heat of the compressed air inside the cylinder for ignition. Here, the concern lies with the duration of cycle where the fresh charge flows through inlet valve and where burnt gases flow through the exhaust valve. Rest of the cycle is however, studied as the *initial conditions* for the flows had to be acquired through a complete engine cycle model. PV (pressure-volume) diagram of a common diesel cycle is attached below:

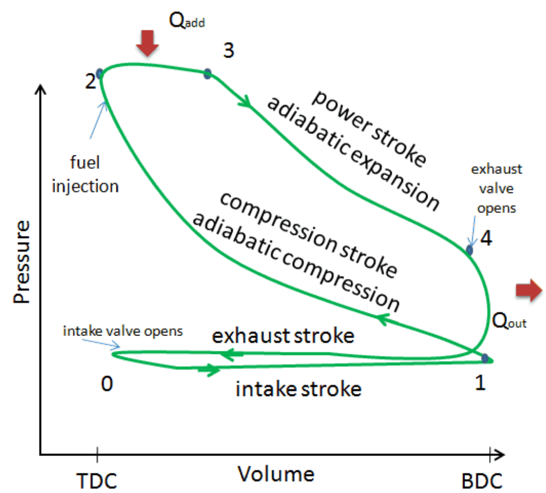

Figure 7 Practical Diesel Cycle [8]

0 – 1 = Intake stroke = Fresh charge of air comes in

1 – 2 = Compression Stroke = Air is compressed as the piston moves up (ideally adiabatically)

2 – 3 = Fuel Injection = Fuel is injected in a controlled fashion and ignites due to the compressed air being hot (ideally isobaric)

3 – 4 = Power Stroke = Energy is extracted from the combustion of fuel as hot gases try to expand moving the piston down (ideally adiabatic)

4 – 0 = Exhaust stroke = Burnt gases flow out

3.2 Adiabatic process:

Adiabatic process is defined as a process where there is no heat or mass transfer to and from the system. Hence from second law of thermodynamics:

Equation 1

$$\delta U = \delta Q - \delta W$$

If there is no heat transfer, the heat added goes to zero. Hence equation 1 reduces to:

$$\delta U = -\delta W$$

Using Ideal gas equation:

$$PV = nRT$$

Where

P	=	Pressure	[Pa]
V	=	Volume	[m^3]
n/m	=	number of moles/mass	[mol/kg]
R	=	Universal Gas Constant	[J/kg.K/J/mol.K]
T	=	Temperature	[K]

And (for and ideal gas):

$$\delta U = mC_v\delta T$$

We can conclude:

$$PV^\gamma = constant$$

This is the adiabatic equation which governs an adiabatic process from one state to another and is extensively used in the project to ***define every subsequent state.*** Another notable difference is between the two types of adiabatic processes namely:

3.2.1 Reversible Adiabatic (Isentropic):

A process in which losses and irreversibility such as turbulence energy losses, frictional losses, mixing of streams, sudden expansion (shockwaves) are ignored and all equations developed assume 100% efficiency of the system under consideration. The equations are:

$$\frac{T_2}{T_1} = \left(\frac{P_2}{P_1}\right)^{\gamma-1/\gamma} = \left(\frac{V_1}{V_2}\right)^{\gamma-1}$$

3.2.2 Irreversible Adiabatic:

In such a flow, irreversibility is not negligible and not ignored, hence it leads to a term called "isentropic efficiency" represented by "$\eta_{isentropic}$" which indicates the percentage ability of the system to conform to isentropic standards i.e. $S_{gen} = 0$. This shows up on the TS diagram as curve/bent line that leads from a lower entropy level to some higher entropy level.

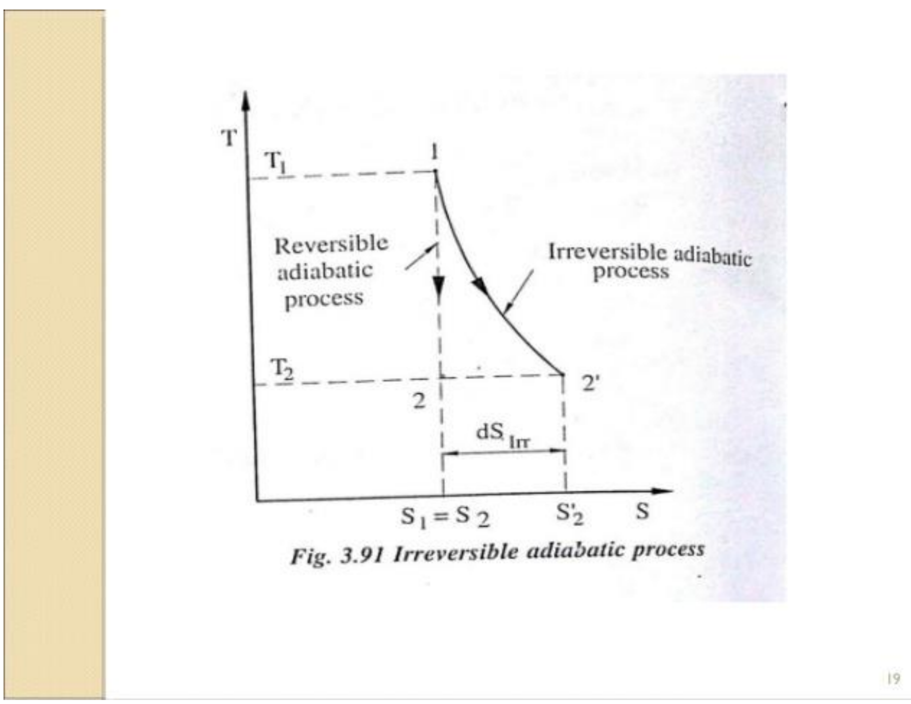

Figure 8 isentropic vs irreversible adiabatic expansion process

It is to be noted, the project relies on isentropic flow equations.

As it is noticeable, the system under consideration is highly dynamic and involves flow of mass from one reservoir to another at every step. This phenomenon has been modelled using isentropic flow equations (3.2.1) and the ideal gas equation (3.2).

The assumption involved in this derivation is "The mass that travels during the discretized time step is negligible, hence the isentropic relationship holds in good approximation". This is then to be noted, the end result of this project applies at a certain discretization level of time, where the mass travelling between reservoirs can be assumed to be negligible.

The final form of equations used has been provided in section 3.4.2.

3.3 Available Approaches:

3.3.1 Computational Fluid Dynamics (CFD):

CFD is probably the latest most used method of solving such complex flows. CFD is the numerical solution of Navier-Stokes's equations, the crux of fluid mechanics that currently do not enjoy the privilege of an analytical solution. It uses numerical methods to convert partial differential equations, ***The continuity, three/two/one (depending on the dimensions under consideration) momentum equations, and an energy equation (usage is problem specific),*** to algebraic equations, that are then solved numerically in matrix formation. It does come with a few limitations but can be appreciably accurate depending on the dexterity of the user. This approach could have been used for the following reasons:

1. It is easy to model and with the availability of packages like ANSYS Fluent, COMSOL Multiphysics etc., much of the arduous work is performed by the computer.
2. It is accurate and several different phenomena can be captured with merely a click.

However, this approach was not used for the following reasons:

1. For such a flow problem, where boundary conditions vary continuously, Volume changes, and mesh must either be regenerated or reshaped, changing the aspect ratio, high computational power is required, and the cost is beyond justifiable.
2. The process of reaching a solution is slow and cannot be used to study the effects of varying parameters, as time required is beyond justifiable.
3. The relationship between parameters or between the volumetric efficiency and parameters of interest cannot be explicitly stated and repetitive simulations with minute changes, although incorporating several or every important phenomenon, is not justified by the afore mentioned point.
4. Absence of development of any understanding of the phenomena.

3.3.2 Experimental study:

Experimental setup is known to be the corroboration for any engineering simulation. This reflects the real-world happenings and is carried out at an exorbitant cost usually for the purpose of verification of simulation setups. For a study of sorts of this project, experimental setup could not be used as:

1. It requires experienced workforce
2. It is extremely expensive
3. It does not help understand the continuum of parameters in a quantifiable manner.

Hence the experimental approach was not used.

3.3.3 Quasi-analytical:

The flow of air that is being modelled in the project to work out the volumetric efficiency is highly dynamic, transient, compressible, and viscid flow. Analytical models to model transient flows are not yet existent. Making assumptions and appropriately simplifying the physics can lead to satisfactory results, for a very small time-step and program the computer to handle all defined time-steps in progression.

This is the approach used here, as:

1. It is much less resource intensive
2. Helps develop the understanding of factors effecting volumetric efficiency in a much more comprehensible manner.

The process of modelling the flow, quasi-analytically involves:

1. Applying/enforcing the correct/appropriate assumptions and decide on which equations to use for a particular time-step.
2. Discretize time and/or space if necessary. Smaller the step size, greater the accuracy, but involves a greater number of calculations.
3. Looping the solution and making sure, the output of one step is being used as an input for the next step or as the physics dictates.

In this case it is to be noted:

3.3.3.1 Set up:

The setup is simple. The inlet and exhaust manifold ends opening into the atmosphere are two nozzle sections. The two pair of valves (intake and exhaust) are also assumed as two converging-diverging nozzles, with variable throat area, installed between three reservoirs (the intake manifold, the cylinder, and the exhaust manifold respectively).

3.3.3.2 Assumptions:

- The flow only happens through the nozzle, the fluid is assumed stagnant in the reservoirs (this allows the flow between two stagnation properties and momentum effects in the flow direction can be accounted for).
- The flow through the nozzles is compressible
- The flow is assumed to be isentropic i.e. no irreversibility exists within the nozzle section 3.4.2.

- The equations for an open system are used to describe the subsequent states of the reservoir (equations in section
- Fluid is an ideal gas

3.3.3.3 Discretization:

The problem has been discretized in time dimension based on degrees of crank shaft. It starts at 341^0 i.e., the point at which the intake valve opens. That is to say, 341^0 has been indexed as the 1st Time-step.

Each time-step in this format of discretization represents 1^0 of crankshaft rotation and hence goes all the way to 720 time-steps i.e., $341^0+720^0 = 1061^0$.

Initial condition has been provided as atmospheric and complete cycle is repeated to attain a stabilized engine cycle.

3.4 Module 1:

Module 1 encompasses everything related to modelling of the engine cycle and studying the evolution of:

1) Mass flow rate through the 4 nozzle sections.
2) Volume of the cylinder (2nd reservoir) at each step.
3) Mass in the 3 reservoirs at each step.
4) Temperature of fluid in each reservoir.
5) Pressure in each reservoir.

The loop exists as:

1. Volume of the cylinder at each step is calculated using a for loop, and equation for volume of cylinder given in section 3.4.2.
2. The initial pressure on both sides of each nozzle section is put into a function that uses equations given in section 3.4.2, to calculate:

$T_{throat} > V_{throat} > P_{throat} > \rho_{throat} >$ mass_flow_rate (Respectively)

3. The mass flow rate is then used to calculate the new mass inside each reservoir using mass that has flown within the stipulated time (mfr * time). The time for rotation of crankshaft through 1^0 is calculated using the RPMs by the equation:

$$Time\ taken\ for\ a\ degree\ rotation\ of\ crankshaft = \frac{1}{6 * N}$$

Where N = RPMs

At 2000 RPMs the equation returns the time for each step = 8.3333e-5 [s]

4. The new mass is then used to calculate new temperature using equations listed in section 3.4.2.
5. The new pressure is calculated either using an approach same as that of temperature or using the ideal gas equation [section 3.2].
6. The new pressures are put into the function and the process repeats.

It is to be noted that all calculations have been performed in MATLAB R2019b.

3.4.1 Physics of Nozzle sections with variable area:

3.4.1.1 Experimental Data:

Experimental data for Peugeot DW10 was acquired with the help of the Supervisor Dr. Sami-ur-Rahman Shah. The data comes from experimentation carried out as a part of a greater project in France.

The data includes:

3.4.1.1.1 The intake and exhaust profiles (Lift and phasing):

The experimental measurement of lift of the valves was provided. This is usually done using a dial gage and the crankshaft is accurately rotated through two complete rotations. This results in 720^0 rotation of crankshaft which translates to 1 complete cycle, i.e., one complete rotation of camshafts. The dial gauge installed and calibrated measures the movement of the valves with high precision. The data is then interpolated to get lift for any crank angle. The lift indicates the formation of two areas, ***Valve flow area*** which is derived using the diameter of valve. This is the area available parallel to the flow direction and the shank of the valve. The flow direction will then be rotated by the valve geometry. The area available to the flow as it exits the valve geometry, is called ***Valve Curtain area***. This involves the circumference of the valve and the lift. The formulae for the two areas are provided below:

$$Valve\ flow\ area = \frac{\pi}{4}(Diameter\ of\ Valve)^2$$

$$Valve\ Curtain\ Area = \pi * diameter\ of\ valve * Instantanous\ Valve\ lift$$

3.4.1.1.2 The intake and exhaust effective flow areas:

The intricacy involved in assigning the flow an effective area, at such high speeds is evident. It quickly escalates into the regime of complex fluid dynamics problems, where losses ought to be approximated at each stage given the two flow areas.

Hence, a simpler approach to experimentally measure the ***effective flow area*** *is generally used where effectiveness of the available area is placed under the umbrella of* C_d *i.e., the discharge coefficient.* C_d *is multiplied with the Valve flow area to calculate the "effective flow area".*

$$Effective\ flow\ area = C_d * \frac{\pi}{4} * (Diameter\ of\ valve)^2$$

Table 2: Coefficients of Discharge of Intake

Lift(intake)	Forward Cd	Reverse Cd
0	0	0
0.036206	0.100472	0.100472
0.072411	0.170643	0.170643
0.108617	0.258356	0.258356
0.144823	0.341285	0.341285
0.181028	0.416241	0.416241
0.217234	0.484817	0.484817
0.25344	0.532661	0.532661
0.289645	0.556582	0.556582
0.325851	0.574125	0.574125
0.362056	0.593263	0.593263
0.044053	0.121902	0.144985
0.088106	0.267247	0.298892
0.132159	0.38915	0.434954
0.176211	0.489953	0.571017
0.220264	0.595446	0.689235
0.264317	0.670463	0.771765
0.30837	0.69625	0.816375
0.352423	0.703282	0.831989
0.396476	0.705627	0.838681
0.440529	0.715004	0.843142

Calculation of C_d is purely experimental. The factor is calculated by equating the experimental and theoretical results and balancing the equation. This is done at a few key points during the valve duration and rest is interpolated. **Interpolation in this project has been performed using MATLAB's built-in spline interpolation method.**

Valve lift and effective flow area graphs

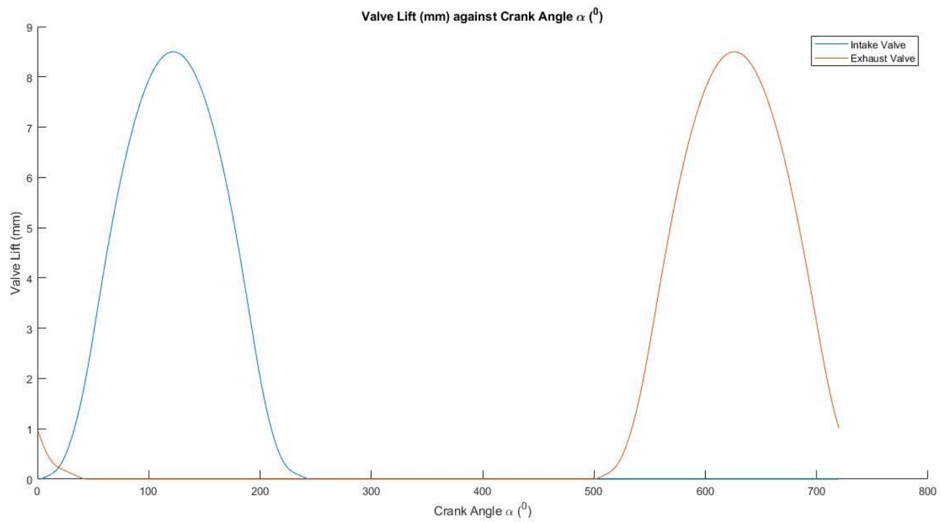

Figure 9: Valve lift (mm)

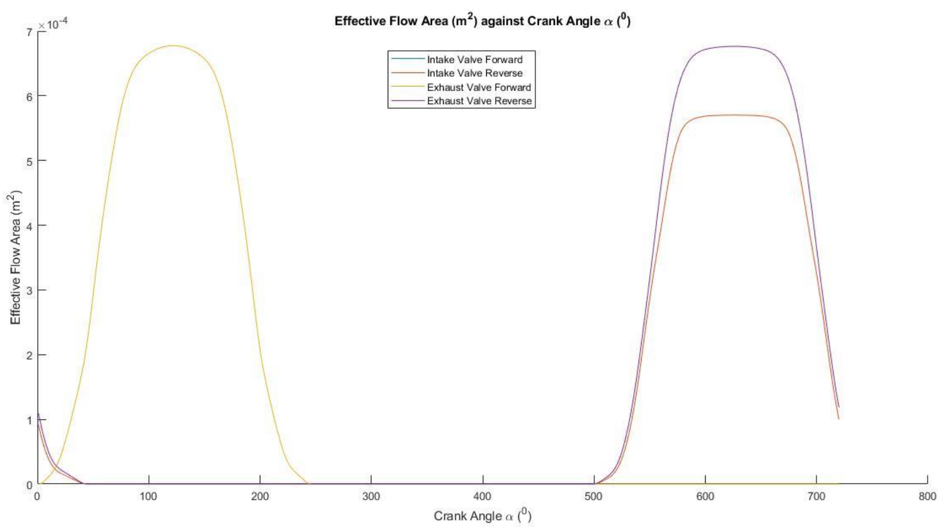

Figure 10: Effective Flow Area (m^2)

3.4.1.2 Analytical Solution:

The analytical analysis revolves around the assumptions stated in section 3.3.3. To start we know, flow only takes place if a pressure gradient exists across the (Converging) nozzle. The flow occurs due to the ability of the fluid to expand into a low-pressure region under its own internal energy by converting the pressure head (P in [Pa])into dynamic head ($\rho V^2/2$ in [Pa]) and vice versa. This is better understandable in terms of temperature which is a direct representative of internal energy.

It is to be clearly understood, the flow here is assumed to be isentropic (Reversible Adiabatic) which indicates the change in enthalpy of the system (by the 1st law of thermodynamics) is zero (no energy is added to or extracted from the system).

This shows,

$$h_0 = h + \frac{V^2}{2}$$

For ideal gas, the internal energy is a function of temperature only, hence:

$$T_0 = T + \frac{V^2}{2C_p}$$

Noting that:

$$C_p = \frac{\gamma * R}{\gamma - 1}$$

And:

$$c^2 = \gamma RT$$

And:

$$Ma = v/c$$

Where v = relative speed of fluid an observer

C = speed of sound in the medium for given conditions

We can then derive following equations for our usage:

$$\frac{T_0}{T} = 1 + \left(\frac{\gamma - 1}{2}\right) Ma^2$$

$$\frac{P_0}{P} = \left(1 + \left(\frac{\gamma - 1}{2}\right) Ma^2\right)^{\frac{\gamma}{\gamma - 1}}$$

The density is then calculated using the ideal gas equation.

The nozzle can undergo, in broader terms, two types of flows:

- Choked Flow
- Unchoked Flow

3.4.1.2.1 Choking of flow:

An interesting phenomenon occurs in flow through nozzles. The flow through nozzles is **due to molecules on one side having higher energy than molecules on the other side. This allows molecules with higher energy to "expand".** Another intertwined important concept is that of speed of sound. This is **the speed at which a disturbance will travel inside a medium. This as observed in earlier is a function of temperature,** i.e., the speed at which one molecule can strike and transfer its additional energy to the next molecule.

At a certain back pressure value, the flow through the nozzle happens as such, that the molecules no longer can achieve higher speeds, as they are expanding as "freely" as possible, this speed is the speed of sound. This is called choking of the nozzle. This means the speeds at the throat (the smallest cross-sectional area along the nozzle length) is the speed of sound i.e., Ma = 1. The thermodynamic properties at this state are designated with a '' and are called critical properties. (This is not to be confused with critical thermodynamic state which pertains to the phase change event of substances).* ***It is to be noted, a 'standing normal shockwave' does form as this undisturbed flow slams into standing flow in the path and dramatically changes its thermodynamic properties. This is a highly irreversible phenomenon.*** *(Such irreversibility has not been considered in the valve as it seldom chokes. Avoiding choking of valve is one of the greatest considerations in engine design).*

Hence inserting Ma = 1 in equations given above, we get:

$$\frac{T^*}{T_0} = \frac{2}{\gamma + 1}$$

$$\frac{P^*}{P_0} = \left(\frac{2}{\gamma + 1}\right)^{\frac{\gamma}{\gamma - 1}}$$

These equations are used for conditions where the flow is choked (Ma = 1 at throat). The condition can be checked using the following manipulation:

$$P_{cylinder} \leq P_{manifold} * \left(\frac{2}{\gamma + 1}\right)^{\frac{\gamma}{\gamma - 1}}$$

Note the pressures switch places when the flow changes direction

If the condition is satisfied, the flow is choked. It is to be noted, the calculation of mass flow rate under this condition is ***INDEPENDENT*** of pressure gradient across the nozzle.

The word "choking" comes from the fact that this is the highest mass flow rate value that can be achieved for the given inlet condition.

3.4.1.2.2 Calculation of mass flow rate:

This mass flow rate through a cross-sectional area 'A' at some density 'ρ' and with certain velocity 'V', ***under any flow condition,*** is given by:

$$\dot{m} = \rho * V * A$$

All the earlier calculations have been performed to calculate the mass flow rate of air through the valve modelled as a nozzle section, to be able to calculate the new masses in each reservoir and hence new thermodynamic properties.

3.4.1.2.2.1 Mass flow rate calculation for unchoked nozzle:

If the nozzle is unchoked, this is to be understood, the flow is assumed to reach the exit pressure value at the exit plane of the nozzle. i.e., $P_{exit} = P_{throat}$.

1. This can be used to calculate the Mach number at the exit plane using a form of the equation provided in section 3.4.1.2 obtained through basic algebraic manipulation, provided below:

$$Ma = sqrt\left(\left(\left(\frac{P_{in}}{P_{ex}}\right)^{\frac{\gamma-1}{\gamma}} - 1\right) * \left(\frac{2}{\gamma - 1}\right)\right)$$

2. The temperature at throat is then calculated:

$$T_{throat} = \frac{T_{in}}{1 + \left(\frac{\gamma - 1}{2}\right) Ma^2}$$

3. The temperature at the throat is then used to calculate the speed of sound or ‘c’ at the throat using equation provided in section 3.4.1.2.

4. The results are then used to calculate the speed of flow in [m/s] using the equation provided in section 3.4.1.2.

5. The density can be calculated in this case using the ideal gas equation [section 3.2]. The pressure and Temperature values used are that of T_{throat} and P_{exit} (due to the assumption of flow achieving the exit pressure at the exit plane).

6. The throat area is calculated using the interpolated experimental data for effective flow area [section 3.4.1.1.2].

7. The mass flow rate is then calculated using equation in section [3.4.1.2.2].

3.4.1.2.2.2 Mass flow rate calculation for choked nozzle:

If the nozzle is choked, this is to be understood, the flow has reached the maximum mass flow rate value at the exit plane of the nozzle. i.e., $\dot{m}_{throat} = \dot{m}_{critical}$. The flow is now independent of the pressure gradient across the nozzle section.

1. The temperature at throat is then calculated using the equation provided in section 3.4.1.2.1 - where choking of flow has been discussed.

2. The temperature at the throat is then used to calculate the speed of sound or ‘c’ at the throat using equation provided in section 3.4.1.2.

3. The flow at the throat is then equal to ‘c’ as during choking, as discussed earlier, Ma = 1.

4. The density can be calculated in this case using the ideal gas equation [section 3.2]. The pressure and Temperature values used are that of T_{throat} and P_{throat} calculated using equations provided in [section 3.4.1.2.1] - where choking of flow has been discussed.

5. The throat area is calculated using the interpolated experimental data for effective flow area [section 3.4.1.1.2].

6. The mass flow rate is then calculated using equation in section [3.4.1.2.2].

3.4.2 Stepwise approach for simulation of complete Diesel engine cycle with equations:

3.4.2.1 The crude design:

The crudest form of the model includes only the intake manifold and the cylinder as two reservoirs and only the intake valve and the manifold intake area have been modelled as converging nozzle section of constant area, i.e., variable area has currently not been introduced. The steps for modelling this flow are given below:

3.4.2.1.1 Functions:

1. A function named ***“Keekay”*** was introduced. This is an empirical relationship proposed in 1936 by ‘Keenan and Keyes’ and the model is known as ‘Keekay C_p Model’. This model/empirical relationship provides considerably accurate C_p (specific heat capacity at constant pressure) values for an air-fuel mixture. *The formula takes in the inlet temperature and fuel equivalence ratio as its arguments and puts out a value of C_p. Any of the 3 empirical relationships is used depending on the value range of the input arguments.* The relationships are given below:

IF Temperature > 600

$$C_p = \left(166.3 + \frac{24.5}{\phi}\right) * \left(\log\left(T - 70 - \frac{120}{\phi}\right)\right)$$

IF Temperature <= 600 & Φ < 8

$$C_p = (975.5 + 0.28 * \phi) - \left((11.92 + 0.06 * \phi) * \log(\phi)\right)$$

Notice the temperature is now independent of temperature.

IF Temperature <= 600 & Φ >= 8

$$C_p = 1000 + 2.85 * \exp\left(\frac{T - 273.16}{100 * 0.88}\right)$$

Note the temperature for input argument is provided in [K] and equivalence ratio 'Φ' is defined as:

$$\phi = \frac{Current\ or\ original\ AFR}{Stoichiometric\ AFR}$$

2. Next a function named ***"Mass_flow"*** was introduced. This function takes in (P_{in}, P_{ex}, T_{in}, throat_area, R (universal gas constant approx. 286.7 [kJ/(kg.K)] for air), AFR (air-fuel ratio)) as input arguments and returns a value of mass flow rate. This is to be noted, the value does not represent the direction of flow. This is then catered for by using *'if, elseif and else conditional statements'* within the calculation code.

The mass flow rate is calculated using stepwise approach explained in [section 3.4.1.2.2].

3.4.2.1.2 Main code (Initializations & Calculations):

3.4.2.1.2.1 Initialization:

3. Time for the intake stroke was discretized into 500 steps. (2000/720) * 180. Matrices of equivalent lengths are initialized for conservation of resource (pre-allocation). Engine specifications (Bore = 85 mm, Stroke = 88 mm, Conrod length = 152 mm, etc.) and other necessary parameters including manifold length, diameter (initialized as *sqrt (2) * Diameter of each valve (4 valves per cylinder)*) and atmospheric and initial cylinder conditions are also introduced.

4. The Volume of the cylinder is then calculated for each step using the following equation under a 'for loop':

$$\mathrm{V_{cylinder}} = \mathrm{V_{clearance}} + \left(\left(\frac{\pi}{4}\right) * (\mathrm{Bore}^2) * \mathrm{Crank\ throw} * \left(1 - \cos(\mathrm{Crank\ Angle\ at\ step}) + \mathrm{n} - \mathrm{sqrt}\left((\mathrm{n}^2) - \left(\sin(\mathrm{Crank\ Angle\ at\ step})\right)^2\right)\right)\right)$$

Where V $_{clearance}$ is calculated by:

$$V_{clearance} = \frac{\frac{\pi}{4} * Bore^2 * Stroke}{Compression\ ratio - 1}$$

Crank throw (Crank pin length) is given by:

$$Crank\ throw = \frac{Stroke}{2}$$

‘n’ or the ratio of conrod length to crank throw is:

$$n = \frac{Conrod\ length}{Crank\ throw}$$

And the Compression ratio for Peugeot DW10 is ***20***.

5. The first values of thermodynamic properties of manifold are initialized with atmospheric conditions, these being (subject to variation between 0.922 – 1.01325 and 298.16 – 303.16 respectively):

$P_{atmospheric}$	=	101.325	[kPa]
$T_{atmospheric}$	=	298.16	[K]

3.4.2.1.2.2 Calculation:

6. A while loop is run with a condition:

$$abs\left(\frac{\left(P_{manifold\ (last)} - P_{manifold\ (initial)}\right)}{P_{manifold\ (last)}}\right) \geq 0.05$$

   a. Under which a for loop from:

$$i = 1{:}\,180$$

      i. Under which ***‘if, elseif and else conditionals’*** run. These conditionals **compare** the value of **$P_{manifold}$ and $P_{cylinder}$** and **feed input arguments to the mass flow rate function accordingly**. Hence, they also assign the flow, its correct direction. A *sample* of using the function (flow from atmosphere to the manifold) in a code is:

$$M_{f_{mat}}(i,1) = Mass\_flow(P_{atm}, P_{mat}(i,1), T_{atm}, Manifold\ orifice\ area, R, AFR)$$

And (flow from manifold to the atmosphere) is:

$$M_{f_{mat}}(i,1) = -Mass\_flow(P_{mat}(i,1), P_{atm}, T_{atm}, Manifold\ orifice\ area, R, AFR)$$

b. Another pressure and temperature matrix captures the evolution of pressure and temperature as the while loop runs.

   i. The next step is to calculate the new mass in the intake manifold and the cylinder. This is done by multiplying the mass flow rate with the time-step and the answer is either added or subtracted to the previous mass held in each reservoir, depending on the direction of flow.

$$\mathrm{M}_{new} = \mathrm{M}_{\mathrm{mat}} + \left(\left(\mathrm{M}_{\mathrm{f}_{\text{through area 1}}} - \mathrm{M}_{\mathrm{f}_{\text{through area 2}}}\right) * \text{Time step}\right)$$

   ii. The new temperature, of each reservoir, is then calculated using the relationship derived below:

We know for an ideal gas

$$PV = mRT$$

For two different states:

$$\frac{P_1V_1}{P_2V_2} = \frac{m_1T_1}{m_2T_2}$$

Assuming the mass that travels during the step time is negligible the isentropic relationship holds:

$$\frac{P_1}{P_2} = \left(\frac{T_1}{T_2}\right)^{\left(\frac{\gamma}{\gamma-1}\right)}$$

Then the relationship between T_1 and T_2 becomes:

$$T_2 = T_1 * \left(\frac{V_2}{V_1} * \frac{m_1}{m_2}\right)^{\gamma-1}$$

The pressure can then be calculated using either the ideal gas equation or a similar approach as that used in temperature calculation. The use of ideal gas equation is recommended to minimize error.

iii. The calculated values are then used to for the subsequent calculation.

c. The Pressure in the manifold after 500^{th} time steps then overwrites the 1^{st} manifold pressure value. The same is done with the temperature value. The Cylinder pressure and temperature however are not changed but are repeated over and over through the cycles.

3.4.2.1 The complete cycle model:

The above model once tested was then extended to take complete shape. Volumetric efficiency directly depends on the mass flow rate through the intake valve. According the current Compressible, Steady-state model, the mass flow rate can either be majorly affected by the flow area (which is currently assumed to be constant) or the velocity of flow through the area available. The velocity of flow is directly dependent the pressure gradient until choking and independently on temperature once the flow gets choked, but a compromise is stipulated on density. Hence, to acquire a much clearer understanding of effects of manifold's and engine's dimensions, RPMs, valve lift profile, valve phasing and duration, injection timing, atmospheric conditions etc. on volumetric efficiency a complete engine cycle was required to be modelled.

3.4.2.1.1 Introducing Valve lift profile:

The valve lift profile was acquired through experimental means [section 3.4.1.1.2]. The phasing was also provided. 279 values were recorded at with varying interval length but approximately 1^0. The data was loaded into MATLAB however, the Crank Angle matrix had to be adjusted to start the cycle neither at top nor at bottom dead center, but at 341^0 which indicates the commencement of intake event.

Hence the crank angle starts at 341^0 and goes up to $341 + 720 = 1061^0$. This can be indexed as 0^0 being the starting point of measurement, however, it is to be noted, the calculations of changing volume with respect to the crank angle assumes the crank angle to be zero at TDC. This then needs to be modified and equation adjusted to incorporate this effect, or the crank angle matrix can simply be started at 341.

The next step is to calculate the effective flow area. The experimental data set available identifies C_d or the coefficient of discharge as a function of the ratio of the lift and diameter of the valve. This has been experimentally determined at 11 ratio values, and the value of C_d against each lift/diameter is provided in a table. This data is then used to interpolate values of C_d for each degree of crankshaft rotation. The obtained value is multiplied by the Valve flow area to get the effective flow area available [section 3.4.1.1.2].

3.4.2.1.2 Introducing Compression and Power stroke:

The compression and power strokes are where the engine produces net power or extracts energy from fuel and delivers it to the crankshaft. This is required to provide the thermodynamic state of cylinder at the time of exhaust valve opening (EVO) and intake valve opening (IVO). The EVC and IVC directly affect the processes inside the cylinder.

It is to be noted all three reservoirs i.e. intake manifold, cylinder and exhaust manifold are initialized with atmospheric conditions.

The compression stroke can be modelled as an isentropic process [section 3.2.1] and each subsequent state can be completely defined as volume is known at both points. Similarly, power stroke is modelled as isentropic expansion. It is without a doubt that heat is actually added to the system and the system is far from isentropic, however, the heat addition process was successfully incorporated using a function called ***"Wiebe's heat release"*** function.

3.4.2.1.2.1 Wiebe's heat release function:

Wiebe's functions to model heat release into the engine during the combustion, have long been used for approximating pressure and temperature trends in the engine.

This function predicts with considerable accuracy, the trend of fraction of fuel mass burnt at each degree. This can then be translated into the addition of heat, if the fuel's energy density is known.

There are majorly 3 types of Wiebe's functions currently being used in literature 1^{st}, 2^{nd}, and 3^{rd} order, with the 2^{nd} order being the best for diesel engines, as it considers, ignition delay and premixed combustion. This keeps the exponential rise in pressure, observed due to use of 1^{st} order Wiebe function, as ignition delay is not considered, in check. However, due to lack of some required experimental data 1^{st} order Wiebe's heat release function was used. A compromise can be made here is the maximum pressures inside cylinder are of no concern here during the compression and power stroke, however, the trends brings values of pressures at EVO and IVO in agreement with the experimental data. Wiebe's 1^{st} order heat release function is generally written as:

$$\mathrm{Wiebe} = 1 - \exp\left(-\mathrm{a} * \left(\frac{\text{Inst. Crank Angle} - \text{Inject start in degrees}}{\text{Total injection duration in degrees}}\right)^{n+1}\right)$$

Where **a** and **n** are constants and are usually determined experimentally for most accurate results, however, a value of 5 and 3 has mostly yielded agreeable results. Here, however, a value of **4** and **1** was used respectively to bring the curves into agreeable dimensions. The two peaks, first at TDC, and 2^{nd} due to heat release can be observed.

3.4.2.1.2.2 Hohenberg's heat loss model:

Hohenberg in 1979 proposed a model to study the heat loss through the walls of an engine's cylinder. This model was used in the study under elucidation, to calculate the heat loss. The model has shown to not affect the pressure and temperature values considerably due to the comparative agility of the other events like combustion, volume change etc.

The persistence of deviation in the peak pressure value by 5 – 10 bars is evidence, the mode, along with the 1^{st} order Wiebe's heat addition function, contributes to the deviation, *however this level of proximity is highly acceptable as this amount of deviation is not of great concern in studying the breathability of an engine.*

The model equations are given below:

$$\begin{aligned}\mathrm{Pos_{piston}} = \mathrm{Inst.\,Piston\ Position} \\ &= \mathrm{Crank\ throw} \\ &* \Big(1 - \cos(\mathrm{Inst.\,Crank\ Angle}) + \mathrm{n} \\ &- \mathrm{sqrt}\big((\mathrm{n}^2) - (\sin(\mathrm{Inst.\,Crank\ Angle})^2)\big)\Big)\end{aligned}$$

$$\mathrm{A_{surf}} = \mathrm{Inst.\,Surface\ Area} = (\mathrm{Inst.\,Piston\ Position} * \pi * \mathrm{Bore}) + \left(\left(\frac{\pi}{2}\right) * \mathrm{Bore}^2\right)$$

$$\begin{aligned}\mathrm{h_{loss}} = \mathrm{Loss\ coefficeint} \\ &= 130 * (\mathrm{Inst.\,Cylinder\ Volume})^{-0.06} * (\mathrm{Cylinder\ pressure\ [bar]})^{0.8} \\ &* (\mathrm{Cylinder\ Temperature})^{-0.4} * (\mathrm{Average\ Piston\ Speed} + 1.4)^{0.8}\end{aligned}$$

Where Average Piston Speed is given by:

$$V_{avg} = \frac{Stroke * RPM}{30}$$

$$\begin{aligned}\mathrm{Q_{loss}} = \mathrm{Inst.\,Heat\ Loss} \\ &= \big(\mathrm{h_{loss}} * \mathrm{A_{surf}} * (Cylidner\ Temperature - 400)\big) * \mathrm{Step\ time}\end{aligned}$$

It is to be noted that model can only be applied with basic temperature and pressure values. The resulting values then overwrite the previous values.

3.4.2.1.3 Introducing Exhaust stroke:

This model is very similar to the intake stroke model, as exactly same type of flow (isentropic compressible quasi steady with effective flow area) is encountered here except that the direction of the flow is assumed to be positive as it happens from cylinder to the exhaust manifold and from manifold to the atmosphere.

As a simple illustration of this model following figure is provided with flow being positive from left to right:

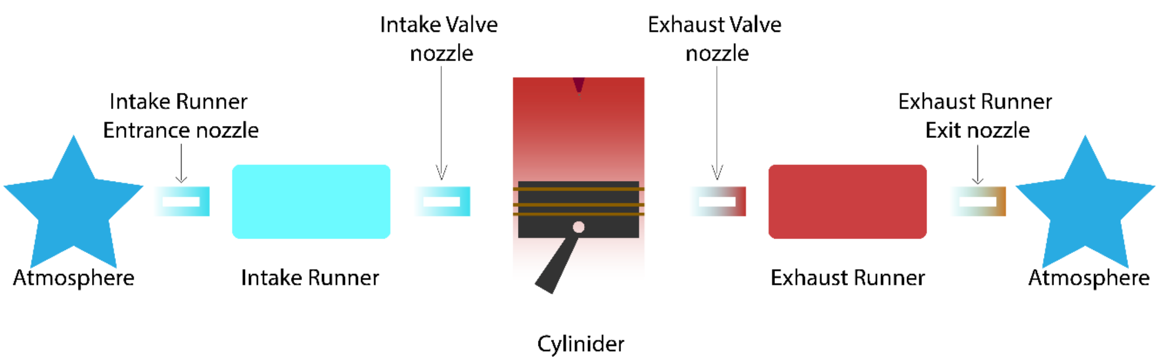

Figure 11: An overview to the general flow model approach

3.4.2.1.4 Other required alterations:

It is to be noted, the model has been broken down into 4 parts:

1. The Overlap region - 1^{st} – 47^{th} step
2. The Intake event - 47^{th} – 249^{th} step
3. The comp/power stroke - 249^{th} – 497^{th} step
4. The exhaust event - 497^{th} – 720^{th} step

3.4.2.1.4.1 Mixing of air at different temperatures:

As the intake valve opens at the 1^{st} step, the temperature difference between the previously charge inside the cylinder and the new charge coming in causes the temperature to fall.

This is important to model to stabilize the cycles. Otherwise, the temperature will go on increasing after each cycle and the volumetric efficiency will keep falling.

The equation for this is the energy balance on the mixing chamber which is the cylinder of $V_{instantaneous}$ here:

$$m_t h_t = m_1 h_1 + m_2 h_2$$

For an ideal gas, the internal energy is function of temperature only hence:

$$h = C_p T$$

then:

$$m_t T_t = m_1 T_1 + m_2 T_2$$

3.4.2.1.4.2 The new stopping criterion:

The stopping criterion for the complete model is stabilization of the cycle. This means that the mass the engine breathes in no longer changes after a few cycles. In this project the cycle is run at least 8 – 10 times to make sure the results are stabilized.

The while loop discussed earlier [section 3.4.2.1.2.1] can now safely be removed, as the cycle is now complete i.e., the mass coming in is now going out.

3.4.2.1.4.3 Re-initialization after each cycle:

The assumption involved in this model, is during the length of time, the intake and the exhaust valves are closed, the pressure inside the manifolds equalizes with the atmosphere. This assumption is logical as the engine under consideration does not rev exceptionally high, and mean piston speed reaches only up to 11 – 11.5 [m/s].

The temperature inside the intake manifold is also re-initialized as atmospheric before the start of the new cycle, the temperature in exhaust manifold, being high, is however, assumed to be equal to the temperature at previous EVC. This, however, did not yield any considerable difference, as the temperature of air by EVC has reached the atmospheric value.

The temperature and pressure inside the cylinder are obviously refed to start the new cycle.

3.5 Module 2:

This module pertains to the study of effect of changing runner dimensions on Volumetric efficiency, which will ultimately dictate the amount of power, the engine produces. Runner here is assumed to be a pipe of certain length $L_{manifold}$ and certain diameter $D_{manifold}$. The diameter, generally, is assumed to be equal to sqrt (2) * Diameter of the Valve.

3.5.1 Studying the effect of runner's cross-sectional area:

3.5.1.1 Initial Selection of diameter:

This is to be kept under consideration, the engine used here PSA DW10 is a 4 cylinder

16 valve assembly, which implies it has 4 valves on each cylinder (2 – intake and 2 – exhaust). Hence the initial diameter is, as a rule of thumb calculated to be:

Equating the area of flow available at the valves and inside the runner:

$$A_{manifold} = A_{valves}$$

$$\frac{\pi}{4} * \left(Dia_{manifold}\right)^2 = 2 * \frac{\pi}{4} * (Dia_{valve})^2$$

$$Dia_{manifold} = sqrt(2) * Dia_{valve}$$

Given the intake valve diameter is 22.7 [mm], the diameter of the manifold comes out to be:

$$Dia_{manifold} = sqrt(2) * Dia_{valve} = 32.103\ [mm]$$

The area is then independently calculated.

Please note, the independent calculation from diameter to the area for the runner and the valves is for availability of liberty for independent changes and separate use later in the program.

3.5.1.2 Changing the diameter:

The diameter of each runner directly decides, the area available for flow between the runner and the assumed atmosphere outside. Hence if the flow inside the runner is limited due to its diameter, the *Volumetric will fall. In case of excessively large diameter, however, the material cost as well the as fixation procedure time and cost go up.*

Hence it is important to know, the trend of V.E. depending on the diameter.

For this purpose, the exact same code was looped with re-initialization of almost all values. The ***range*** of diameters chosen is

$$[0.55 * sqrt(2) * Dia_{valve}, 2.5 * sqrt(2) * Dia_{valve}].$$

The results are discussed in the results section, however, this statement is with mentioning, the relationship was not found to be linear, as the curve flattens out after a certain value of diameter.

3.5.2 Attempt to introduce momentum effects:

3.5.2.1 The Ram effect:

The Ram effect [section 2.6] is the forced induction of air, under its own momentum. The air that gets accumulated at the intake valve travels up-stream and due to the existence of the manifold (common intake pipe), gets reflected and may travel back and forth several times before it gets inducted back into the cylinder when it opens up for the next cycle, if the length has been tuned.

This, however, is NOT very prominent at low piston speeds where flow is prominently dictated by the pressure gradient. However, at considerably high piston speeds ***"Ram effect"*** becomes prominent and is used to achieve higher V.E. at higher RPMs.

The limitations to calculate the increased V.E. with the current model has been explained below:

The approach discussed so far has been explicitly stated to be compressible, quasi-static in nature. This modelling method leads to some discrepancies at higher RPMs, the physics of which will be explained, along with the available workarounds, in the following sections.

3.5.2.2 Effect of piston speed on flow of air:

The air is a fluid and carries some mass. Due to this mass, air has momentum. The model used by-far, is essentially application of steady state equations for a very short period and evaluating the changes occurring in the reservoirs on each side.

This approach then assumes, the mass flow in the nozzle has achieved the value indicated by the steady state equations during the stipulated time constraint, during regions of positive as well as negative acceleration.

This, however, is not the case at very high V_{p_avg}. At very high piston speeds where the change in volume is considerably rapid and time taken by the crankshaft to rotate one degree drops, the air is not provided enough time to accelerate and decelerate enough to achieve steady state within the given time.

Hence one may state, the mass starts lagging the pressure variation.

This is close to not being the case for low piston speeds (0 – 5 [m/s]) and is somewhat the case for mid-range piston speeds (5 – 8 [m/s]) but is considerable at high piston speeds (8 – 15 [m/s]).

Under the pronounced effects of momentum, the air cannot accelerate to the desired levels of velocity under a certain temperature gradient within the given time, nor can it decelerate similarly.

3.5.2.3 The required model:

The flow under discussion, if it neither accelerates nor decelerates to levels predicted by compressible steady state design, then the flow becomes time dependent. A time dependent flow is also known as transient or unsteady flow.

This is to be noted, the flow cannot be accurately modelled through further discretization of time. This approach will, although certainly help reduce the discretization error, it will not model the ***"lagging of mass"***.

The flow, as explained earlier, is of compressible type and expands under the internal energy available. Hence the compressible effects cannot be completely ignored. Hence to conclude:

The required model for this flow should be of Compressible, un-steady type.

The difficulty with this model is, however, the absence of completely analytical approach to it. Due to compressibility, within a given volume, mass tends to change due to change in density. The developing expansion then holds a different momentum at each step with different amount of mass experiencing acceleration due to the force from fluid behind it. Hence, to improve the approximation of compressible, steady state model, the project considers combination of ***compressible, steady-state, and incompressible unsteady flow model.***

3.5.2.4 The developed model:

The developed model is a combination of the compressible, steady, and incompressible unsteady equations. The alterations to develop the current model are:

1. The velocity and mass flow rate functions are redefined with incorporation of the following equation:

$$F = ma$$

This is the ***Newton's second law of motion***. It's application to a differential fluid element leads to differential form of the famous ***Navier-stokes equations***, but its application to the entire mass in a reservoir, leads to a simple, incompressible flow model. *Analytical solution to Navier-stokes under time dependence is currently unavailable.* Application of this equation to the entire mass in the reservoir leads to an equation which can then be used to calculate a velocity depending upon the *time given to the force to act* and *the initial velocity*.

2. The Force acting on the mass is given by the pressure difference across the throat cross-section, multiplied by the instantaneous area of the throat (effective flow area [section 3.4.1.1.2]).

$$F = \left(P_{manifold} - P_{cylinder}\right) * Effective\ flow\ area$$

3. Notice the equation yields a positive or a negative force depending on the pressure gradient.

4. The equation yielding velocity then becomes:

$$V_f = \frac{\left(\left(P_{manifold} - P_{cylinder}\right) * Effective\ Area\right)}{mass_{inlet}} + V_i$$

5. The velocity yielded by this equation is then compared to the velocity and mas flow rate functions [section 3.4.1.2.2], ***if the velocity is <u>in the same direction as the pressure gradient</u>, the velocity is capped by the steady-state velocity, i.e., the velocity CANNOT exceed the steady state velocity in any condition.***

6. The mass used to calculate this velocity depends on *the cause of this motion, i.e., where the flow is generated. If the velocity is* ***positive*** *through the* ***inlet*** *valve, the mass that needs to move is the* ***mass inside the runner****. If there is* ***back-flow***

*however, the mass that dominates momentum is **mass inside the cylinder**. Similarly, if the flow is **positive** through the exhaust valve, the **opposite is true**.*

3.5.2.5 Increased Volumetric Efficiency:

In practical scenario the volumetric efficiency increases due to the combination of two intertwined phenomena:

- As the air bombards with the closed intake valve, it loses its dynamic pressure head and converts it into static pressure head. This means an increase in pressure is observed, but this is equal to the stagnation pressure used till yet. The pressure, however, keeps rising as the air compresses under its own momentum. This, by the conservation of energy, should increase <= the factor $\frac{\rho V^2}{2}$.
- This increased pressure implies higher density, which implies more mass. This high-pressure wave then travels back and forth at the speed of sound, but the mass travels with velocity 'V' (manifold velocity) *(can be understood with analogy with a slinky axially hitting a wall)*, however, the high-pressure region continuously oozes out mass thus losing its additional energy until the pressure wave diminishes to P_0 i.e., the initial stagnation pressure upon which the converging nozzle model works.

Thus, the program developed to model this phenomenon:

- Adds a factor $\frac{\rho V^2}{2}$ to stagnation pressure, and $\frac{V^2}{2C_p}$ to the stagnation temperature.
- Changes the initial velocity inside the manifold to the velocity at the instance of IVC.

3.5.2.6 Tuned Runner Length: [9]

The tuned runner length is the length that, in a multicylinder engine, resonates the air inside the manifold thus providing higher pressures at the top of the valve as it opens. This can be calculated by the following method:

As we know, the high-pressure wave travels at the speed of sound, the distance that it travels during a given time with *no loss assumption and zero acceleration* can then be calculated using:

$$Distance\ Travelled = Velocity * Time$$

The speed of sound in the air for a given set of conditions can be calculated using [section 3.4.1.2]:

$$c = sqrt(\gamma * R * T)$$

The time available is the difference between the IVC of the current cycle and IVO of the next cycle. This can be calculated with some basic math, given the duration of intake event and RPMs:

$$Time\ for\ rotation\ through\ 1^0 = \frac{60}{360 * RPMs}$$

As the intake event lasts for 249^0, the remaining time for the wave to travel up and back down is: $720^0 - 249^0 = 471^0\ then\ t = \left(471^0 * \frac{60}{360*RPMs}\right)$

For the calculation of speed of sound, the model itself has been used as the temperature varies through the cycle, the distance covered in each step against calculated value of speed increases accuracy by a small amount. The tuned runner length calculated is provided in the results section.

3.5.2.7 The shortcoming:

As the model under discussion here is a combination of incompressible unsteady and compressible steady state equations, the model fails to predict results with considerable accuracy in a particular regime of flow, besides which the flow follows the accurate pattern.

This regime lies between two such points, where the pressure gradient is reducing. E.g., when the piston starts moving from BDC to TDC during the intake event, the pressure inside the cylinder is slowly approaching the manifold pressure. The situation persists until the gradient reverses. During this time, the flow velocity reduces, as it TRIES to approach the steady state velocity. ***In practical scenario, the velocity is more than the steady state velocity but shows a negative acceleration. In the model however, the equation used does not take this into account as the force is considered external but limited and not internal (expansion). This then dictates the velocity to go up, but the function, to limit the velocity, switches to steady state equations. This considerably reduces the volumetric efficiency (which should have been comparable to the compressible steady state), as the mass that should have been breathed in is now forcibly curbed from entering the cylinder.***

It is, however, important to note, the % increase in volumetric efficiency, is of concern in this module, the increase in V.E. can be predicted with appreciable accuracy with this model. the overall V.E., however, can be calculated using the compressible steady state model with appreciable accuracy.

3.6 Module 03

The opening and closing of intake and exhaust valve is governed by cam operated valve train. The lift of valve controls the area through which flow is possible. If somehow this variation of lift is not according to what is required or predetermined by the fixed mechanism of cam and follower, the mass-flow through the intake and exhaust will deviate from what is needed.
Although there are many components that are involved in the cam follower mechanism but

the design of all of these is mostly dependent upon structural strength based on MEP of engine. All of the components involved, and the concepts of mechanics involved in their design will be discussed one by one.

3.6.1 Cam and Follower Mechanism [10]

Cam Mechanism can be stated as a four-bar linkage mechanism with a half joint present instead of coupler. Cam mechanisms are used to convert rotatory motion into linear motion. The most important factor for perfect operation of this mechanism is force that allows constant contact between the follower and the cam. Cam is an eccentric shaft that rotates. Follower is a rolling or a flat surface that moves back and forth due to geometry of cam shaft.

Cam Mechanism is used to actuate the valves of intake and exhaust in most engines today. The method might be different such as over-head cams, cams with push rod and rocker arm assembly, SOHC, DOHC. In our particular model the under-discussion method will be DOHC. The engine EW 10 uses a Dual over-head cam for operating intake and exhaust valves.

3.6.1.1 Dual Over-head Cam Mechanism

In DOHC, two separate cam shafts are used for intake and exhaust. The cam shafts are present on top of piston in orientation. The lobes of each cam and phasing are set as per the required timing and lift required.

3.6.2 Design of Components involved

In DOHC mechanism, components involved are:

1. Cam (shaft design and lobe Geometry)

Cam shaft in this case operates 8 valves. 4 cylinder and 2 valves for intake per cylinder. Similarly, another camshaft is used for exhaust side. Each camshaft will have total 4 pair of lobes for actuating valves for each cylinder.

The phasing of these lobes is an important part of camshaft design. This setting of angles depends on which cylinder is undergoing intake or exhaust and what is the firing order.

The other part of design is the lobe geometry. The lobe geometry is determined by what valve lift profile is needed.

2. Follower selection

Follower types vary for different applications. These type generally are

- Knife point followers
- rolling followers
- Flat followers

Based on applications follower geometry may vary. in our given scenario a very precise fit and contact force regulation is required and similarly in most engines with DOHC flat followers are used.

3. Valve

Valve is the main component acting as a doorway between the manifolds and the cylinder. Generally, a fat plate with a stalk is used and the connected between both parts is tapered to get a smooth flow of air.

4. Valve spring

All the components discussed above have their importance. But for them to work properly, maintaining a contact between cam and follower is very necessary. The valve spring present in this mechanism serve to provide this role

3.6.3 Valve lift and Valve Float

Valve lift is the amount of valve displacement by which cam causes it to rise and create a pathway for air. The area is varied as it opens and closes, and valve lift determines this flow area. Thus, the control of flow of intake and exhaust lies at the mercy of valve lift. In our project as we have not proposed any change in cam profile for valve timing or lift. Our main focus is to study the flow by keeping the scenario with involvement of these phenomenon to the minimum.

Valve float occurs when the contact between the follower and the cam lobe is disturbed such that even when actually the cam turns so that the valve should have been shut but the valve remains open under the action of different forces acing on valve. Valve float control is desirable to us as it is a requirement of our project.

There is only one way to eliminate or reduce the possibility of valve float to the lowest possible chance. This way is to generate enough force between the follower and the cam. This can be achieved through variety of ways.

By using a fixed linkage mechanism, this is not a feasible application and several design and space constraints do not allow the usage of bar linkage

By using electromagnetic/ solenoid actuator for controlling valve motions. This method is very expensive and will require several design changes

By changing the spring that forces the hold of follower and cam together.

In our project, our study revolves around the fluid flow and to make sure that what recommendation for any engine be suggested based on the developed model the flow is as nearly same as described or dictated by valve lift profile. The design changes that might be required is only the valve spring if the mass-flow is increased

All other design and structural strengths are dictated by MEP of the operating cycle and even by increasing the mass-flow that does not change and the design of all parts such as valve, camshaft, cylinder head etc. will be good enough to operate without any changes in design.

3.6.4 Forces on Valves

In order to suggest necessary design changes the calculation of force that tries to compress the spring is important. Frist of all, the forces that act upon the valve should be discretized. There are 3 main forces that are trying to pull the valve down and break the contact between follower and cam lobe.

3.6.4.1 Force due to mass (weight of components)

Due to mass of valve, and spacer (flat follower), a preload is experienced by the spring and in our design consideration this force plays a vital role for designing the spring.

3.6.4.1.1 Mass of valve:

A solid model of valve based on experimentally achieved measurements is created in solid works. Using the software analysis of mass properties. The mass of valve is achieved by setting the material to be a Tribaloy having the density of about 8700 kg/m^3. Dimensions of the valve model are also indicated in the picture below.

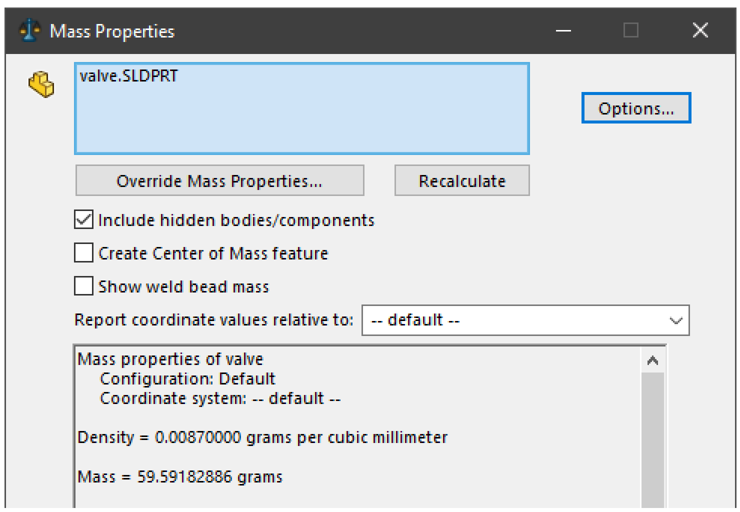

Figure 12: Mass of Valve using SolidWorks

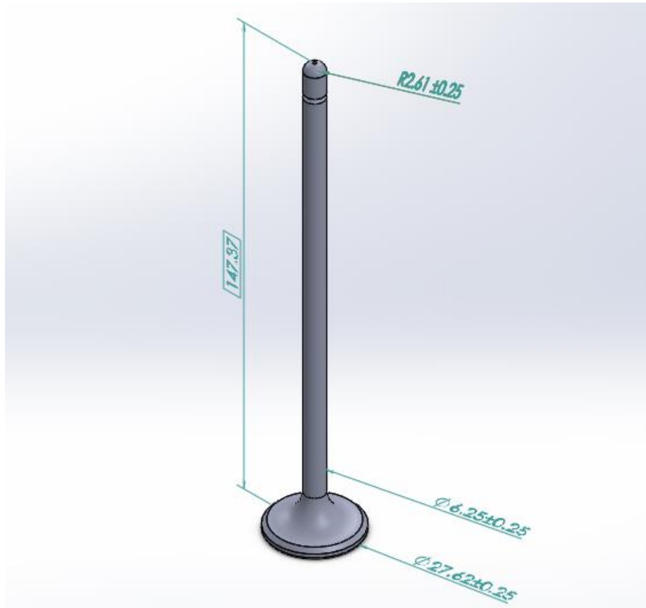

Figure 13: A 3D depiction of engine valve

3.6.4.1.2 Mass of flat attachment

Valve is not in direct contact to the cam and a spacer flat follower is used. The mass of this attachment is also calculated as per the method explained above.

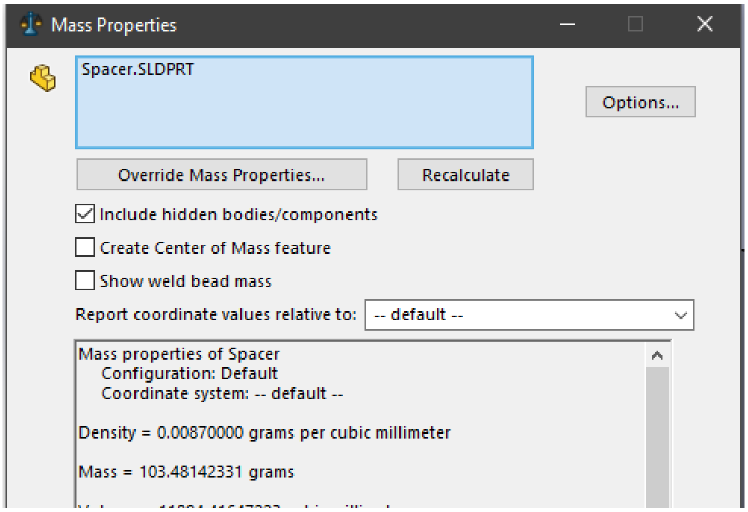

Figure 14: Mass of follower attachment using SolidWorks

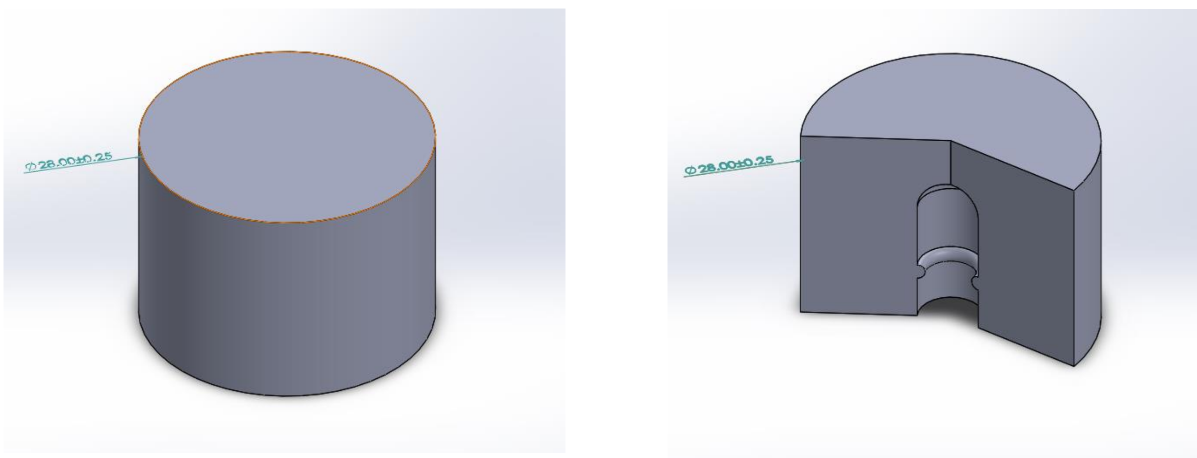

Figure 15: 3D view and Section View of Follower attachment

3.6.4.1.3 Calculation of weight:

$$Total\ weight = (Mass\ of\ valve + Mass\ of\ attachement) * g$$

$$W = (m_v + m_a) * g$$

$$W = (60g + 120g) * \frac{9.81m}{s^2}$$

$$W \approx 2N$$

3.6.4.2 Force due to acceleration produced by the Cam movement

SVAJ profile of cam can be obtained from valve lift profile that is generated from experimentally obtained data. Using the value of acceleration and the total mass of the follower and the valve the force impacted due to the lift generated in valve can be calculated.

Using the MATLAB code for valve lift, derivative w.r.t is calculated twice and a curve for acceleration of valve assembly is obtained. The maximum values of acceleration are then used to find the maximum push force of the valves.

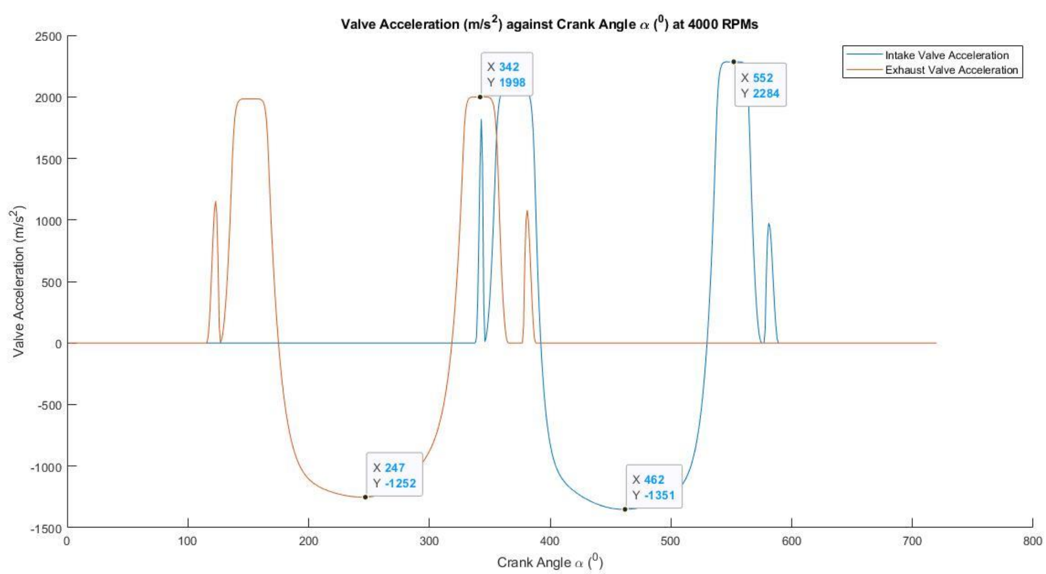

Figure 16: Acceleration of Valve using second differential of Valve lift profile

Calculation of force

$$Maximum\ acceleration = 2284\ m/s^2$$

$$Mass\ of\ accelerated\ bodies = \ m_a + m_v \approx 200g$$

$$F\ due\ to\ acceleraion \approx 457\ N$$

3.6.4.2 Force due to impact of air flow

Air is flowing continuously and causing the valve to resist the contact with cam. When the valve has to close the pressure of flow present between the valve top surface and the valve seat is forcing it to stay open. This force hence generated is the major culprit of valve float. In our earlier modules of our project, we have worked upon studying and trying to maximize the flow of air in and out. Due to this increased flow the consideration for valve float is very important.

A pressure gradient from manifold towards cylinder causes the air the to flow inside but also while flowing this air impacts the area around the valve seat and tries to push the valve down with it. This force can be a main contributor to valve float.

A comparison based on the pressures is made and a maximum pressure gradient of 73950 Pa is noted. The area on which this pressure is impacted directly is measured to be 590mm^2. The plots and SW measure indicating pressures and area are indicated below.

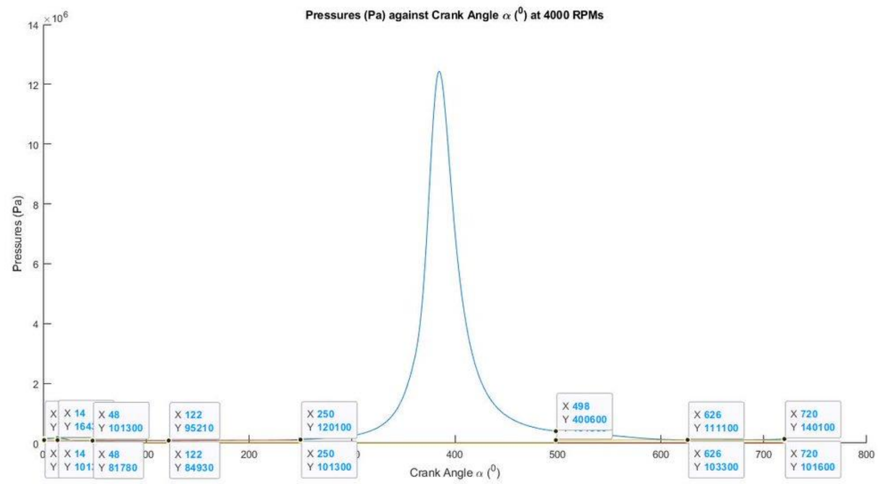

Figure 17: Pressure propagation inside cylinder

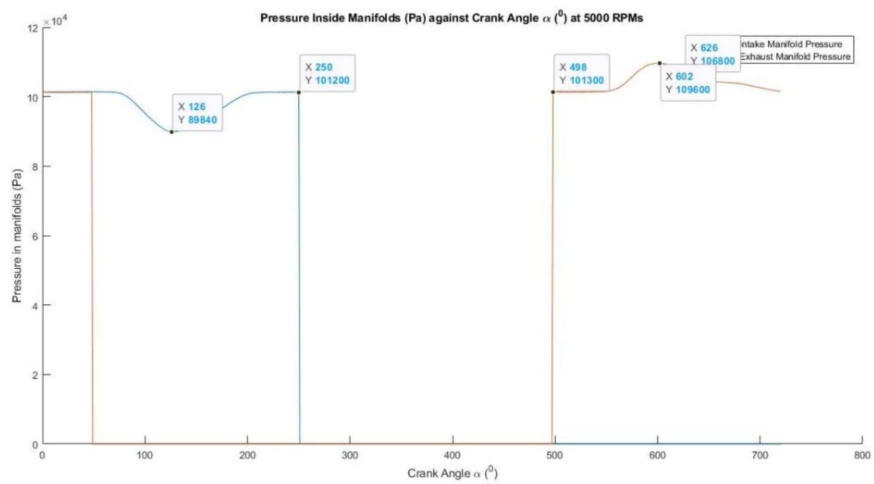

Figure 18: Pressure propagation inside manifolds

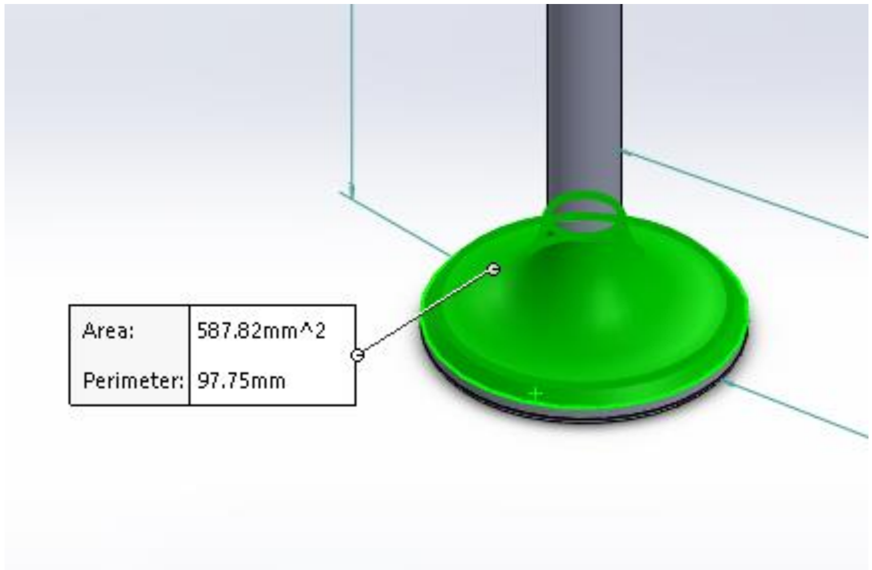

Figure 19: Upper area of Valve

$$Total\ force = F_{max} = W + F\ due\ to\ acceleration + F\ due\ to\ flow$$

$$F_{max} \approx 805\ N$$

This F_{max} will be used for designing the spring.

3.6.5 Helical Compression Spring Design [11]

To cater for the changes in loading condition of the cam mechanism (valve), the change in the design of spring is needed. A procedural attempt at this design change is made. The most important physical laws and theorems will be discussed before continuing with the approach.

3.6.5.1 Hooke's law

According to the statement of Hooke's law, the deformation in any elastic object is proportional to the stress applied to it. Springs are considered to be an elastic material and this law holds true for general operating conditions of spring.

$$F = -kx$$

In this equation, ***"F"*** is the force applied to compress one end of the spring. ***"x"*** describes the compression that the spring undergoes on application of the force F. According to Hooke's Law this deformation is proportional to the applied force F. To equate the proportionality, a constant is introduced. This constant is "***k***". This represent the material property of the spring wire and is called the spring constant.

3.6.5.2 Castigliano's theorem

This theorem uses the ability of spring to store strain energy in a quantified manner to find out the deflection it is undergoing at that particular moment when a particular loading condition is applied.

$$k = \frac{d^4 G}{8D^3 N}$$

"d" represents the diameter of the wire of spring

"G" represents the shear modulus of the material

"D" represents the mean diameter of the spring

"N" represents the number of active coils in the spring

3.6.6 Approach

A methodological approach is used for designing the spring for this particular application. Stepwise description and important finding will be discussed below.

3.6.6.1 Selection of material

Materials is selected on the base of application by referring to published and tested overtime literature. Shigley's Machine Design has a list of potential spring material and description for the particular material based on their application area.

A Chromium Vanadium based steel alloy is selected for the design ASTM A232. This material has a good cyclic loading life and has good potential of dealing impact forces as well. In most car engines and even aircraft engines this material has application in manufacture of valve springs.

All of the required material properties are also referred from the same book as mentioned.

3.6.6.2 Category of Use

The valve spring is used in a preloaded orientation in between two flat plates. The spring will be present inside a hole. The geometry is not considered to be wrapped around a shaft as the shaft in this case is valve which is actually in motion.

A squared and grounded on both sides spring is selected.

3.6.6.3 Diameter of wire "d"

A range in which the selected material wire is available for used is used. The diameter of wire may range from 0.8 mm to 12 mm

This list will be shortlisted based on later calculations.

3.6.6.4 Mean Diameter of Spring "D"

According to our particular orientation as described in point 2. The mean diameter is calculated by using equation

$$D = d_{hole} - d - allowance$$

D_{hole} is the diameter of hole this in our particular geometry is 29 mm.

Allowance is the gap that will be allowed between the hole wall and the spring. 1mm is defined as allowance for this particular scenario.

3.6.6.5 Spring Index

For any practical design of spring the ration between the mean diameter of spring and the wire diameter is called the spring index.

$$C = \frac{D}{d}$$

The allowable range for this factor is

$$4 < C < 12$$

The range of available diameter is shortened after this calculation from 2.2mm to 5.6mm.

3.6.6.6 Curvature effect and Bergestraser's factor

The curvature of the wire increases the stress on the inside of the spring but decreases it only slightly on the outside. This curvature stress is primarily important in fatigue because the loads are lower and there is no opportunity for localized yielding. For static loading, these stresses can normally be neglected because of strain-strengthening with the first application of load. To cater for this curvature effect, a correction factor is used. A close approximation of Bergestraser's factor is used

$$K_B = \frac{4C + 2}{4C - 3}$$

3.6.6.7 Maximum allowable torsional stress and Factor of safety at closure

Every material accepted by society of materials have a specific coding and experimentally derived set of allowable material properties is defined. ASTM232 also has a defined stress-strain curve that signifies its material strength and behaviour. Ultimate tensile strength is one of these properties that plays important role in dictating the design.

$$S_{ut} = \frac{A}{d^m}$$

Where "A" is the intercept of the stress strain curve and "m" is the slope.

Based on experimental observations, a percentage of this S_{ut} is decided. This percentage factor only serves as the Maximum allowable torsional stress.

For chromium vanadium, this Max. allowable torsional stress can be defined as

$$S_{sy} = (0.65)S_{ut}$$

A comparison between the stress arising in the spring due to loading scenario and this S_{sy} is built resulting in a factor of safety.

To find the stress due to particular loading condition the equation used is

$$\tau_s = K_B 8(1+\xi)F_{max}D/(\pi d^3)$$

Factor of safety determines how safe is the component to be used under specific loading condition and how good will it hold up compared to maximum allowable stress.

$$n_s = \frac{S_{sy}}{\tau_s}$$

This calculation also leads to minimizing the possibility of use of thickness of wire.

3.6.6.8 Active coils

In our spring configuration squared and grounded on both sides, active coils are present between 2 inactive coils.

$$N_a = Gd^4 y_{max}/8D^3 F_{max}$$

3.6.6.9 Spring dimension and geometric constraints of application

Condition of overall length, solid length, Inner diameter and outer diameter are applied to minimize the number of possibilities as well.

3.6.6.10 Buckling and Critical length

If the design height of spring is too long as compared to the diameter. A safe length is decided fir sring to not buckle based on

$$L_o < \frac{\pi D}{\alpha}[\frac{2(E-G)}{2G+E}]^{1/2}$$

3.6.6.11 Fatigue loading

The spring has to undergo countless loadings in a single run of engine. The amount of loading in its complete lifetime can be easily considered to be infinity. Sines and Zimmerli gave a concept to design spring taking in consideration this fact.

3.6.6.12 Fatigue factor of safety

For infinite loading a safe criterion of design is established and calculated to compare the max allowable stresses for infinite life to actual stresses.

3.6.6.13 Fundamental frequency wave

A wave of compression and rarefaction travels along the length of the spring at a particular fundamental frequency and the stresses can arise if the frequency of loading is not matched properly.

Figure 10-3

Helical coil compression spring design flowchart for static loading.

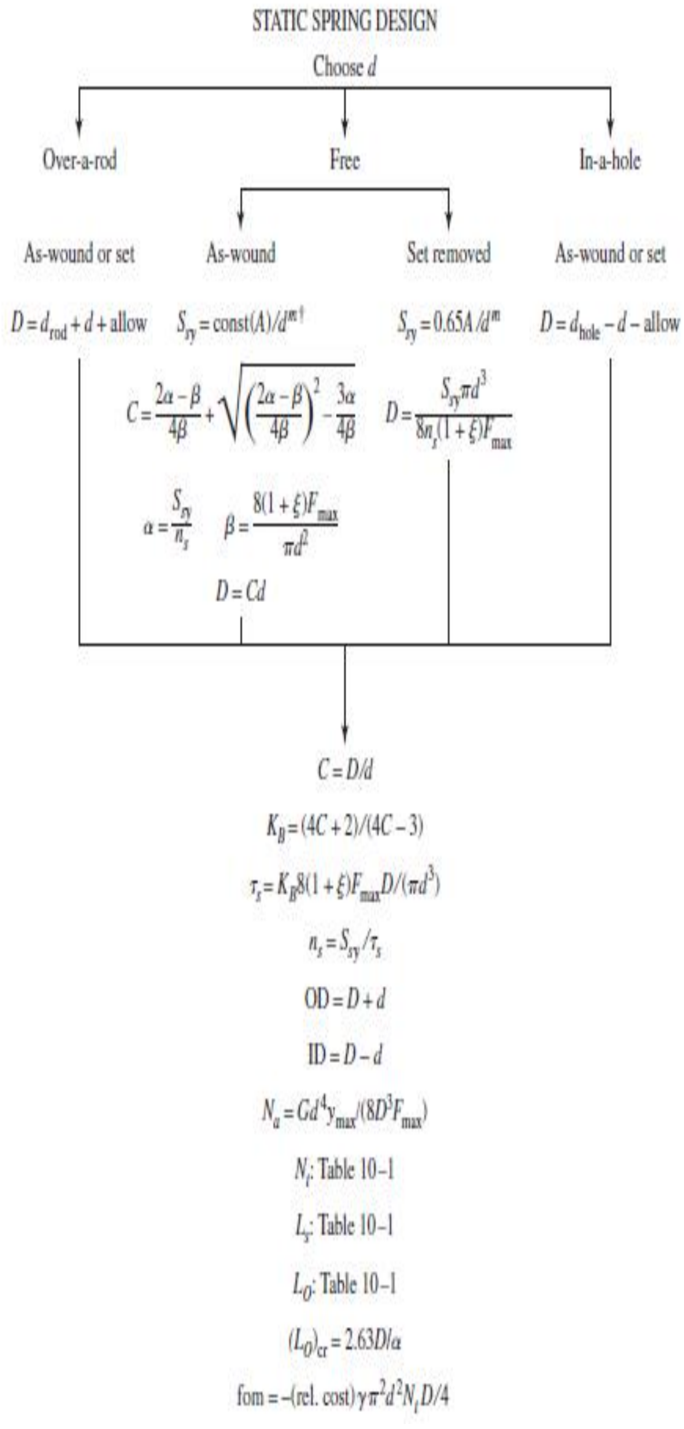

Figure 20: Reference figure indicating calculation strategy for spring design

3.6.7 Calculation

Before starting to calculate the dimensions for spring, it is very important to select a material. The material selection is totally based on literature and a reference is attached.

Chrome-vanadium	UNS G61500 AISI 6150 ASTM 231-41	This is the most popular alloy spring steel for conditions involving higher stresses than can be used with the high-carbon steels and for use where fatigue resistance and long endurance are needed. Also good for shock and impact loads. Widely used for aircraft-engine valve springs and for temperatures to 220°C (425°F). Available in annealed or pretempered sizes 0.8 to 12 mm (0.031 to 0.500 in) in diameter.

Figure 21: Reference image for material property

Table 3: Material properties of ASTM A232

Density	7800 kg/m^3
Specific Weight	0.076518 kg/mm^{2}s^2
Elastic Modulus	203.4 GPa
Shear Modulus	77.2 GPa
Stress-strain Intercept, A	2005 MPa.mm^m
Slope of stress-Strain, m	0.168
Percent elastic limit to Tensile	88%
Percent Elastic Limit to Torsion	65%

Selection calculations table:

Based on the strategy explained earlier the calculations for all the available diameters of wire are performed the results are indicated in a tabular form below:

Table 4: Results from Calculation and Selection of spring

d:	**1mm**	**2mm**	**3mm**	**4mm**	**5mm**	**6mm**	**7mm**	**8mm**
D	27mm	26mm	25mm	24mm	23mm	22mm	21mm	20mm
ID	26mm	24mm	22mm	20mm	18mm	16mm	14mm	12mm
OD	28mm	28mm	28mm	28mm	28mm	28mm	28mm	28mm
C	27	13	8.33	6	4.6	3.67	3	2.5
N_a	0.0081	0.14	0.833	2.9	8.26	19.5	41.34	82.34
L_s	1.90mm	4.3mm	8.5mm	19.91mm	51.38mm	129.7mm	305.2mm	674.5mm
L_o	16.40mm	18.8mm	23mm	34.41mm	70mm	143.4mm	320.2mm	689.27mm
$(L_o)_{CR}$	142mm	137mm	131.5mm	126mm	120mm	115.2mm	110mm	105.2
n_f	0.0128	0.10	0.33	0.7	1.5	2.5	3.8	5.4
n_s	0.0187	0.12	0.39	0.8	1.6	2.6	3.8	5.4
f_n	59466 Hz	7158Hz	2039Hz	825Hz	400Hz	224.5	134Hz	86Hz

fom	-0.00317	-0.0135	-0.037	-0.117	-0.345	-0.991	-2.62	-6.31

CHAPTER 4: RESULTS AND DISCUSSIONS

Since we have already taken into account the physics on which our concept is based and the experimental data for valve lift and co-efficient of drag has been obtained. Subsequently, we have developed a code in MATLAB, to solve the flow equation and the creation of pressure gradient due to combustion. The engine dimensions and data were taken as input and an analytical solution of engine based on these available resources were produced. The code mainly generates the process through which air and fuel charge goes and power is generated. The concepts of diesel combustion, flow properties of air in intake and exhaust, energy losses are modeled in the code under discussion. The code seconds as a practical engine was actually being observed during its operation.

As the engine starts it takes time of about 5 cycles to stabilize itself. After this the mass-flow of air, pressures and temperature are noted at the point of interest and will be discussed in detail during the course of this chapter.

4.1 Model of Complete Diesel Cycle

Thermodynamic cycle has been modeled with every degree of crankshaft rotation as a single step. The importance of the compression and power stroke modeling for our project is due to the reason that pressure gradients for the flow of air into and out of the cylinder i.e., intake and exhaust cannot occur without these.

The model is based on the state present inside the engine cylinder. How the mass inside the cylinder changes and what pressure and temperature it is present at. The model also indicates energy lost due to heat losses and energy addition due to combustion.

The graph below indicates the results generated from this part of the code and an interpretation of this results will be presented below.

4.1.1 Mass inside the cylinder

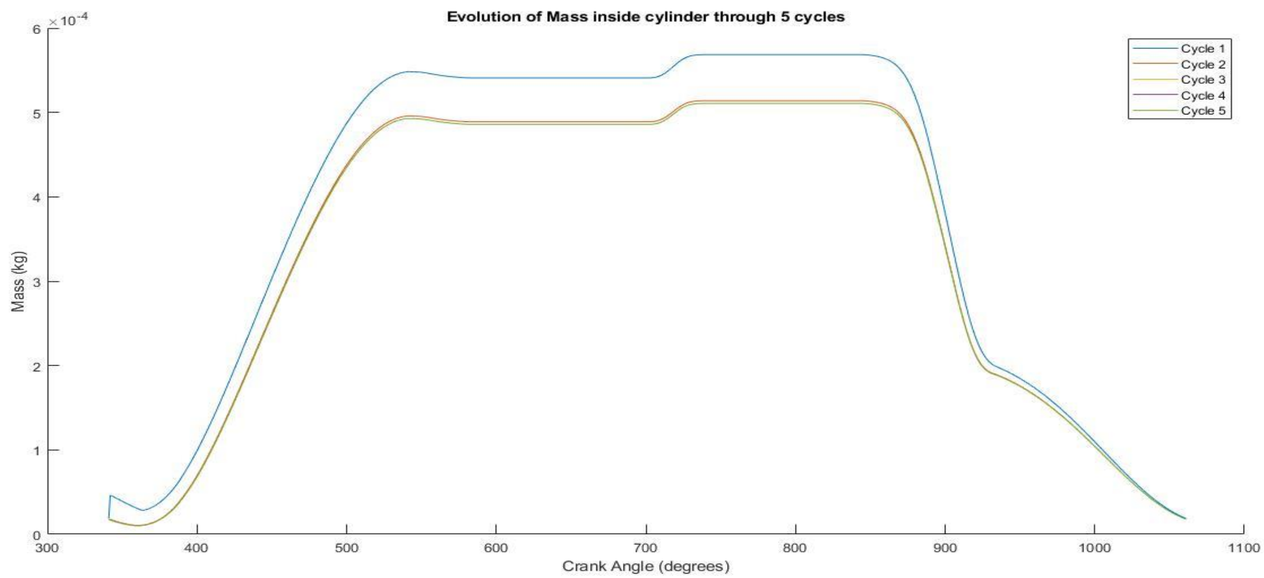

Figure 22: Evolution of Mass inside the cylinder

The operation of engine stabilizes after 5 cycles. First cycle is indicated in blue color which has a higher mass intake and then the mass efficiency falls due to development of pressure. The indicated cycle is starting at 341^o revolution of crank shaft i.e., when the intake valve starts to open. From 341^{o,} intake stroke starts and then air is compressed, combust, and exhaust gases are removed. The cycle takes place in 720^o ending at 1061^o.

Table 5 Mass breathed through 5 cycles (2000 RPMs)

Cycle #	***Total breathed mass (kg)***
1	6.080e-4
2	5.554e-4
3	5.530e-4
4	5.529e-4
5	5.529e-4

4.1.2 Pressure inside the cylinder

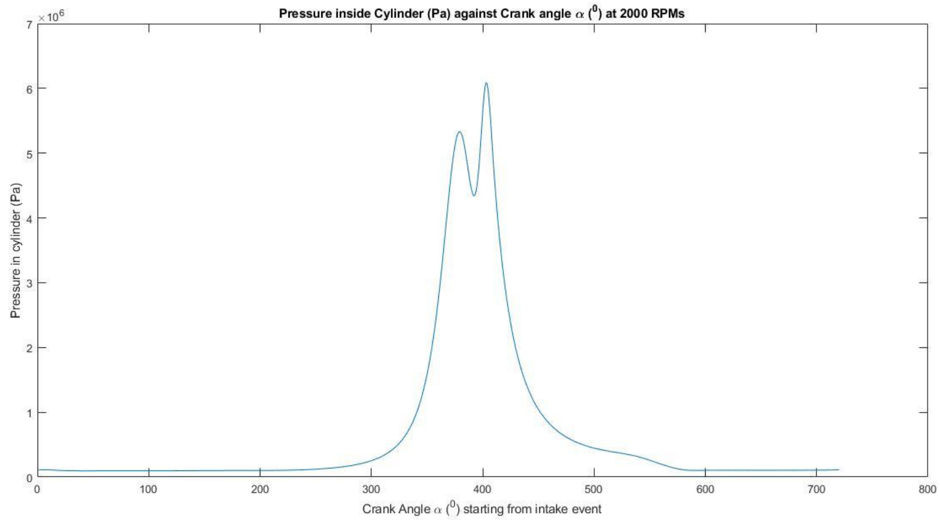

The change in pressure inside the cylinder after the process stabilizes is indicated by the graph. The pressure before the start of compression stroke remains almost at P_{atm} equal to 0.92 bar or indicated on the scale as 0.092 MPa. The pressure then rises as it should and finally drops again to P_{atm} during exhaust stroke.

Figure 23: Pressure inside the cylinder

4.1.3 Temperature inside the cylinder

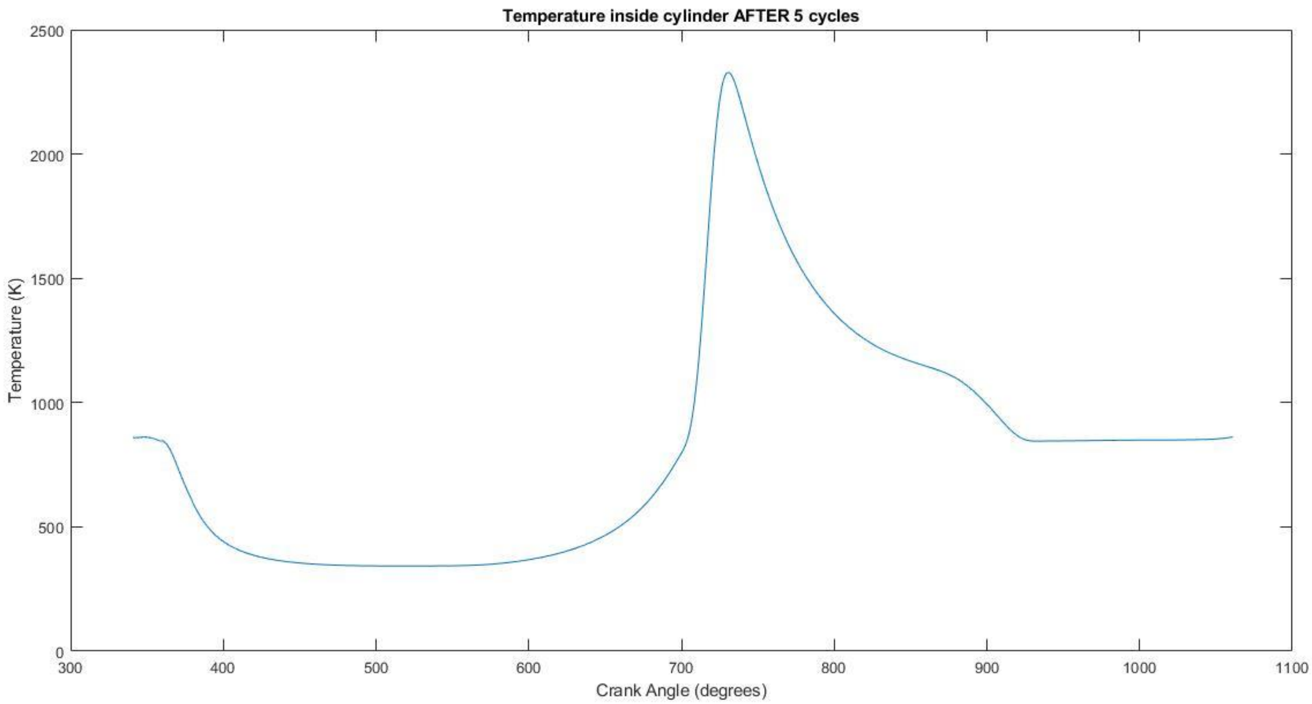

Figure 24: Temperature inside the cylinder

At the opening of intake valve, the exhaust has not been fully expelled and the temperature inside the cylinder is still comparatively high. As soon as the fresh air enter the temperature starts to drop towards room conditions. When compression stroke starts temperature starts to rise again due to increase in pressure, the temperature keeps on rising in the power stroke as well as heat is being added on combustion. In the later part of stroke, the volume increases and pressure decreases so temperature starts to fall. On the onset of exhaust, the temperature falls and normalizes itself to almost room conditions.

4.2 Intake flow

The important part of our project is to study the intake flow of air inside the runner. As per the assumptions mentioned in the earlier portion of methodology. The logic is built such that result for the state of runner in the form of mass flow rate, pressure inside the intake manifold, and temperature inside the manifold are obtained. The graphical results obtained will be interpreted and discussed here.

4.2.1 Mass flow during intake

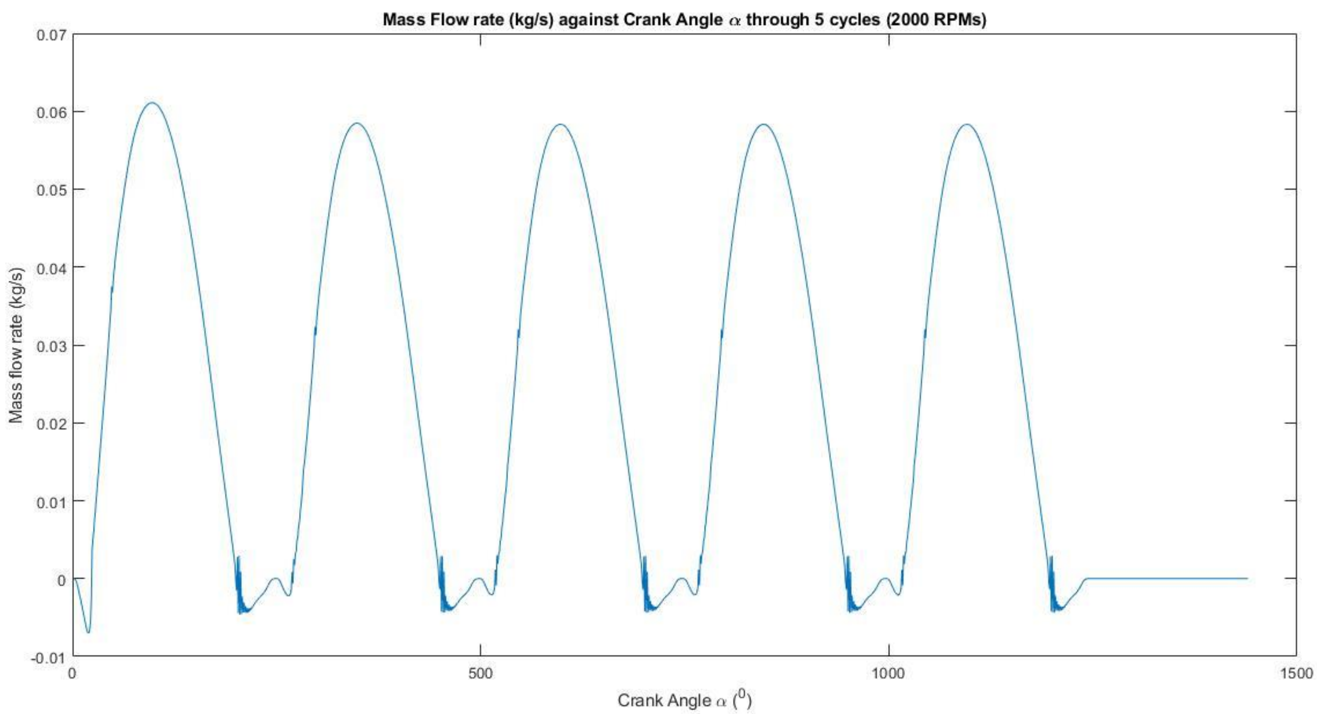

Figure 25: Mass flow through the intake valve

This plot shows 5 cycles and it can be observed that the process of intake at the specific initial condition has started to repeat itself. The repetitive stability indicates that the state of manifold has developed fully. The initial drop is due a bit of back pressure as the piston was still in upward motion. After this the mass-flow rises as the pressure gradient between cylinder and manifold increases. The fluctuations in the graph tail are due the numerical solution which shifts its direction at every instant due to the overlap condition.

Table 6 Peak Mass flow rate through intake valve cycles 1 through 5 (2000 RPMs)

Cycle #	***Peak mass flow rate (kg/s)***
1	0.06109
2	0.05847
3	0.05833
4	0.05831
5	0.05833

4.2.2 Pressure inside intake runner

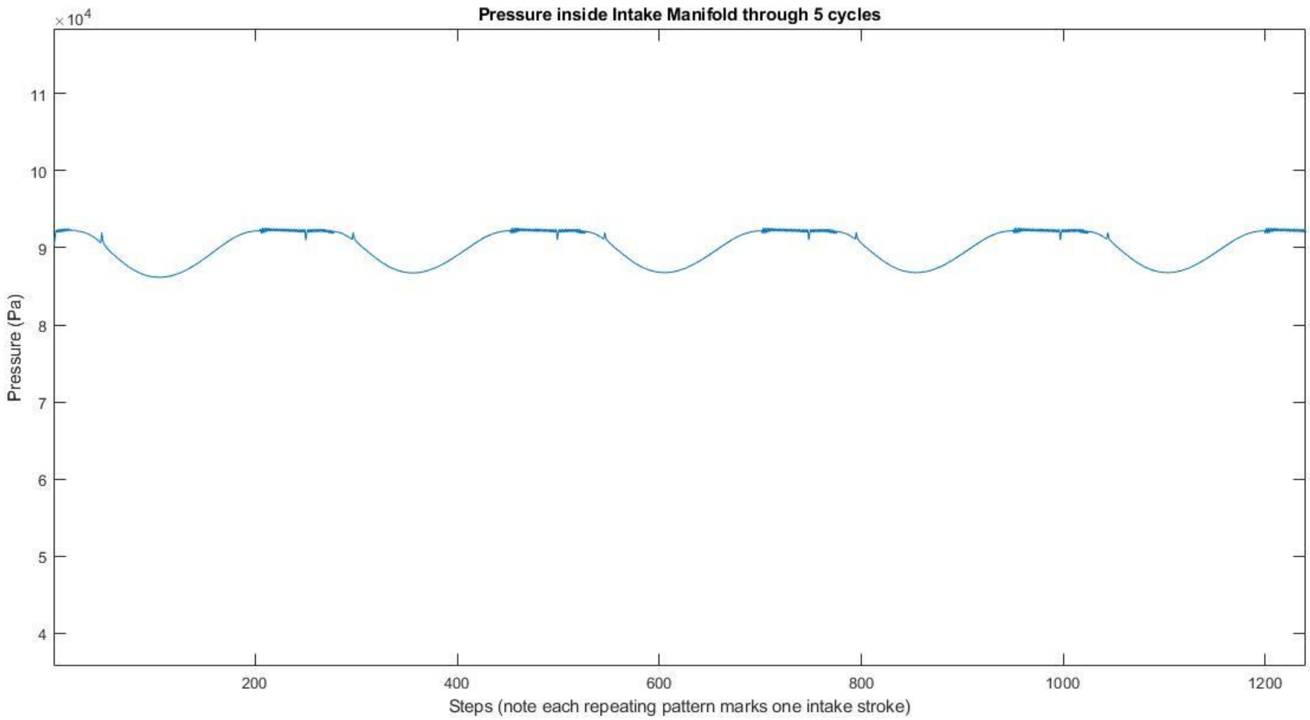

Figure 26: Pressure variation inside intake manifold

As the engine is naturally aspirated and operating at low RPMs, the pressure plot is close to a harmonic behaviour. With the change in volume and pressure of cylinder due to the movement of piston air is sucked into the cylinder through the valve rather than a push of air from intake manifold. The graph is symmetrical about the initial condition pressure. This phenomenon is comparable to a well establish pressure curve from the Internal Combustion Engine Fundamentals book.

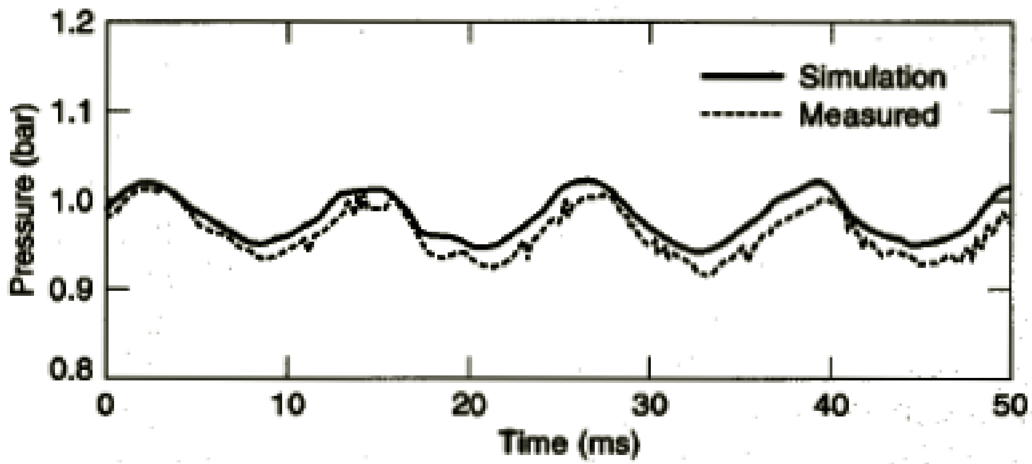

Figure 27: Reference figure for trend comparison [5]

The figure is presented in chapter 6 of the book. The operating conditions in both the graphs are a bit different but the trend of graph generated by our pseudo-numerical analysis is comparable and similar. This proves the accurateness of our program. The comparison proves that the engine model designed on MATLAB performs well close to a practical model and thus the flow of air inside the manifold is behaving as it should practically.

4.2.3 Temperature of Intake

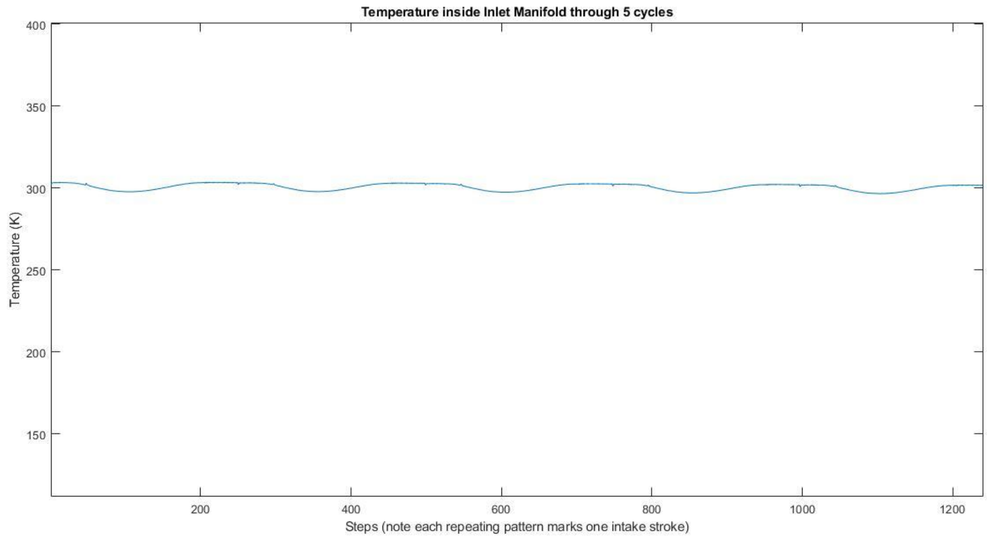

Figure 28: Temperature variation of intake manifold

The temperature of air inside the manifold remains pretty close to the initial condition. This is the behaviour it should have shown because no heat is added, no pressure in applied, no very dramatic change in density occurs so temperature should remain constant.

4.3 Exhaust Flow

A similar approach to study the flow inside the exhaust manifold is adopted. Graphical results based on analytical calculations are obtained and their validity is checked by explaining the behaviour of the plots. Exhaust flow through the orifice created by the opening of valve, the pressure and temperature inside the manifold

4.3.1 Mass flow during exhaust

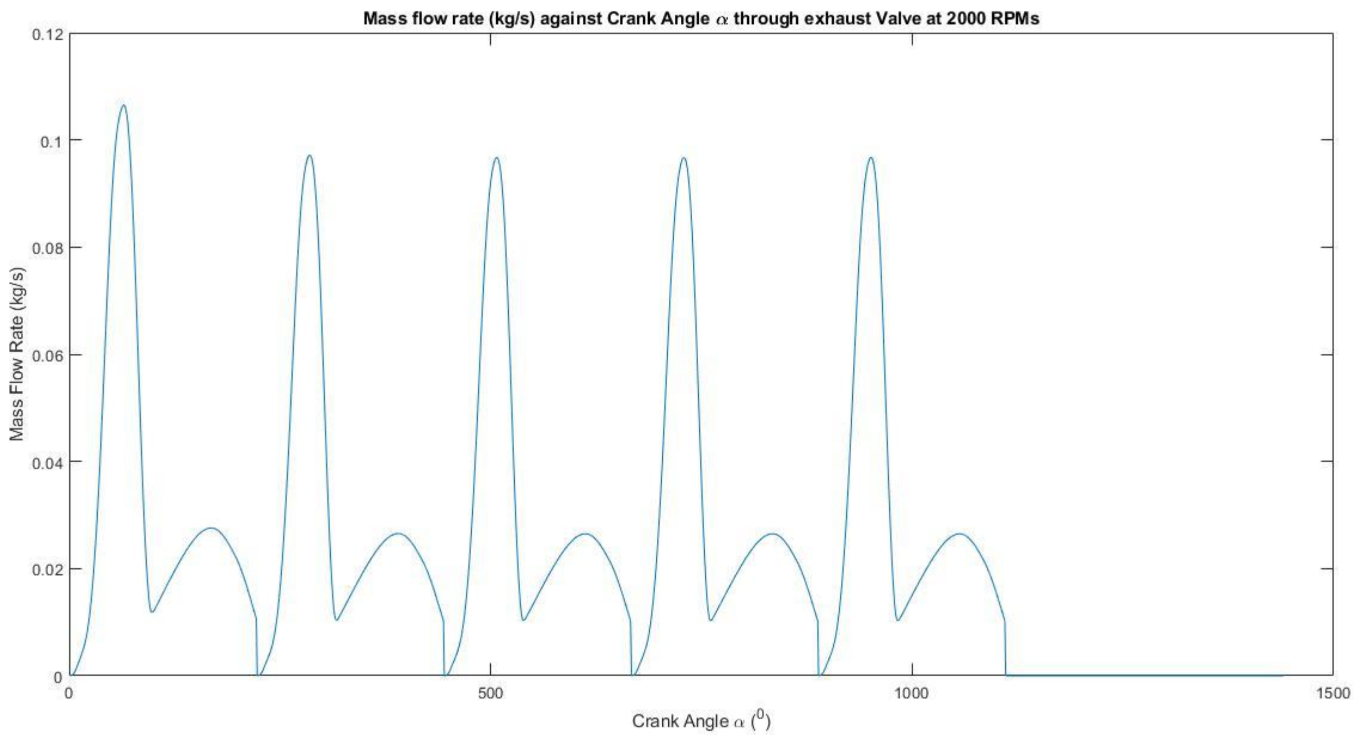

Figure 29: Mass flow through exhaust valve

During the very start of the exhaust stroke the pressure inside the cylinder is very large because this charge was created due to combustion of fuel at high temperature and pressure. The large pressure exhaust pushes itself at a very high rate to the exhaust manifold. This high mass-flow rate drops as the pressure effect dilutes but soon enough the rate rises again because now the piston has moved quite close to the TDC and the reduction in volume creates a high-pressure effect. This is an explanation to the second smaller peak. According to physical interpretation this behaviour of exhaust flow seems to follow practical situation.

Table 7 Peak Mass flow rate through exhaust Valve through 5 cycles at 2000 RPM

Cycle #	***Peak mass flow rate (kg/s)***
1	0.1065
2	0.09717
3	0.09673
4	0.09659
5	0.09672

4.3.2 Pressure and Temperature inside exhaust manifold

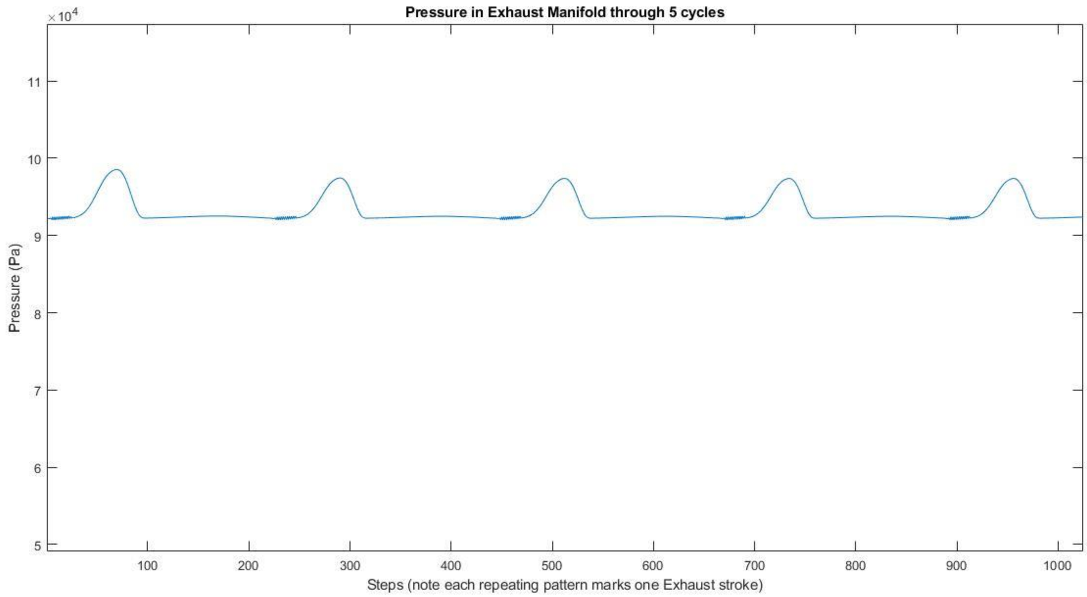

Figure 30: Pressure propagation of exhaust valve

A pressure bump is observed during the very start of the exhaust flow due to the very high pressure inside the cylinder but after the flow develops the pressure normalizes to

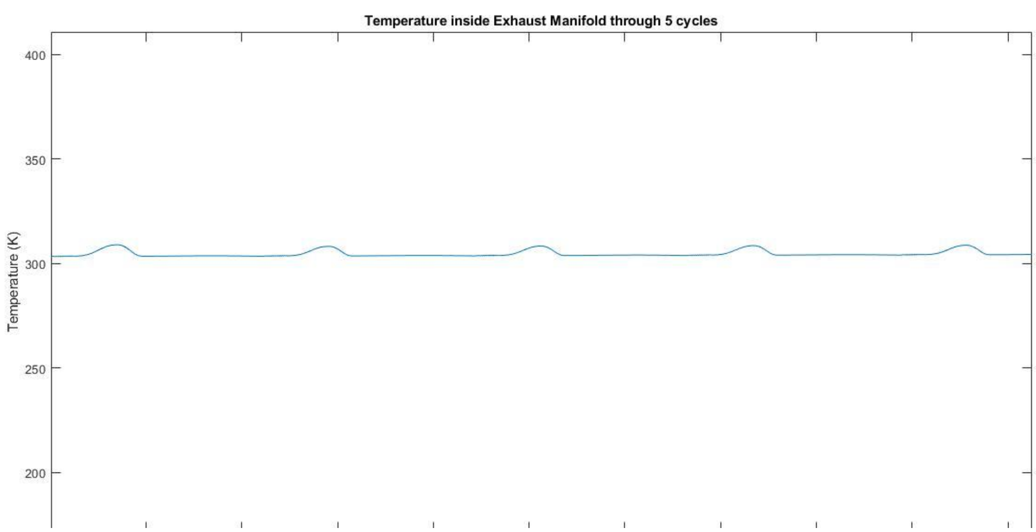

Figure 31: Temperature state of exhaust manifold

initial condition i.e., around 0.92 bar. The temperature plot is almost a straight line expect a small bump in the start due to the same reason as pressure curve.

4.4 Volumetric efficiency and Comparison

One of the important parameters using which we can generate satisfactory results for our design and validate our model is volumetric efficiency. Volumetric efficiency is a direct product of mass-flow or in other words the amount of total mass present inside the cylinder before the start of compression stroke defines the volumetric efficiency.

From figure 1 of the section, it is evident that the amount of mass taken inside the cylinder is around 5×10^{-4} kg. Using ideal gas equation, the maximum swept mass that can be breathed into the cylinder of this engine is 5.4×10^{-4} kg. By calculation it is observed that the engine model gives a volumetric efficiency roughly around 90%. A comparison based on this calculated value and experimentally observed data (general for Diesel Engines; from literature) is made.

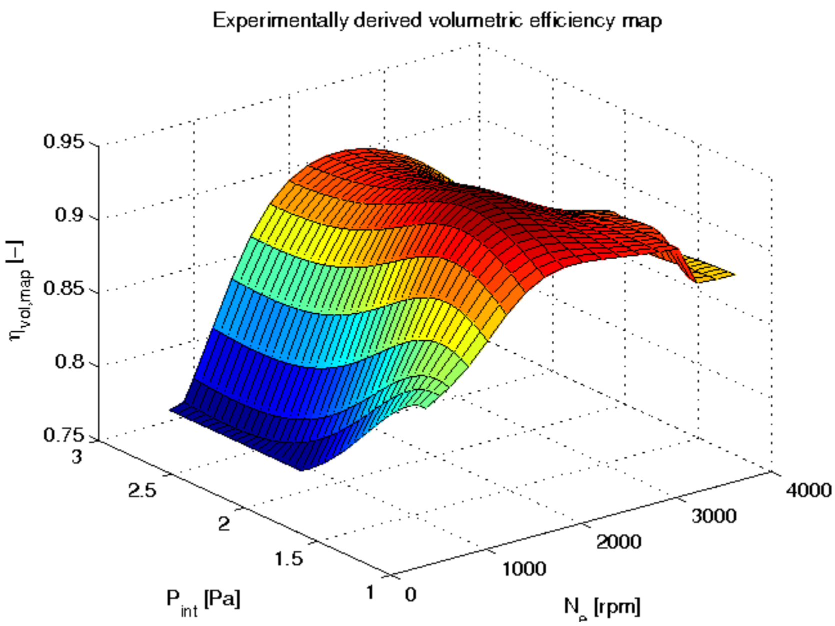

Figure 32: Experimentally plotted volumetric efficiency v/s RPM plot (reference image) [12]

Based on this experimental data, it is observed that for naturally aspirated engines operating at around 2000 RPMs, volumetric efficiency is about 90%. This is a generic map and will hold true for any diesel engine. The comparison of this map to our model's volumetric efficiency proves the correctness and validates our results.

Another piece of literature is used to back our claim and compare our results in this perspective. Again, ICE Fundamental by John B. Heywood has proved useful and a similar observation and plot is present in his work.

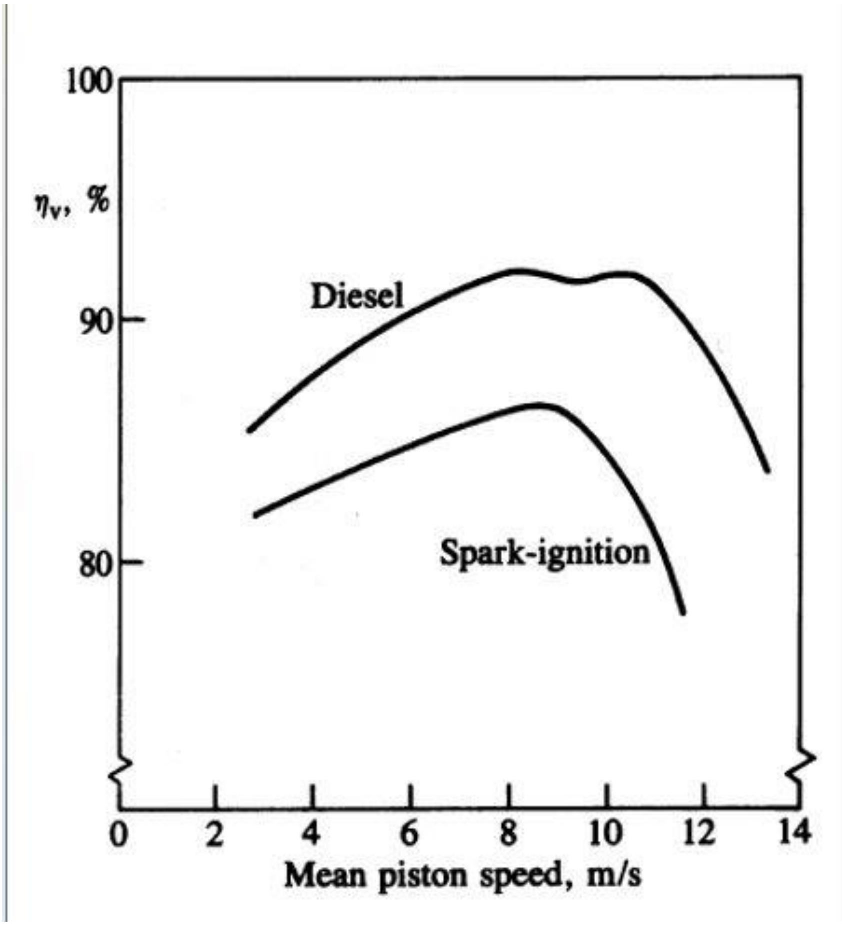

Figure 33: Reference image for volumetric efficiency trend from ICE book [5]

For a mean piston speed of about 6m/s, is 90%. This scenario matches our model and double validates that the experimental data claims are right and so is our model. Model has a good relevance to the practicality of operations and comparison of volumetric efficiency has made it clearer.

4.5 Tuned Runner

As discussed in earlier sections, runner dimensions are tuned to get optimal performance from the engine. This process is generally based on RPMs of engine. Iterative technique in on our engine model are applied to tune our engine for specific conditions.

This can be categorized as a Low RPM tuning and High RPM tuning.

4.5.1 Low RPM

The compressibility has negligible effect on lower RPMs, pistons mean speed is lower and changing the length of runner will not create a difference. Rather the diameter of runner is changed and optimal diameter is selected keeping in view the usage of material and cost incurred due to it.

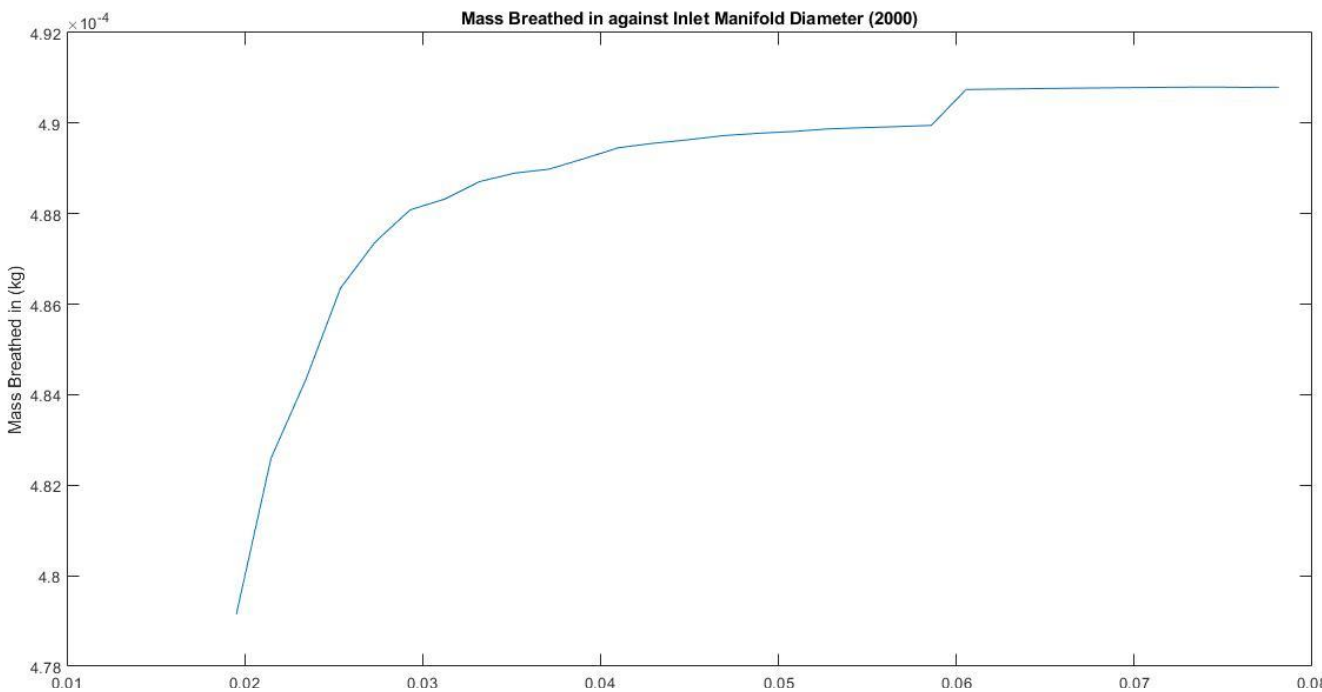

Figure 34: Mass Breathed v/s change in diameter of runner

As the diameter is increased the breathability of engine increases but after increasing the diameter further from a point the slope has straightened drastically. This indicates that increasing the diameter further from this point results in heavy material cost and the exchange in term of efficiency or mass-flow rate will not be very fruitful.

Same phenomenon in term of manifold cross-sectional area can be seen. This gives a better idea of cost terms. As increasing area of a pipe uses more material.

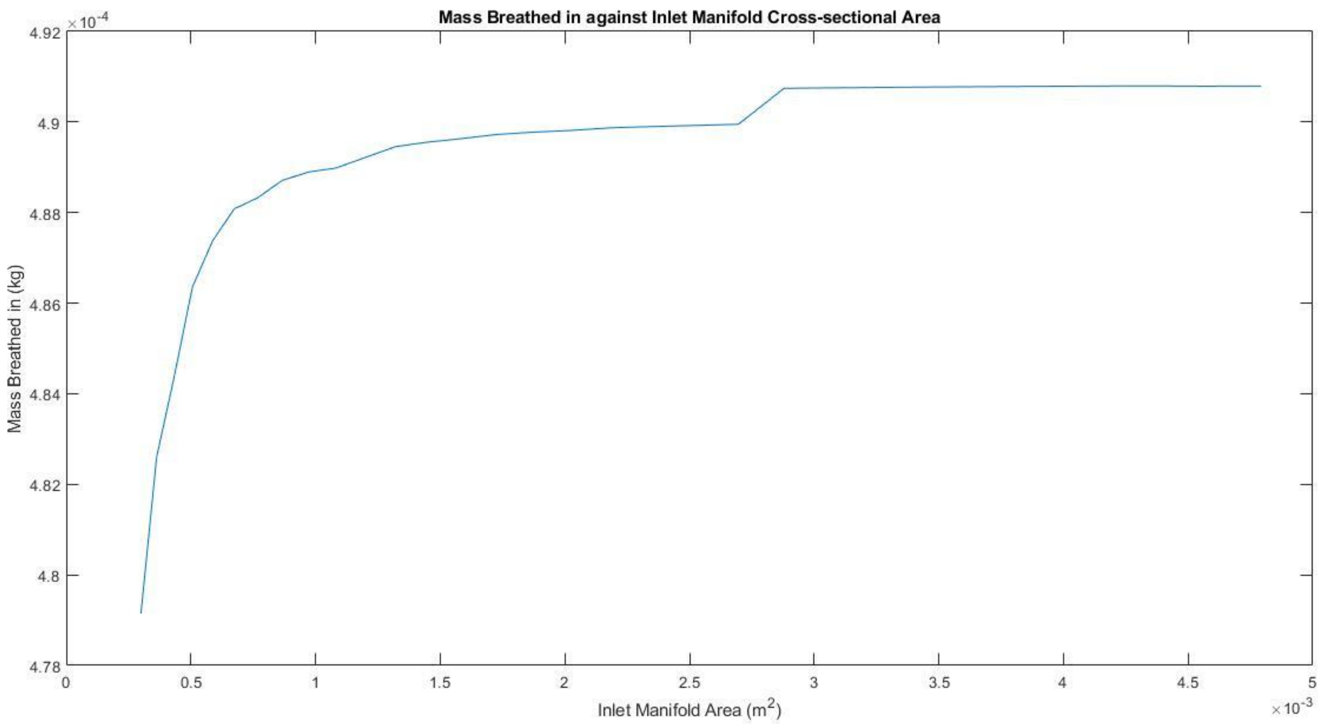

Figure 35: Mass breathed v/s Area of manifold

4.5.2 Higher RPM

In this case the velocity of intake flow is greater and compressibility wave will be generated. The length is tuned such that the compressional part of pressure wave occurs to be on the opening of intake valve. This causes the volumetric efficiency to rise.

4.6 Comparison of compressible – steady state model and incompressible – unsteady model with experimental data

4.6.1 Compressible – steady state model (better results at low RPMs):

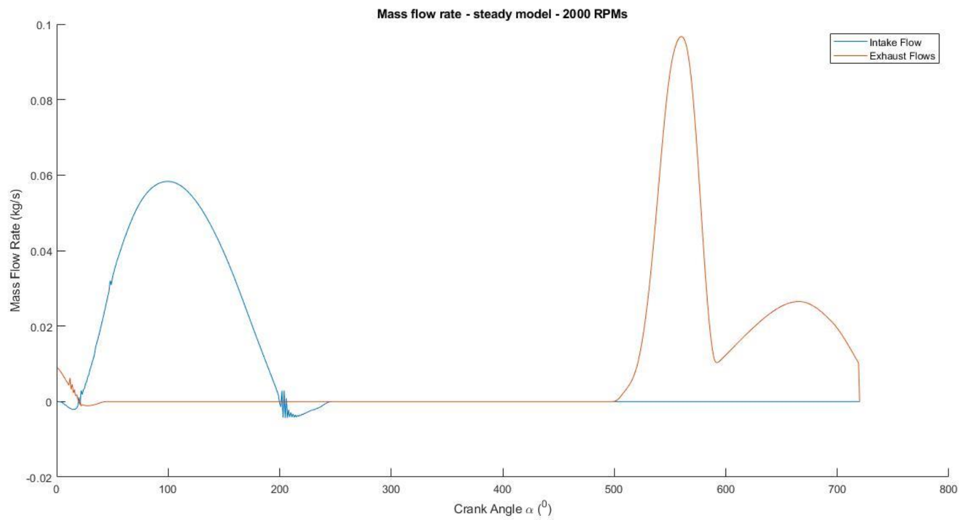

Figure 36 mass flow rate graph at 2000 RPMs

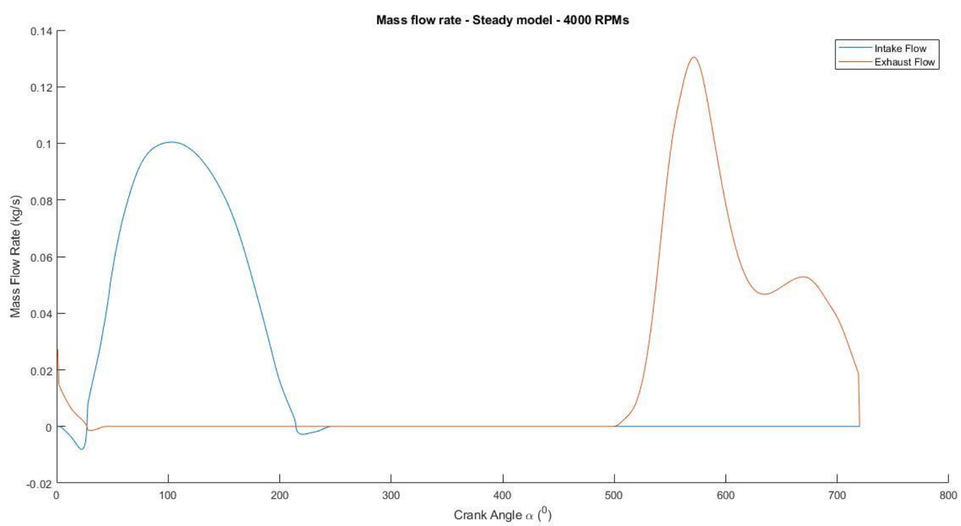

Figure 37 mass flow rate graph at 4000 RPMs

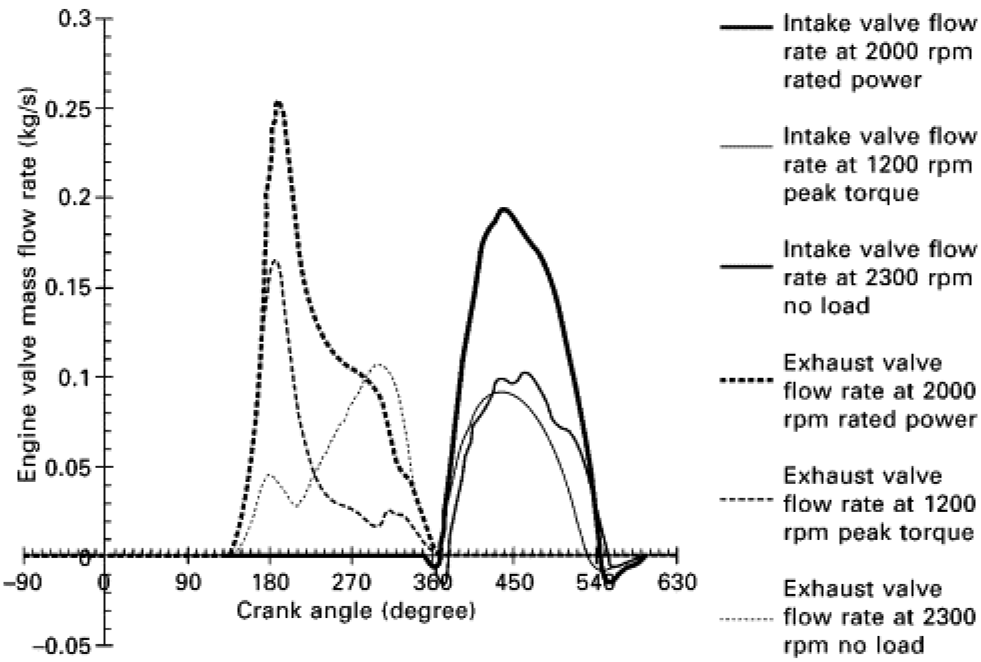

Figure 38 Experimental data 2000 RPMs Comparison [13]

- The intake mass flow rate is very similar to the result of steady state model at 2000 RPMs. (The numerical value is not of concern here as the engine is stationary i.e., probably a large generation engine having much larger flow area).
- Notice the reversal of the flow at the start and the end of the intake event.
- This is present in the model's results, AS THE FLOW HAS ENOUGH TIME TO ACHIEVE THE STEADY STATE I.E., IT IS DICTATED BY THE PRESSURE GRADIENT AND MOMENTUM EFFECTS (TENDEDNCY OF INERTIA CAUSING THE MASS TO FLOW AGAINST THE PRESSURE GRADIENT IS LOW).
- The exhaust is somewhat similar however there is a dip in the model's result. THIS IS BECAUSE OF THE BLOW-DOWN PHENOMENON (THE SUDDEN GUSHING OF GAS) WHICH GREATLY DEPENDS ON 1) VALVE TIMING 2) VALVE PROFILE 2) CYLINDER PRESSURE AT THE TIME OF EXHAUST VALVE OPENING 3) THE RATE OF CHANGE IN VOLUME OF THE CYLINDER. THIS EFFECT ALSO REDUCES PUMPING LOSSES WHEN IT STARTS DYING OUT, HOWEVER, AT LOW RPMS MUCH GREATER LOSS IN POWER IS INCURRED.

Blowdown phenomenon can be observed to have reduced at a higher RPM. This is in accordance with the physical understanding as well as the statement "High RPM engines need to have the exhaust valve open sooner so the pressure has a better chance to exit the cylinder. However, at lower RPMs, opening the exhaust valve too soon means you didn't take full advantage of the power stroke.” – source: Valve Timing & Performance (austincc.edu).

4.6.2 Incompressible – unsteady state model (better results at high RPMs):

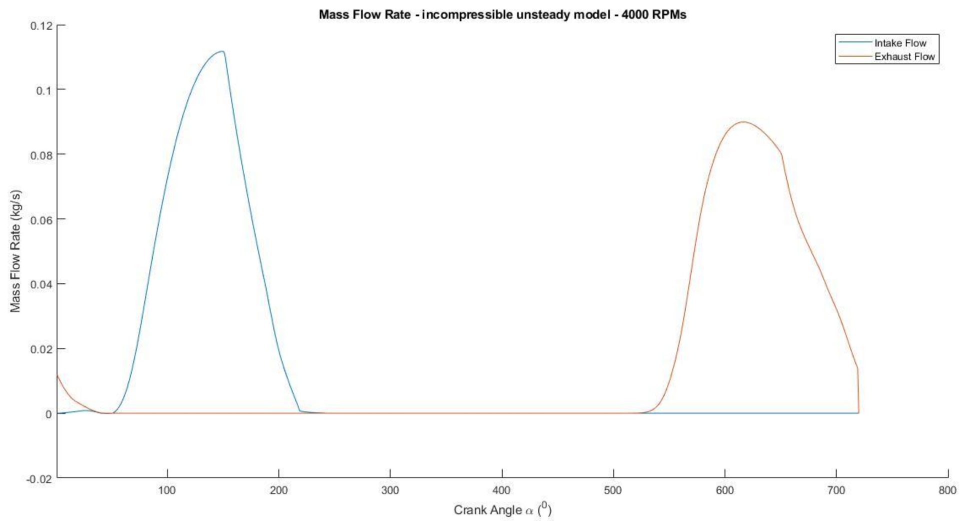

Figure 39 momentum effects incorporated at most points - 4000 RPMs.

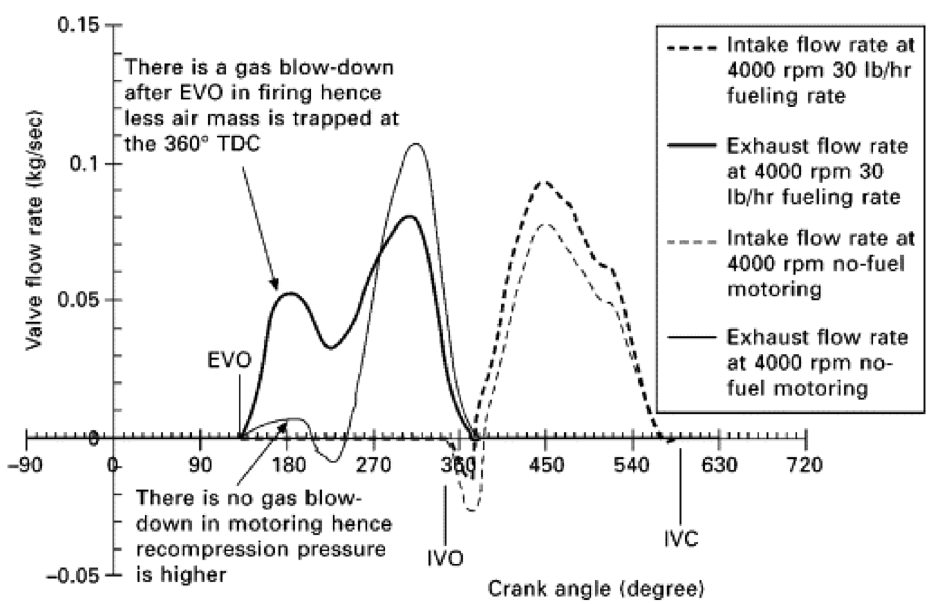

Figure 40 Experimental results 4000 RPMs [13]

- Mass flow rate does not go negative due to carrying large momentum.
- Mass flow rate is reduced.

- Sharp corners occur due to sudden change of physics (momentum included to momentum excluded. This is due to the fact that either some kind of empirical relationship is required or experimental data describing reduction of velocity towards a steady condition)
- Blowdown is not observable anymore due to high piston speeds.
- Here blowdown is observable because, as the author states, “This effect may happen when the exhaust valve is opened very suddenly and rapidly.”, i.e., due to aggressive valve lift.

4.6.3 Increased Volumetric Efficiency:

An increase of approximately ***5%*** was observed after performing the necessary alterations to the code regarding increased pressure, temperature, and velocity. For detailed explanation refer to [section 3.5.2.5]. *This is in comparison to the model incorporating incompressible, unsteady effects, without increased pressure and velocity values. For exact values refer to [Appendix 2].*

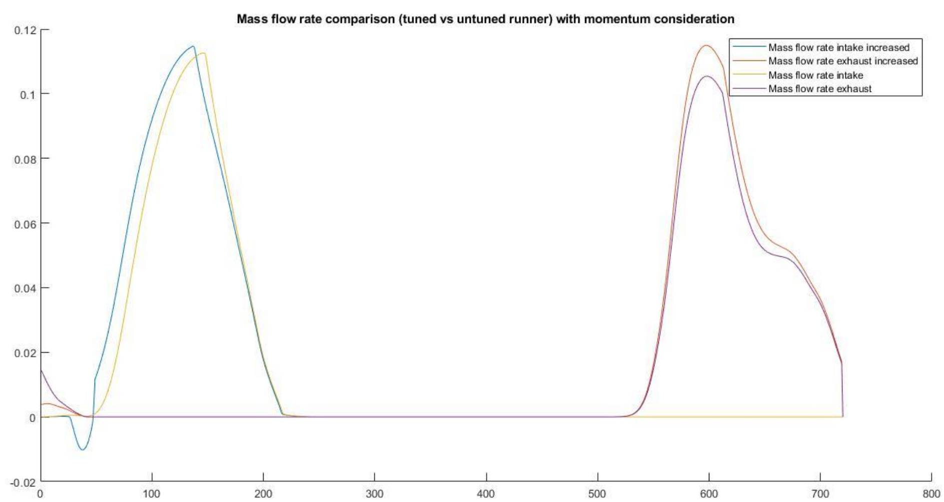

Figure 41 Comparison between tuned an untuned runner (mass flow rate)

4.6.4 Volumetric Efficiency Comparison:

In the following table Volumetric Efficiencies achieved by different models are compared:

Table 8: Volumetric Efficiency Comparison

RPMs	*Steady State equations only*	*Incompressible, unsteady equation only*	*Combined equations*	*Equations from literature*
1500	89.1327	93.7473	82.5624	89.5
2000	88.7325	97.2589	80.0781	88.8121
2500	88.1495	109.0202	76.8375	88.3756
3000	87.3948	110.8203	74.8157	87.5916
3500	86.373	101.0791	72.619	86.5804
4000	85.0192	87.1347	69.3229	85.109

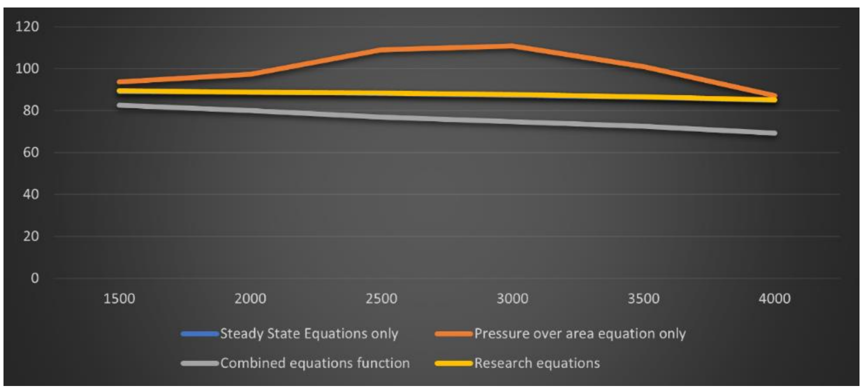

Figure 42 Volumetric Effciency Comparison between different models

Notice: The pressure over area equation or Incompressible, unsteady equation only follows the correct curve path but gives questionable results. For the reason of combined equations' model to do so, read [section 3.5.2.7]. Closet result to the experimental values are achieved by using steady state model.

4.7 Change in Mechanism Components

As per the explanation in section 3.6 of the report. The final design of the required spring is achieved to be as indicated in the results below.

4.7.1 Design Calculation Results

Based on the calculations performed for module 3 we have now the spring that will be able to provide enough return force to the valve in order to maintain a continuous contact between cam and the follower. The resultant finalized dimensions and characteristics of the selected spring are presented below

Table 9: Final Design of spring

Diameter of wire	**d:**	**5mm**
Mean Diameter of Spring	**D**	**23mm**
Internal Diameter	**ID**	**18mm**
Outer Diameter	**OD**	**28mm**
Spring Index	**C**	**4.6**
Number of Active Coils	N_a	**8.26**
Solid Length	L_s	**51.38mm**
Overall Length	L_o	**70mm**
Critical Length	$(L_o)_{CR}$	**120mm**
Fatigue factor of safety	n_f	**1.5**
Factor of safety	n_s	**1.6**
Fundamental Freqquency	f_n	**161Hz**
Figure of merit	**fom**	**-0.345**

All the vitals, C, N_a, L_o, are within normal range. The critical length is larger than the overall length indicating that the spring will nor buckle. The fundamental frequency is 161Hz which is greater than about 16 times of frequency of the forcing function (10.6Hz). The factors of safety are greater than 1.5 and the design is good enough to undergo estimated infinite loading and will not fail either due to fatigue or due to stresses.

Figure 43: Final render of designed spring

Figure 44: Final Render of valve spring Assembly

4.7.2 Stress Analysis and Verification

In order to verify the design, stress analysis was also performed using the SolidWorks simulator. The results of general von mises stress plots and comparison to the yield strength is indicated below

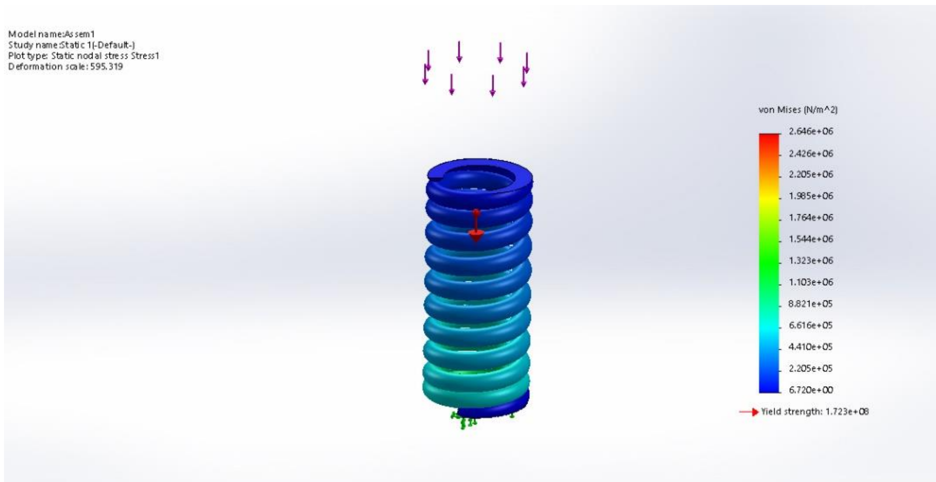

Figure 45: Stress analysis of spring

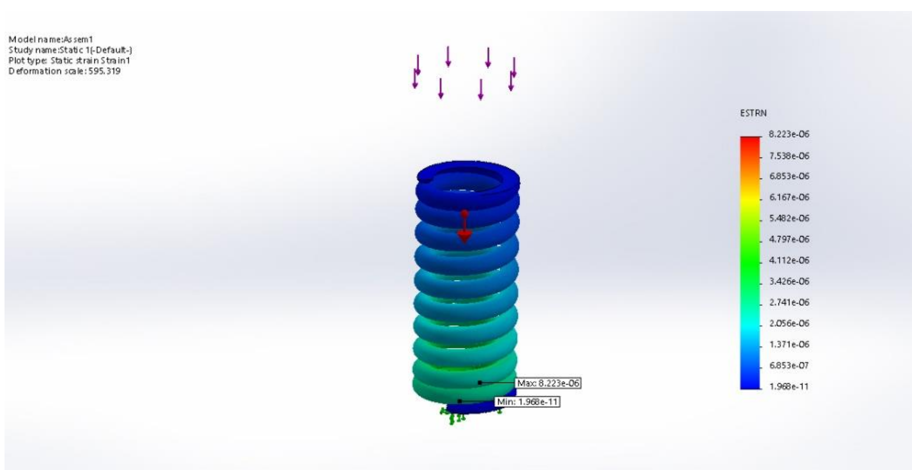

Figure 46: Max and Minimum strain in the designed spring

CHAPTER 5: CONCLUSION AND RECOMMENDATION

A 4-stroke DW 10 PSA diesel engine was modeled on MATLAB to study integral flows of engine i.e., intake and exhaust. After successfully analyzing the flows through them, we have got a complete picture of the fluid flow. The different curves of Temperature, Pressure and Mass flow rate were plotted that help visualize the state of fluid at different points along the flow. After completing the project, we have a few achievements at our hands:

5.1 Final Product:

The project gives a complete picture of the initially set targets. Designing and modeling of the intake and exhaust flows with relevant spring design are key deliverable of the end product that have yielded valuable information about the following domains:

5.1.1 Interpretation of Flows:

We have successfully developed an understanding of flows through the intake and exhaust systems. Now, we have an idea of the temperature and pressure profiles throughout the flow. These results lie in close approximation with the actual experimental results that further validate the interpretation.

The parameters that affect the fluid flow as it goes from intake manifold to the engine cylinder and then to the exhaust manifold, have been studied in detail. Their effect on the fluid profile and their relationship with engine's volumetric efficiency are also a part of the study we have obtained through this project. Further, we have established a relationship between the breathed mass and the intake manifold diameter. This led us to determine the critical diameter.

The relationship of engine parameters like volumetric efficiency, maximum cycle temperature and profile of curves with the fluid flow was studied too. This further helps visualize the system of cause and effect going on in an engine cylinder.

5.1.2 A Model with near Accuracy:

The fluid flow was successfully modeled on MATLAB. This helped us study and visualize effects like compressibility, concept of pressure wave resonation, momentum effects etc.

Now, we have the MATLAB code available for the complete flow analysis that undermines the usage of these key concepts. Our MATLAB code explains and matches our results with those obtained from the theory. However, it can be used with modification for any engine.

For studying the different flows, we have used different models to get closer to the real picture. Starting from the very basic model of compressible and unsteady flow, our final model is an amalgam of it with incompressible and unsteady flows. This takes substantial compressibility effects into consideration. Further, this model produces identical results to the real picture when engine is operating at low rpms. Even at high rpms, the results are similar to the real scenario with slight non-linearity.

A key outcome of the project is the study on the tuned runner geometry. This concept was studied in detail and a model of tuned runner diameter and length was obtained with the available knowledge at hand. However, more experimental data is needed for it to achieve better approach for tuning lengths.

5.1.3 Modified Components:

After obtaining the desired results, it was necessary to design the related crucial components for ideal performance. Therefore, our study then expanded to the design of the valve spring assembly. The force requirements were calculated numerically on SolidWorks. It was then used to design the best spring for valve so as to reduce the valve gap. Different factors like cost effectiveness, high yield material and feasibility were used to finalize the material for spring.

5.2 APPLICATIONS:

The results obtained from the study can be used in many different types of industries. Provided that adequate modification is made to the code itself, the base project can be developed into any of the following sectors:

5.2.1 Automotive:

- This particular segment of industry was also the target industry of our project. The MATLAB code from our project can be used to better understand the dynamics of an automobile engine.

- Engine repair shops can use this work to understand and modify engine performances.
- If suitable experimental results are amalgamated into the code, it can be used to tune intake runner lengths. A dynamometer-based software can be developed from it.

5.2.2 Engine Development Labs:

- There are many research labs still working to control emissions and reduce their impact. Since, this model provides the complete hidden scenario of what happens to air-fuel mixture, this can help with their study.
- The temperature and pressure profiles are very much specific regarding crank angle. The results lie in close approximation to actual scenario. This can be used to upgrade the existing material and check its feasibility computationally.

5.2.3 Spare Parts and OEM:

- If workshop operators have access to a similar model such as ours, they can use the data obtained from the results to computationally design other parts. Just as we have designed the valve spring, other parts can be designed and tested without any actual material cost.
- Original Equipment Manufacturers (OEM) can also extend this study to incorporate their own designs on numerical models. Especially, the newer companies that are emerging, like UNITED, could always use additional data.

5.2.4 Research and Development:

- There is still research going on in the world to understand fluids better. An empirical method such as ours could surely be beneficial.
- Furthermore, HCCI and RCCI are fuel injection techniques that are still under study. To extend study on them and to bring them in action, scientists need a working model, computational success and a finalized design. Our study can help as the very basic study especially for students who want to enter the domain of injection techniques.

5.3 Recommendations:

We have successfully presented the basic study of flows through the intake and exhaust systems. The results are much similar to the actual scenario and provide a very good and accurate picture. Our project involves modeling the compressibility effects, designing related components and studying the effect of different parameters. The analysis surrounds the thermal and fluid domains and present a thorough picture of the engine.

However, automotive is a vast field and similarly, our project certainly has great room for further study and improvement. A few recommendations to highlight the crucial workable domains are:

- The model that we have used is a bland mixture between steady & compressible flows and unsteady and incompressible flows. If suitable experimental data is available that lies close to the desired conditions, the MATLAB model can be upgraded. It can then show better results at high rpms. But first, reasonable trials have to be conducted to combine experimentation and computation.
- Our model can also be upgraded into a commercial software with proper user interface. It can then be integrated to form a type of engine simulator which can be used to obtain basic data regarding flows, profiles and operating conditions of any engine.
- This model can also be used a key step for extending the research on recent studies regarding injection techniques. It is a workable model that can be modified to match the require engine specifications. It can then provide reasonable data about the overview of temperature & pressure curves, flow of fluid and effects of different parameters on them.

REFERENCES

[1] "Wikipedia," [Online]. Available: https://en.wikipedia.org/wiki/Diesel_engine.

[2] PSA, "DW10 FC," [Online]. Available: https://site.groupe-psa.com/content/uploads/sites/32/2018/04/Fiche_Mot_Diesel-DW10_FC.pdf.

[3] A. M. S. R. S. Xavier Tauzia, "Experimental study of inlet manifold water injection on combustion and emissions of an automotive direct injection diesel engine," *Pergamon Press*, 2010.

[4] M. S. a. A. Noorpoor, "Flow Simulation in Engine Cylinder with Spring Mesh," *American Journal of Applied Sciences 5 (10): 1336-1343, 2008.*

[5] J. B. Heywood, Internal Combustion Engine Fundamentals, McGraw Hill.

[6] R. P. Georgiev, "Design a four-cylinder Internal Combustion Engine," Pamplona, 27.06.2011.

[7] R. N. S. B. Shrinath Potul, "Analysis Of Change In Intake Manifold Length And Development Of Variable Intake System," *INTERNATIONAL JOURNAL OF SCIENTIFIC & TECHNOLOGY RESEARCH VOLUME 3, ISSUE 5, MAY 2014 - ISSN 2277-8616.*

[8] "Nuclear-power.net," [Online]. Available: https://www.nuclear-power.net/nuclear-engineering/thermodynamics/thermodynamic-cycles/diesel-cycle-diesel-engine/actual-and-ideal-diesel-cycle/.

[9] f. t. i. speed, "Exhaust pressure pulsation observation from turbocharger instantaneous speed," *INSTITUTE OF PHYSICS PUBLISHING,* 2004.

[10] M. Husselman, "Modeling and Verification of Valve train Dynamics in Engine," Matieland, South Africa, 2005.

[11] Budynas−Nisbett, Mechanical Engineering - Shigley's Mechanical Engineering Design, Mcraw-Hill, 2006.

[12] N. P. P. R. C. V. J . Chauvin, "Air Path Estimation on Diesel HCCI Engine," *Society of Automotive Engineers, Inc.*, 2006.

[13] Q. Xin, Diesel Engine System Design, Woodhead Publishing, 2011.

APPENDIX I: MATLAB CODE FOR MODULE 01

COMPLETE FLOW MODEL

RESULTS FROM MATLAB

```
Vol_eff     =   (M_mat(275,2)/((P_atm*max(V_c))/(R*T_atm)))*100
```

```
Vol_eff = 88.7325
```

mass flow rate function:

```
function m_f_r  =   Mass_flow(P_in,P_ex,T_in,th_a,R,AFR)
C_p_k    =   Keekay(T_in,AFR/14.5);
y_k      =   C_p_k/(C_p_k-R);
if  (P_in/P_ex) >=  ((y_k + 1)/2)^(y_k/(y_k-1))
    %M_th     =   1;
    T_th     =   T_in*(2/(y_k + 1));
    V_th     =   sqrt(T_th * R * y_k);
    P_th     =   P_in*((2/(y_k+1))^(y_k/(y_k-1)));
    Rho_th   =   P_th/(R*T_th);
    m_f_r    =   Rho_th * th_a * V_th;
else
    M_th     =   sqrt((2/(y_k - 1))*(((P_in/P_ex)^((y_k - 1)/y_k))-
1));
    T_th     =   T_in/(1+(((y_k - 1)/2)*(M_th^2)));
    V_th     =   M_th*(sqrt(y_k * R * T_th));
    P_th     =   P_in/((1+((y_k-1)/2)*(M_th)^2)^(y_k/(y_k-1)));
    Rho_th   =   P_th/(R * T_th);
    m_f_r    =   Rho_th * th_a * V_th;
end
end
```

Velocity function:

```
function V_th   =   Velocity(P_in,P_ex,T_in,R,AFR)
C_p_k    =   Keekay(T_in,AFR/14.5);
y_k      =   C_p_k/(C_p_k-R);

P_th     =   P_in * ((2/(y_k + 1))^(y_k/(y_k - 1)));

if  P_ex     <=  P_th
```

```
    %M_th    =   1;
    T_th    =   T_in*(2/(y_k + 1));
    V_th    =   sqrt(T_th * R * y_k);

else
    M_th    =   sqrt((2/(y_k - 1))*(((P_in/P_ex)^((y_k - 1)/y_k))-
1));
    T_th    =   T_in/(1+(((y_k - 1)/2)*(M_th^2)));
    V_th    =   M_th*(sqrt(y_k * R * T_th));

end
end
```

Keekay Function:

```
function C_p_k = Keekay(L, K)
if L>600
    C_p_k = (166.3+24.5/K)*log(L-70-120/K);
else
    if K<8
        C_p_k = (975.5+0.28*L)-((11.92+0.06*L)*log(K));
    else
        C_p_k = 1000+2.85*exp((L-273.16)/100*0.88);
    end
end
end
```

After looping the same calculation for changing diameters from 0.55*sqrt (2) *Valve Diameter to 2*sqrt (2) *Valve Diameter. The diameter chosen is 0.84*sqrt (2) *Valve Diameter.

APPENDIX II: MATLAB CODE AND CALCULATIONS FOR MODULE 02

COMPLETE FLOW MODEL

```
Vol_eff     =   (M_mat(275,2)/((P_atm*max(V_c))/(R*T_atm)))*100
```

```
Vol_eff = 75.1271 @ 4000 RPMs
```

mass flow rate function nozzle 2 and 3:

```
function m_f_r_v  =
Mass_flow_val(P_in,P_ex,T_in,T_out,th_a,R,t_step,m_man,V_last,AFR)

 if  P_in     >=  P_ex

     C_p_k   =   Keekay(T_in,AFR/14.5);
     y_k     =   C_p_k/(C_p_k-R);

     if  (P_in/P_ex) >=  ((y_k + 1)/2)^(y_k/(y_k-1))
         %M_th_st    =   1;
         T_th_st     =   T_in*(2/(y_k + 1));
         V_th_st     =   sqrt(T_th_st * R * y_k);
     else
         M_th_st     =   sqrt((2/(y_k - 1))*(((P_in/P_ex)^((y_k -
1)/y_k))-1));
         T_th_st     =   T_in/(1+(((y_k - 1)/2)*(M_th_st^2)));
         V_th_st     =   M_th_st*(sqrt(y_k * R * T_th_st));
     end

 else

     C_p_k   =   Keekay(T_out,AFR/14.5);
     y_k     =   C_p_k/(C_p_k-R);

     if  (P_ex/P_in) >=  ((y_k + 1)/2)^(y_k/(y_k-1))
         %M_th_st    =   1;
         T_th_st     =   T_out*(2/(y_k + 1));
         V_th_st     =   sqrt(T_th_st * R * y_k);
     else
         M_th_st     =   sqrt((2/(y_k - 1))*(((P_ex/P_in)^((y_k -
1)/y_k))-1));
         T_th_st     =   T_out/(1+(((y_k - 1)/2)*(M_th_st^2)));
         V_th_st     =   M_th_st*(sqrt(y_k * R * T_th_st));
     end

 end

 V_th    =   (((P_in-P_ex)*th_a*t_step)/m_man)   +   V_last;

 if      P_in    >=  P_ex    &&  V_th    >=  0    &&  V_th    >=
V_th_st
     V_th    =   V_th_st;
 elseif  P_in    <  P_ex    &&  V_th    <  0     &&  abs(V_th)    >=
abs(V_th_st)
```

```
    V_th    =   -V_th_st;
end

if  V_th    >=  0

    C_p_k   =   Keekay(T_in,AFR/14.5);
    y_k     =   C_p_k/(C_p_k-R);
    T_cr    =   T_in*(2/(y_k + 1));
    M_th    =   (abs(V_th)/(sqrt(y_k*R*T_cr)));
    T_th    =   T_in/(1+(((y_k - 1)/2)*(M_th^2)));
    P_th    =   P_in/((1+((y_k-1)/2)*(M_th)^2)^(y_k/(y_k-1)));
    Rho_th  =   P_th/(R*T_th);
    m_f_r_v =   Rho_th * th_a * ((V_th + V_last)/2);

else    %V_th   <   0

    C_p_k   =   Keekay(T_out,AFR/14.5);
    y_k     =   C_p_k/(C_p_k-R);
    T_cr    =   T_out*(2/(y_k + 1));
    M_th    =   (abs(V_th)/(sqrt(y_k*R*T_cr)));
    T_th    =   T_out/(1+(((y_k - 1)/2)*(M_th^2)));
    P_th    =   P_ex/((1+((y_k-1)/2)*(M_th)^2)^(y_k/(y_k-1)));
    Rho_th  =   P_th/(R*T_th);
    m_f_r_v =   Rho_th * th_a * ((V_th + V_last)/2);


end
end
```

Velocity function nozzle 2 and 3:

```
function V_th  =
fin_velocity_val(P_in,P_ex,T_in,T_out,th_a,R,t_step,m_man,V_last,AFR
)

if  P_in     >=  P_ex

    C_p_k   =   Keekay(T_in,AFR/14.5);
    y_k     =   C_p_k/(C_p_k-R);

    if  (P_in/P_ex) >=  ((y_k + 1)/2)^(y_k/(y_k-1))
        %M_th_st    =   1;
        T_th_st    =   T_in*(2/(y_k + 1));
        V_th_st    =   sqrt(T_th_st * R * y_k);
```

```
    else
        M_th_st    =   sqrt((2/(y_k - 1))*(((P_in/P_ex)^((y_k -
1)/y_k))-1));
        T_th_st    =   T_in/(1+(((y_k - 1)/2)*(M_th_st^2)));
        V_th_st    =   M_th_st*(sqrt(y_k * R * T_th_st));
    end

 else

    C_p_k   =   Keekay(T_out,AFR/14.5);
    y_k     =   C_p_k/(C_p_k-R);
    if  (P_ex/P_in) >=  ((y_k + 1)/2)^(y_k/(y_k-1))
        %M_th_st    =   1;
        T_th_st    =   T_out*(2/(y_k + 1));
        V_th_st    =   sqrt(T_th_st * R * y_k);
    else
        M_th_st    =   sqrt((2/(y_k - 1))*(((P_ex/P_in)^((y_k -
1)/y_k))-1));
        T_th_st    =   T_out/(1+(((y_k - 1)/2)*(M_th_st^2)));
        V_th_st    =   M_th_st*(sqrt(y_k * R * T_th_st));
    end

 end

 V_th    =   (((P_in-P_ex)*th_a*t_step)/m_man)   +   V_last;

 if      P_in    >=  P_ex    &&  V_th    >=  0   &&  V_th    >=
V_th_st
    V_th    =   V_th_st;
 elseif  P_in    <  P_ex    &&  V_th    <  0     &&  abs(V_th)    >=
abs(V_th_st)
    V_th    =   -V_th_st;
 end

 end
```

mass flow rate function nozzle 1 and 4:

```
 function m_f_r_m  =   Mass_flow_man(P_in,P_ex,T_in,th_a,R,AFR)
 C_p_k   =   Keekay(T_in,AFR/14.5);
 y_k     =   C_p_k/(C_p_k-R);
 if  (P_in/P_ex) >=  ((y_k + 1)/2)^(y_k/(y_k-1))
     %M_th    =   1;
```

```
    T_th     =   T_in*(2/(y_k + 1));
    V_th     =   sqrt(T_th * R * y_k);
    P_th     =   P_in*((2/(y_k+1))^(y_k/(y_k-1)));
    Rho_th   =   P_th/(R*T_th);
    m_f_r_m =   Rho_th * th_a * V_th;
else
    M_th     =   sqrt((2/(y_k - 1))*(((P_in/P_ex)^((y_k - 1)/y_k))-
1));
    T_th     =   T_in/(1+(((y_k - 1)/2)*(M_th^2)));
    V_th     =   M_th*(sqrt(y_k * R * T_th));
    P_th     =   P_in/((1+((y_k-1)/2)*(M_th)^2)^(y_k/(y_k-1)));
    Rho_th   =   P_th/(R * T_th);
    m_f_r_m =   Rho_th * th_a * V_th;
end
end
```

Velocity function nozzle 1 and 4:

```
function V_th  =   fin_velocity_man(P_in,P_ex,T_in,R,AFR)
C_p_k    =   Keekay(T_in,AFR/14.5);
y_k      =   C_p_k/(C_p_k-R);
if  (P_in/P_ex) >=  ((y_k + 1)/2)^(y_k/(y_k-1))
    %M_th     =   1;
    T_th     =   T_in*(2/(y_k + 1));
    V_th     =   sqrt(T_th * R * y_k);
else
    M_th     =   sqrt((2/(y_k - 1))*(((P_in/P_ex)^((y_k - 1)/y_k))-
1));
    T_th     =   T_in/(1+(((y_k - 1)/2)*(M_th^2)));
    V_th     =   M_th*(sqrt(y_k * R * T_th));
end
end
```

Keekay Function:

```
function C_p_k = Keekay(L, K)
if L>600
    C_p_k = (166.3+24.5/K)*log(L-70-120/K);
else
    if K<8
        C_p_k = (975.5+0.28*L)-((11.92+0.06*L)*log(K));
    else
        C_p_k = 1000+2.85*exp((L-273.16)/100*0.88);
    end
```

```
end
end
```

TUNED LENGTH CALCULATION

```
    Dis_wave       =    (sqrt((Keekay(T_mat(In_end,1),AFR/14.5) / (Keekay(T_mat(In_end,1),AFR/14.5) - R)) * R * T_mat(In_end,1)) * (Step_time * (Array_size_1 - In_end)));
```

Calculated travel distance by pressure wave: 6.72 m

As wave travels back and forth = 6.72/2 = 3.36 m

Thus, runner length after 5 reflections = 3.36/5 =0.672 m

INCREASE IN VOLUMETRIC EFFICIENCY

At 4000 RPMs, after making necessary changes, mentioned in methodology [3.5.2.5] the volumetric efficiency increased from 69.3229 to 75.1271.

APPENDIX III: CALCULATIONS FOR MODULE 03

Diameter of wire:

$$d := 5\ mm$$

Diameter of Hole:

$$d_{hole} := 29\ mm$$
$$Allowance := 1\ mm$$

Mean Diameter of Spring:

$$D := d_{hole} - d - Allowance$$
$$D = 23\ mm$$

Spring Index:

$$C := \frac{D}{d}$$

$$C = 4.6$$

Curvature Effect: Bergstrasser Factor

$$K_B := \frac{4 \cdot C + 2}{4 \cdot C - 3}$$

$$K_B = 1.325$$

Ultimate Tensile Strength:

$$S_{ut} := 2005\ MPa$$

Torsional Stress Limit:

$$S_{sy} := S_{ut} \cdot 0.65$$

$$S_{sy} = \left(1.303 \cdot 10^3\right)\ MPa$$

Maximum Loading Condition:

$$F_{max} := 870\ N$$

Valve lift:

$$Valvelift := 8.5\ mm$$

Pre-compression:

$$precompression := 6\ mm$$

Maximum Compression:

$$y := Valvelift + precompression$$
$$y = 14.5\ mm$$

Spring Constant:

$$k := \frac{F_{max}}{y}$$
$$k = \left(6 \cdot 10^4\right)\ \frac{kg}{s^2}$$

Fractional Overrun:

$$\xi := 0.15$$

Stress Due to Loading Condition:

$$\tau := \frac{K_B \cdot 8 \cdot (1+\xi)\ F_{max} \cdot D}{\pi \cdot d^3}$$

$$\tau = 620.99\ MPa$$

Stress Factor of safety:

$$n_s := \frac{S_{sy}}{\tau}$$

$$n_s = 2.099$$

Outer diameter:

$$OD := D + d$$
$$OD = 28\ mm$$

Inner diameter:

$$ID := D - d$$
$$ID = 18\ mm$$

Shear Modulus:

$$G := 77.2\ GPa$$

Elastic Modulus:

$$E := 203.4\ GPa$$

Number of Active Coils:

$$N_a := \frac{G \cdot d^4 \cdot y}{8 \cdot D^3 \cdot F_{max}}$$

$$N_a = 8.262$$

Number of Total coils:

$$N_t := N_a + 2$$

$$N_t = 10.262$$

Solid Length of Spring:

$$L_s := d \cdot N_t$$

$$L_s = 51.309\ mm$$

Overall Length of Spring

$$L_o := L_s + y + precompression$$

$$L_o = 71.809\ mm$$

Critical Length:

$$L_{CR} := 5.26 \cdot D$$

$$L_{CR} = 120.98\ mm$$

Specific weight:

$$\gamma := 76518 \frac{kg}{m^2 \cdot s^2}$$

Weight of Spring:

$$W := \frac{\pi^2 \cdot d^2 \cdot D \cdot N_a \cdot \gamma}{4}$$

$$W = 0.897\ N$$

Fundamental Frequency of Spring:

$$f_n := \frac{1}{2} \cdot \left(\frac{k \cdot g}{W}\right)^{\frac{1}{2}}$$

$$f_n = 404.98\ \frac{1}{s}$$

Table 10: Complete calculation Table generated on Excel

d	D	C	Kb	Sut	Ssy	Ts	ns	OD	ID	Na	Nt	Ls	Lo	Lcr	fom	W	k	f	Ta	Tm	Ts-	nf	ns-
0.8	27.2	34	1.0376	2081.6	1353	140509	0.0096	28	26.4	0.0033	2.0033	1.6026	16.103	143.07	-0.002	1E-05	60000	117006	36514	85668	140509	0.0066	0.0096
1	27	27	1.0476	2005	1303.3	72102	0.0181	28	26	0.0082	2.0082	2.0082	16.508	142.02	-0.003	4E-05	60000	59467	18737	43960	72102	0.0129	0.0181
1.2	26.8	22.333	1.0579	1944.5	1263.9	41823	0.0302	28	25.6	0.0173	2.0173	2.4208	16.921	140.97	-0.005	0.0001	60000	34159	10869	25500	41823	0.0222	0.0302
1.4	26.6	19	1.0685	1894.8	1231.6	26403	0.0466	28	25.2	0.0328	2.0328	2.846	17.346	139.92	-0.006	0.0003	60000	21351	6861.2	16098	26403	0.0351	0.0466
1.6	26.4	16.5	1.0794	1852.8	1204.3	17733	0.0679	28	24.8	0.0573	2.0573	3.2917	17.792	138.86	-0.008	0.0007	60000	14196	4608.4	10812	17733	0.0523	0.0679
1.8	26.2	14.556	1.0905	1816.5	1180.7	12488	0.0945	28	24.4	0.0939	2.0939	3.769	18.269	137.81	-0.01	0.0015	60000	9894.5	3245.3	7614.1	12488	0.0743	0.0945
2	26	13	1.102	1784.6	1160	9129.7	0.1271	28	24	0.1464	2.1464	4.2928	18.793	136.76	-0.013	0.0029	60000	7158	2372.5	5566.4	9129.7	0.1016	0.1271
2.2	25.8	11.727	1.1139	1756.3	1141.6	6879.6	0.1659	28	23.6	0.2194	2.2194	4.8826	19.383	135.71	-0.016	0.0052	60000	5336.6	1787.8	4194.5	6879.6	0.1348	0.1659
2.4	25.6	10.667	1.1261	1730.8	1125	5315.5	0.2116	28	23.2	0.3181	2.3181	5.5633	20.063	134.66	-0.02	0.0088	60000	4078.7	1381.3	3240.8	5315.5	0.1745	0.2116
2.6	25.4	9.7692	1.1386	1707.6	1110	4194.3	0.2646	28	22.8	0.4485	2.4485	6.3661	20.866	133.6	-0.025	0.0145	60000	3182.9	1090	2557.2	4194.3	0.2211	0.2646
2.8	25.2	9	1.1515	1686.5	1096.2	3369.6	0.3253	28	22.4	0.6177	2.6177	7.3297	21.83	132.55	-0.03	0.023	60000	2528.3	875.65	2054.4	3369.6	0.2752	0.3253
3	25	8.3333	1.1648	1667.1	1083.6	2749.3	0.3941	28	22	0.8338	2.8338	8.5013	23.001	131.5	-0.037	0.0354	60000	2039.3	714.45	1676.2	2749.3	0.3373	0.3941
3.2	24.8	7.75	1.1786	1649.1	1071.9	2273.7	0.4714	28	21.6	1.1057	3.1057	9.9381	24.438	130.45	-0.046	0.053	60000	1666.9	590.87	1386.3	2273.7	0.4079	0.4714
3.4	24.6	7.2353	1.1927	1632.4	1061.1	1902.9	0.5576	28	21.2	1.4437	3.4437	11.709	26.209	129.4	-0.057	0.0774	60000	1378.5	494.51	1160.2	1902.9	0.4873	0.5576
3.6	24.4	6.7778	1.2074	1616.8	1050.9	1609.5	0.6529	28	20.8	1.8596	3.8596	13.895	28.395	128.34	-0.071	0.1109	60000	1151.8	418.27	981.33	1609.5	0.5762	0.6529
3.8	24.2	6.3684	1.2225	1602.2	1041.4	1374.3	0.7578	28	20.4	2.3663	4.3663	16.592	31.092	127.29	-0.089	0.156	60000	971.35	357.14	837.91	1374.3	0.6748	0.7578
4	24	6	1.2381	1588.4	1032.5	1183.5	0.8724	28	20	2.9784	4.9784	19.914	34.414	126.24	-0.112	0.2157	60000	825.93	307.55	721.57	1183.5	0.7836	0.8724
4.2	23.8	5.6667	1.2542	1575.5	1024.1	1027	0.9971	28	19.6	3.7123	5.7123	23.992	38.492	125.19	-0.14	0.294	60000	707.52	266.9	626.18	1027	0.903	0.9971
4.4	23.6	5.3636	1.2709	1563.2	1016.1	897.54	1.1321	28	19.2	4.5862	6.5862	28.979	43.479	124.14	-0.176	0.3952	60000	610.19	233.24	547.23	897.54	1.0333	1.1321
4.6	23.4	5.087	1.2882	1551.6	1008.5	789.42	1.2775	28	18.8	5.6203	7.6203	35.053	49.553	123.08	-0.221	0.5249	60000	529.48	205.15	481.31	789.42	1.1748	1.2775
4.8	23.2	4.8333	1.3061	1540.5	1001.3	698.43	1.4337	28	18.4	6.8372	8.8372	42.418	56.918	122.03	-0.276	0.6893	60000	462.04	181.5	425.83	698.43	1.3278	1.4337
5	23	4.6	1.3247	1530	994.49	621.3	1.6006	28	18	8.2618	10.262	51.309	65.809	120.98	-0.345	0.896	60000	405.26	161.46	378.81	621.3	1.4926	1.6006
5.2	22.8	4.3846	1.3439	1519.9	987.96	555.49	1.7785	28	17.6	9.9217	11.922	61.993	76.493	119.93	-0.43	1.1537	60000	357.14	144.35	338.68	555.49	1.6695	1.7785
5.4	22.6	4.1852	1.3639	1510.3	981.72	498.98	1.9675	28	17.2	11.847	13.847	74.776	89.276	118.88	-0.534	1.4726	60000	316.11	129.67	304.22	498.98	1.8586	1.9675
5.6	22.4	4	1.3846	1501.1	975.74	450.18	2.1674	28	16.8	14.073	16.073	90.008	104.51	117.82	-0.66	1.8645	60000	280.93	116.99	274.48	450.18	2.06	2.1674
5.8	22.2	3.8276	1.4062	1492.3	970	407.83	2.3784	28	16.4	16.635	18.635	108.08	122.58	116.77	-0.814	2.3432	60000	250.6	105.98	248.65	407.83	2.2739	2.3784
6	22	3.6667	1.4286	1483.8	964.49	370.89	2.6005	28	16	19.576	21.576	129.45	143.95	115.72	-0.999	2.9242	60000	224.33	96.384	226.13	370.89	2.5004	2.6005
6.2	21.8	3.5161	1.4519	1475.7	959.19	338.53	2.8334	28	15.6	22.939	24.939	154.62	169.12	114.67	-1.222	3.6256	60000	201.46	87.973	206.4	338.53	2.7395	2.8334
6.4	21.6	3.375	1.4762	1467.8	954.09	310.05	3.0772	28	15.2	26.775	28.775	184.16	198.66	113.62	-1.489	4.468	60000	181.48	80.573	189.04	310.05	2.9911	3.0772
6.6	21.4	3.2424	1.5015	1460.3	949.17	284.9	3.3316	28	14.8	31.139	33.139	218.72	233.22	112.56	-1.806	5.4749	60000	163.94	74.037	173.7	284.9	3.2551	3.3316
6.8	21.2	3.1176	1.528	1453	944.42	262.6	3.5964	28	14.4	36.091	38.091	259.02	273.52	111.51	-2.183	6.673	60000	148.5	68.242	160.11	262.6	3.5315	3.5964
7	21	3	1.5556	1445.9	939.83	242.77	3.8714	28	14	41.698	43.698	305.88	320.38	110.46	-2.629	8.0926	60000	134.85	63.088	148.01	242.77	3.8201	3.8714
7.2	20.8	2.8889	1.5844	1439.1	935.4	225.07	4.1561	28	13.6	48.03	50.03	360.22	374.72	109.41	-3.154	9.768	60000	122.74	58.488	137.22	225.07	4.1205	4.1561
7.4	20.6	2.7838	1.6146	1432.5	931.1	209.23	4.4502	28	13.2	55.17	57.17	423.06	437.56	108.36	-3.771	11.738	60000	111.97	54.372	127.57	209.23	4.4324	4.4502
7.6	20.4	2.6842	1.6463	1426.1	926.94	195.01	4.7532	28	12.8	63.203	65.203	495.55	510.05	107.3	-4.492	14.046	60000	102.35	50.678	118.9	195.01	4.7555	4.7532
7.8	20.2	2.5897	1.6794	1419.9	922.9	182.23	5.0646	28	12.4	72.227	74.227	578.97	593.47	106.25	-5.334	16.742	60000	93.751	47.355	111.1	182.23	5.0892	5.0646
8	20	2.5	1.7143	1413.8	918.99	170.69	5.3838	28	12	82.347	84.347	674.77	689.27	105.2	-6.313	19.88	60000	86.034	44.359	104.07	170.69	5.433	5.3838
8.2	19.8	2.4146	1.7509	1408	915.18	160.28	5.7101	28	11.6	93.678	95.678	784.56	799.06	104.15	-7.448	23.523	60000	79.092	41.651	97.719	160.28	5.7862	5.7101
8.4	19.6	2.3333	1.7895	1402.3	911.48	150.84	6.0427	28	11.2	106.35	108.35	910.11	924.61	103.1	-8.761	27.74	60000	72.833	39.199	91.967	150.84	6.1481	6.0427
8.6	19.4	2.2558	1.8301	1396.7	907.89	142.29	6.3807	28	10.8	120.49	122.49	1053.4	1067.9	102.04	-10.28	32.608	60000	67.176	36.976	86.751	142.29	6.5178	6.3807
8.8	19.2	2.1818	1.873	1391.4	904.39	134.52	6.7233	28	10.4	136.27	138.27	1216.8	1231.3	100.99	-12.02	38.215	60000	62.053	34.957	82.013	134.52	6.8943	6.7233
9	19	2.1111	1.9184	1386.1	900.98	127.45	7.0694	28	10	153.85	155.85	1402.6	1417.1	99.94	-14.02	44.657	60000	57.403	33.12	77.705	127.45	7.2765	7.0694
9.2	18.8	2.0435	1.9664	1381	897.66	121.02	7.4177	28	9.6	173.4	175.4	1613.7	1628.2	98.888	-16.32	52.042	60000	53.175	31.448	73.783	121.02	7.6634	7.4177
9.4	18.6	1.9787	2.0173	1376	894.42	115.15	7.7671	28	9.2	195.14	197.14	1853.1	1867.6	97.836	-18.94	60.49	60000	49.322	29.925	70.209	115.15	8.0534	7.7671
9.6	18.4	1.9167	2.0714	1371.2	891.26	109.81	8.1162	28	8.8	219.28	221.28	2124.3	2138.8	96.784	-21.94	70.134	60000	45.805	28.537	66.952	109.81	8.4452	8.1162
9.8	18.2	1.8571	2.129	1366.4	888.18	104.94	8.4635	28	8.4	246.07	248.07	2431.1	2445.6	95.732	-25.35	81.125	60000	42.59	27.272	63.983	104.94	8.8371	8.4635
10	18	1.8	2.1905	1361.8	885.17	100.51	8.8072	28	8	275.78	277.78	2777.8	2792.3	94.68	-29.23	93.625	60000	39.645	26.118	61.278	100.51	9.2273	8.8072
10.2	17.8	1.7451	2.2562	1357.3	882.23	96.464	9.1457	28	7.6	308.69	310.69	3169	3183.5	93.628	-33.64	107.82	60000	36.943	25.068	58.814	96.464	9.6138	9.1457
10.4	17.6	1.6923	2.3265	1352.9	879.36	92.79	9.4769	28	7.2	345.12	347.12	3610.1	3624.6	92.576	-38.64	123.91	60000	34.461	24.113	56.573	92.79	9.9945	9.4769
10.6	17.4	1.6415	2.4021	1348.5	876.55	89.455	9.7988	28	6.8	385.44	387.44	4106.8	4121.3	91.524	-44.29	142.13	60000	32.177	23.247	54.54	89.455	10.367	9.7988
10.8	17.2	1.5926	2.4835	1344.3	873.8	86.437	10.109	28	6.4	430.02	432.02	4665.8	4680.3	90.472	-50.68	162.71	60000	30.072	22.462	52.7	86.437	10.729	10.109
11	17	1.5455	2.5714	1340.2	871.11	83.719	10.405	28	6	479.29	481.29	5294.2	5308.7	89.42	-57.89	185.95	60000	28.131	21.756	51.043	83.719	11.077	10.405
11.2	16.8	1.5	2.6667	1336.1	868.48	81.283	10.685	28	5.6	533.73	535.73	6000.2	6014.7	88.368	-66.01	212.14	60000	26.337	21.123	49.558	81.283	11.409	10.685
11.4	16.6	1.4561	2.7702	1332.2	865.9	79.119	10.944	28	5.2	593.84	595.84	6792.6	6807.1	87.316	-75.16	241.63	60000	24.678	20.561	48.238	79.119	11.721	10.944
11.6	16.4	1.4138	2.8831	1328.3	863.37	77.216	11.181	28	4.8	660.2	662.2	7681.5	7696	86.264	-85.44	274.79	60000	23.141	20.066	47.078	77.216	12.01	11.181
11.8	16.2	1.3729	3.0068	1324.5	860.9	75.57	11.392	28	4.4	733.43	735.43	8678.1	8692.6	85.212	-96.99	312.03	60000	21.716	19.638	46.075	75.57	12.272	11.392
12	16	1.3333	3.1429	1320.7	858.47	74.179	11.573	28	4	814.22	816.22	9794.6	9809.1	84.16	-110	353.82	60000	20.393	19.277	45.226	74.179	12.502	11.573